NOVEL THERAPEUTIC COMPOUNDS MODULATE THE INFLAMMATORY RESPONSE OF STIMULATED EQUINE SYNOVIOCYTES

by

Krista M. Huff

A Thesis

Submitted to the Faculty of Purdue University

In Partial Fulfillment of the Requirements for the degree of

Master of Science

Department of Basic Medical Sciences

West Lafayette, Indiana

May 2022

THE PURDUE UNIVERSITY GRADUATE SCHOOL
STATEMENT OF COMMITTEE APPROVAL

Dr. Marxa Figueiredo, Chair

Department of Basic Medical Sciences

Dr. Timothy Lescun

Department of Veterinary Clinical Sciences

Dr. Herman Sintim

Department of Chemistry

Dr. Dianne Little

Department of Basic Medical Sciences

Approved by:

Dr. Laurie Jaeger

In loving memory of
Michael Joseph Huff
March 17, 1958 – May 20, 2021

I would like to dedicate my thesis to my beloved father, Michael Joseph Huff, who always encouraged me to be the greatest version of myself and taught me that nothing comes free-handedly – I must put forth the work to achieve my goals. He is my strength and will to move forward, my motivator to give my best effort, no matter the outcome. I will be forever grateful.

ACKNOWLEDGMENTS

I would like to express my gratitude to those that have supported and encouraged me throughout my academic accomplishments.

First, a special mention goes to my principal investigator and my mentor, MLF, for introducing me to the field of research and for providing me with the opportunity to be part of the lab as an undergraduate student and transition into a graduate student. I am thankful for her kindness, understanding, patience, and enthusiasm and for continuously motivating me to strive beyond what I thought was possible. It was a great privilege to work and study under her guidance.

Secondly, my sincere thanks go to my committee members, TBL, DL, and HOS, for providing me with advice and suggestions throughout my project. The attention-to-detail questions and feedback regarding current findings and future directions of the project led to the finished product that my thesis is today.

Thirdly, I want to thank my fellow lab members for teaching me and for always being open and available for questions and random tasks. I have been fortunate to meet many commendable colleagues who became friends, especially CMRC, who has taught many valuable tasks since day one and gave me priceless advice, even beyond academic and professional topics.

Lastly, I am grateful to my parents, MJH and JTH, my siblings, KMH and AGH, my extended family, and my close friends for advocating for me, for believing that I could achieve things beyond my imagination, and for pushing me to my greatest heights, even in times of self-doubt. And, of course, I am beyond thankful for my significant other, TAB, for being my rock and for being by my side and supporting me every step of the way as I endlessly worked to complete my degree.

I cannot express my gratitude enough for the individuals that have made an imprint on my life as I made the journey through my academic career.

TABLE OF CONTENTS

LIST OF TABLES

LIST OF FIGURES

LIST OF ABBREVIATIONS

Abbreviation	Meaning
ADAM	A disintegrin and metalloproteinase
DAMP	Damage-associated molecular pattern
DMEM	Dulbecco's Modified Eagle's Serum
DMSO	Dimethyl sulfoxide
DPBS	Dulbecco's Phosphate Buffered Solution
ECM	Extracellular matrix
eqFLS	Equine fibroblast-like synoviocytes
FBS	Fetal Bovine Serum
FLS	Fibroblast-like synoviocytes
GAPDH	Glyceraldehyde 3-phosphate dehydrogenase
GFP	Green fluorescent protein
HA	Hyaluronic acid
IL-1β	Interleukin-1 beta
IL-6	Interleukin-6
LAMR1	Laminin Receptor 1
LPS	Lipopolysaccharide
MLS	Macrophage-like synoviocytes
MMPs	Matrix metalloproteinases
NF-κB	Nuclear factor kappa B subunit 1
OA	Osteoarthritis
PAMPs	Pathogen-associated molecular patterns
PEDF	Pigment epithelium derived factor
PG	Proteoglycan
PRRs	Pathogen recognition receptors
PTOA	Post traumatic osteoarthritis
RA	Rheumatoid arthritis
TLR	Toll-like receptor

ABSTRACT

Osteoarthritis (OA) is prevalent in equine and can be career-ending for performance horses due to lameness limitations and decreased quality of life. OA is a progressive, multifactorial disease that compromises the synovial joints' normal function, resulting in subchondral bone and articular cartilage deterioration over time. OA is a complex disease that impacts the entire joint, wherein activation of the innate immune system has an essential role in the disease progression and the development of pain. The synovial membrane, or the synovium, is a crucial contributor to the inflammation of diseased joints, regardless of the intra-articular tissue type initially affected. Synoviocytes are a predominant cell type of the synovium and contribute to inflammation by releasing key mediators and degradative enzymes, such as interleukin (IL)-6, IL-1β, a disintegrin, and metalloproteinase (ADAM) domains, and matrix metalloproteinases (MMPs). The production of pro-inflammatory molecules sequentially influences the expression of degradative enzymes and cartilage destruction. Therefore, the pathophysiological processes within synovial joints afflicted by OA can be further understood by studying the characteristics of synoviocytes.

We aimed to investigate the inflammatory component of OA in an *in vitro* model using a primary cell line of equine fibroblast-like synoviocytes (eqFLS) stimulated with tumor necrosis factor-alpha (TNF-α) to represent an initial inflammatory stimulus. Our studies have shown that stimulating eqFLS with TNF-α for 24 hours significantly increased the gene expression of pro-inflammatory biomarkers. Among several pro-inflammatory candidate genes assayed, only pro-inflammatory cytokine IL-6 gene expression could be detected reproducibly following stimulation with the TNF-α gene in eqFLS. We characterized the pro-inflammatory response of eqFLS and utilized this system to examine the impact of novel therapeutic compounds designed *in-silico* with the goal of reducing the inflammatory response of eqFLS. A piperazine-based compound (C3) and its derivative (02-09) were primarily designed to mimic the interactions of the growth factor pigment epithelium-derived factor (PEDF) with its receptor, the non-integrin laminin receptor 1 (LAMR1). Based on previous *in vitro* studies in the laboratory, C3 and 02-09 had been proposed to have a strong potential for inhibiting inflammation while reducing angiogenesis and chondrocyte hypertrophy. The efficacy of these two novel compounds on eqFLS was examined in the present work by assessing the gene expression levels of inflammatory biomarkers, including

IL-6, IL-1β, IL-8, ADAMs, and MMPs relative to a control housekeeping gene, glyceraldehyde 3-phosphate dehydrogenase (GAPDH) in various study designs. An *in-vitro* screen with the IL-1β promoter driving a reporter green fluorescent protein (GFP) was also designed to detect and track the inflammatory response of eqFLS by imaging following stimulation with or without (+/-) TNF-α relative to controls. This screen will be utilized in future studies to potentially identify more effective compounds in the LAMR1-interacting series. The current findings suggest that the novel compounds, especially 02-09, might exhibit an anti-inflammatory effect on eqFLS; therefore, it is a potential therapeutic agent in modulating inflammation during OA development.

CHAPTER 1. INTRODUCTION

1.1 Impact of osteoarthritis (OA) in the equine industry

The equine industry encompasses diverse occupations comprised of sport, work, and leisure and considerably impacts the United States (U.S.) economy. A study conducted by the American Horse Council (2018) determined that the equine industry has an annual economic impact of $38.8 billion in the U.S. and a total contribution of more than $101.5 billion to the gross domestic product (GDP) (Lord, 2019). Over 7.1 million people in the U.S. participate in the industry as owners, volunteers, service providers (e.g., farriers or veterinarians), employees, or spectators, with an equine population greater than 7.2 million (Lord, 2019). Few diseases have been identified to affect the horse regardless of breed, age, management, or purpose of use (United States Department of Agriculture, 2000). However, the deteriorating joint disease osteoarthritis (OA) has shown adverse effects on all types of horses and raises much concern in the equine industry.

Horses are commonly withdrawn from their occupational roles, or their primary use permanently changes due to OA diagnosis, thus causing considerable economic losses within the equine industry (United States Department of Agriculture, 2000). For instance, there is a correlation between a horse's economic value and its 'soundness,' i.e., the absence of clinical signs of illness or lameness (Lord, 2019). A horse lacking performance ability would have a reduced functional life, ultimately decreasing its economic value. There are indirect and direct costs in interventions targeting OA. OA's direct expenses commonly consist of diagnostic and treatment fees charged by the veterinarian practitioner, and indirect costs might include loss of income and increased efforts by the owner to maintain the needs of their diagnosed horse (Oke et al., 2010). For instance, one year of direct medical costs can exceed $3,000 per horse, with indirect costs estimated at $15,000 per year (Oke et al., 2010). Considering the direct and indirect costs necessary to treat a horse diagnosed with OA, it is evident that OA has a significant impact on the equine industry and the horse's overall well-being and economic value.

An example of how OA can place a substantial burden on the equine industry includes a study from Great Britain that indicated OA could affect at least 13.9 % of an equine population examined (Ireland et al., 2013). This study provided valuable information regarding the prevalence of chronic musculoskeletal disorders and the importance of identifying clinical signs and risk factors in the prevention and/or treatment strategies for these disorders (Ireland et al., 2013). The apparent clinical sign of lameness, i.e., abnormality of movement, is the initial reason horses are examined for an underlying issue, such as OA (Caron & Genovese, 2003; United States Department of Agriculture, 2000). At least 60% of the lameness caseload is associated with OA, according to questionnaire responses of 14 members of the American Association of Equine Practitioners, who reported treating an estimated 17,000 horses annually (Caron & Genovese, 2003).

OA can be detected by other indicators, including but not limited to the presence of cartilage lesions. Cartilage (or chondral) lesions can be visualized in the joint space by utilizing specialized imaging modalities (i.e., computed tomography (CT)) (Myller et al., 2019). Most lesions may cause changes in the biomechanical response of articular cartilage, indicating an elevated risk for tissue degeneration (Myller et al., 2019). Moreover, cartilage lesions often result in further degeneration of articular cartilage without medical intervention, thus leading to OA progression (Kajabi et al., 2021). For reference, a study of 50 Thoroughbred racehorses deceased of natural causes or euthanized after 60 days of racing identified that 33% of the 2- and 3-year-old horses examined had at least one detectable cartilage lesion in the metacarpophalangeal joint (Neundorf et al., 2010). This study concluded that young equine athletes (less than three years of age) are more susceptible to musculoskeletal injury and the potential development of OA and are more likely to undergo career limitations (Neundorf et al., 2010). Although age and gender (male) were the factors that correlated the most with OA progression, conclusions from this study were limited by its relatively small (~0.3) correlation coefficients, consistent with the small population size (Neundorf et al., 2010). The burden of OA within the equine population has been reflected in the literature and several studies; however, limitations remain in developing an equine model that demonstrates both clinical and morphological evidence of OA-associated changes. Thus, characterizing OA joint disease in equine and understanding its translational factors to human medicine via experimental models has been of interest in defining targets for therapeutic interventions (Bertoni et al., 2020; McIlwraith et al., 2012).

1.2 OA joint disease characterization and its diagnosis

OA is a multifactorial, chronic degenerative arthritis disease that impacts the mobility of synovial joints of many species, such as humans and horses. OA has traditionally been deemed a "wear and tear" disease of the articular cartilage and subchondral bone. However, it is recently considered a whole-joint disease, with all joint tissues contributing to its symptoms (Hsia et al., 2017). The most encompassing definition considers OA a group of related diseases with unique etiologies but similar morphologic, biologic, and clinical outcomes of joint destruction comprising the entire joint (McIlwraith et al., 2012; Sokolove & Lepus, 2013). Many studies have supported that all tissues undergo alterations at some point during disease progression due to shifts in joint homeostasis – even though controversy remains on which tissues play a role in the early and later stages of the disease (Heinegård & Saxne, 2011; Scanzello & Goldring, 2012; Sokolove & Lepus, 2013; Suri & Walsh, 2012). In general, tissues in an OA-affected joint progressively undergo structural and biological changes that alter the joint's primary function – smooth, frictionless movement (van Weeren, 2016).

Humans are commonly diagnosed with OA due to symptoms of pain, swelling, stiffness, loss of flexibility and mobility, grating sensations, and formation of bone spurs in the joint (Guillemin et al., 2019; Hunter et al., 2009). Joint swelling and pain can result from inflammation, another common sign of OA, as it promotes increased amounts of synovial fluid in the joint space, which can cause evident protrusions of the joint (Manzano et al., 2015). OA-associated pain has been identified in two distinctive ways – severe erratic pain and tenacious 'background' aching pain – and many people living with knee and hip OA described it as unpredictable nociceptive pain (Hawker et al., 2008). Even though joint stiffness and pain are commonly associated with early OA development, articular cartilage degeneration and subchondral bone alterations commonly occur before any intervention, resulting in irreversible damage to the joint (Hawker et al., 2008). Furthermore, whereas some limitations remain in studying human OA, recent studies have recognized the horse as a suitable model for human OA. There is much clinical effort with OA in horses, and experimental approaches provide a predictable OA model that can help define targets for therapeutic approaches (McIlwraith et al., 2012). Generally, the joint of a horse is comparable to that of a human due to the thickness, mechanical properties, and structure of equine articular cartilage, for example (Bertoni et al., 2020). Horse models of OA can provide

insight into OA pathobiological events. Understanding how the disease is detected and treated in horses is essential for better detection and treatment of the condition in humans.

The change in a horse's behavior or conformation (i.e., evaluation of the bone structure, musculature, and body proportions) often indicates an OA-associated problem (Ross, 2003b). Conformational defects are commonly associated with lameness, and veterinarians are often asked to comment on a horse's conformation during examinations to ensure a horse is sound for an intended use (Ross, 2003b). Moreover, specific gait characteristics, the degree of lameness, and palpation findings allow a veterinarian to suspect the development of a disease like OA unless the disease has advanced into later stages (Ross, 2003b). Some findings during palpation examination of a horse with suspected OA might include joint deformation and stiffening, as well as increased temperature and swelling of the affected area (Martig et al., 2020; McIlwraith et al., 2012; Olive et al., 2014) . Even though physical examination reveals the clinical signs of OA, many detectable lesions develop later, generally after joint deterioration is already initiated. Thus, further validated diagnostic methods are necessary to detect OA in its initial stages to prevent joint deterioration.

Several diagnostic imaging methods are utilized in veterinary medicine to detect and track the development of OA in equine. Detection methods include, but are not limited to, radiography (Dyson, 2003), ultrasonography (De Lasalle et al., 2016), computed tomography (CT) (Lee et al., 2021; Nelson et al., 2021), magnetic resonance imaging (MRI) (Kajabi et al., 2021), and arthroscopic evaluation (Cohen et al., 2009). Interpretation of these imaging findings can be complicated and must be evaluated appropriately and comprehensively (Dyson, 2003). Moreover, combining these imaging modalities can assist in evaluating normal tissue from degenerative tissue, considering that each method is distinctive in how it detects and localizes abnormal tissue structures within a potentially OA-affected joint.

Radiography, for instance, has the vital role of providing information about the bones that are comprised in the joint (Dyson, 2003). Joint space reduction or fractured bones can be detected under radiography; however, this method is remarkably insensitive to pathologic features of OA's initial stages. The absence of radiographic findings should not be interpreted as a lack of disease within the joint space, considering its primary function is to confirm the presence of OA and

eliminate other possible conditions (Dyson, 2003; Ley et al., 2014). Gray-scale ultrasonography is considered standard for examining soft tissue alterations (e.g., ligaments, tendons, joint capsule) during OA development. However, this modality provides morphological information rather than a precise measurement of tissue strain (Lustgarten et al., 2014). An advancement in this modality, elastography, measures tissue stiffness and evaluates mechanical properties and is considered a noninvasive "stall-side" imaging modality for evaluating potential OA-affected joints (Straticò et al., 2021). CT, or contrast-enhanced CT (CECT), has been a promising imaging technique in recent years due to its wide availability and shorter acquisition times during evaluation (Nelson et al., 2021). The state of normal and degenerative articular cartilage can be reflected by utilizing CECT due to its ability to exploit the high-level extracellular matrix negative charges using cationic contrast agents (Joshi et al., 2009; Nelson et al., 2021). Data collected from CT can also be used for biomechanical three-dimensional and functional anatomical modeling, which can characterize equine conformation associated with changes in tissue integrity during OA progression (Lee et al., 2021). Nevertheless, radiography, ultrasonography, and CT cannot evaluate both subchondral bone and articular cartilage independently; thus, MRI imaging is often utilized to overcome some limitations in recognizing tissue alterations due to OA (Bertoni et al., 2020).

The main features detected by MRI include ligament and tendon injuries, fractures, subchondral bone remodeling, and articular cartilage defects that appear as a cross-sectional and three-dimensional evaluation plane (Bertoni et al., 2020). MRI imaging is sensitive to subtle changes within these structures; however, its most significant disadvantages are its expense, the potential anesthesia requirement, and limitations on what can be placed within the magnetic field for imaging (Roemer et al., 2020; Whitton et al., 2003). The other mentioned detection method is arthroscopic evaluation, which remains the gold standard for detecting changes in articular cartilage and other soft tissues (e.g., synovium, menisci, ligaments) in OA-affected joints (Ross, 2003a). However, arthroscopic evaluation has limitations in detecting subchondral bone and accessing all joint structure regions compared to CT and MRI. Beyond discussed methods, other modalities are available for clinically diagnosing OA, and recent advances in developing biomarkers for therapeutic approaches have taken place. Ultimately, using an equine model of OA

furthers our understanding of the progression of this condition and better defines targets for therapeutic intervention that are translatable to human medicine.

1.3 High-impact joint loading in the development of OA

Performance horses are more prone to developing OA due to the extensive and intensive exercise demands of training and competitive events. Several loading profiles have been defined during physical activities in horses (i.e., walking, trotting, galloping, and jumping) (Byström et al., 2021; Johnson & Symons, 2019; Parsons et al., 2011). For example, Thoroughbred racehorses perform by galloping with maximum speed around a controlled track, or Warmblood showjumpers perform by jumping over obstacles within a show arena. Both athletic performances increase extensive, recurrent load and stress, particularly on the forelimb joints. Forelimbs receive the load from landing and are more weight-bearing as a horse's center of gravity is closer to the forelimbs relative to the hindlimbs (Ross, 2003b). Lameness is commonly found on the forelimbs, with the forelimb/hindlimb weight load distribution being close to 60:40% (Ross, 2003b). It has been demonstrated previously that a horse with forelimb lameness would compensate for its loading from the lame forelimb to the diagonal hindlimb to shift the load to a limb that can withstand the additional stress (Weishaupt et al., 2006). However, more recent studies have provided significant evidence that forelimb lameness promotes compensatory load distribution in contralateral hindlimbs during trotting, indicating that an actual lame limb can be determined on a diagonal axis (Maliye et al., 2015; Uhlir et al., 1997). The abnormal motion of the head can be seen during diagnostic evaluations of a horse undergoing forelimb lameness (Buchner et al. 1996). Even though forelimb lameness is more common among performance horses, hindlimb lameness is still of much concern in the equine industry, especially considering that it enhances the difficulty in detecting and diagnosing OA (Leelamankong et al., 2020). Horses experiencing hindlimb lameness are often evaluated for an abnormal motion of the pelvic region – the examiner would evaluate the amplitude of vertical or rotational movement of the tuber coxae and compare its motion to the opposing pelvic region (Kramer et al. 2000; Kramer et al. 2004). A horse undergoing hindlimb lameness may use abnormal pelvis rotations when landing on a lame limb, like a horse may use its head to compensate for forelimb lameness. Overall, conformational traits of a lame horse become evident due to the shift in load distribution, which may aid in diagnosing the initial cause of the lame limb (Ross, 2003a).

Approximately 95% of lameness issues of the forelimb occur distal to the carpus, i.e., "knee," and should be examined prior to the upper limb when excluding potential sources of lameness (Ross, 2003b). Joints of the forelimb include the metacarpophalangeal (MCP), proximal, and distal interphalangeal joint, antebrachiocarpal, middle carpal, and carpometacarpal joints. These joints are dynamic load-bearing structures comprised of elastic biomaterial (cartilage and tendons/ligaments) and a specialized lubricant (synovial fluid). These joints are commonly exposed to low-level continuous loading in weight-bearing activities, recurrent loading during movement, and elevated and abrupt loading while training or competing in events (Harrison et al., 2014; Hyttinen et al., 2009). Overall, the excessive amount of high-impact load on synovial joints due to galloping or jumping, for instance, is generally a common contributor to OA development and its resulting pain (i.e., lameness) (Boyce et al., 2013; Harrison et al., 2010). OA that develops because of an initial trauma to the joint is commonly deemed post-traumatic osteoarthritis (PTOA). High-impact joint loading, or trauma, makes performance horses more predisposed to developing PTOA at a young age, potentially ending the careers of many horses, and it can be life-threatening to some (Bailey et al., 1999)

In recent years, much knowledge has been gained relative to PTOA pathogenesis with *in vivo* models, human subjects, and *in vitro* studies using tissues isolated from animal and human sources (Kramer et al., 2011). Moreover, many studies have found that the pathological changes that occur after joint trauma in equine are translatable to humans (Frisbie et al., 2006) as well as to a variety of other mammalian species (Kim et al., 2018; Martin et al., 2017). Regardless of the species or the type of trauma initiating PTOA (i.e., single acute traumatic loads or repetitive overloading), an imbalance is formed between the joint load being applied and how the tissues within the joint absorb the load (Harrison et al., 2010; Shaktivesh et al., 2020). Joint instability leads to increased degeneration of the articular cartilage, changes in soft tissue composition, and subchondral bone alterations (Li et al., 2013; Simmons et al., 1999). The normal function of chondrocytes, cells of the articular cartilage, is disrupted due to the imbalance of load within an OA-affected joint (Novakofski et al., 2014). Past studies have reported that disruption to the collagen network and proteoglycan content of cartilage can increase strain within the joint space, contributing to the loss of tissue structure and integrity (Myller et al., 2019). The articular cartilage cannot undergo repair processes to preserve its structure under strain, resulting in chondrocyte loss

of viability and cartilage extracellular matrix (ECM) degradation (Martel-Pelletier et al., 2008; Novakofski et al., 2014). The primary simultaneous degeneration of articular cartilage and subchondral bone generally leads to ongoing damage to the articular cartilage due to a loss of structural support in the joint or the release of inflammatory cytokines, which may accelerate OA progression (McCoy et al., 2020; van Weeren, 2016). Subsequently, high-impact joint loading results in a cascade of events that ultimately lead to histological, clinical, and radiographic signs of OA (Kramer et al., 2011) – understanding how normal tissue components function is critical for elucidating how abnormalities may predispose the joint to OA development.

1.4 Components and functions of a healthy joint

1.4.1 General synovial joint structure

Synovial or diarthrodial joints are elaborate structures that allow maximal movement. They are composed of specialized tissues, i.e., articular cartilage, synovial membranes, articular capsule, ligaments, menisci, and subchondral bone, organized into reciprocally positioned subchondral bone covered by articular cartilage, which is stabilized by intra- and extra-joint ligaments and insulated by a synovial membrane and a thick surrounding articular capsule filled with synovial fluid (Figure 1.1) (Zhang et al., 2015). The unique organization of the joint allows for locomotion, requiring joints to have smooth surfaces for articulation and resilience for absorbing load (van Weeren, 2016). It is challenging to accommodate these functions within a single, complex structure; thus, any malfunction within the structure or in its biomechanical properties may lead to disease development, such as OA (van Weeren, 2016). The general structure of a synovial joint is translatable across a range of mammalian species (e.g., human, equine, canine, feline, bovine, mice), which is beneficial in studying the interactions among tissue types among diverse animal models (Bendele, 2001; Boyce et al., 2013; Kim et al., 2018). Consequently, understanding the general structure of synovial joints and their constituents is vital in identifying abnormalities within the joint – the deterioration of articular cartilage, formation of osteophytes, or inflammation within the synovium – all of which occur during OA development. The specialized tissue constituents comprised in a synovial joint are discussed next in this section.

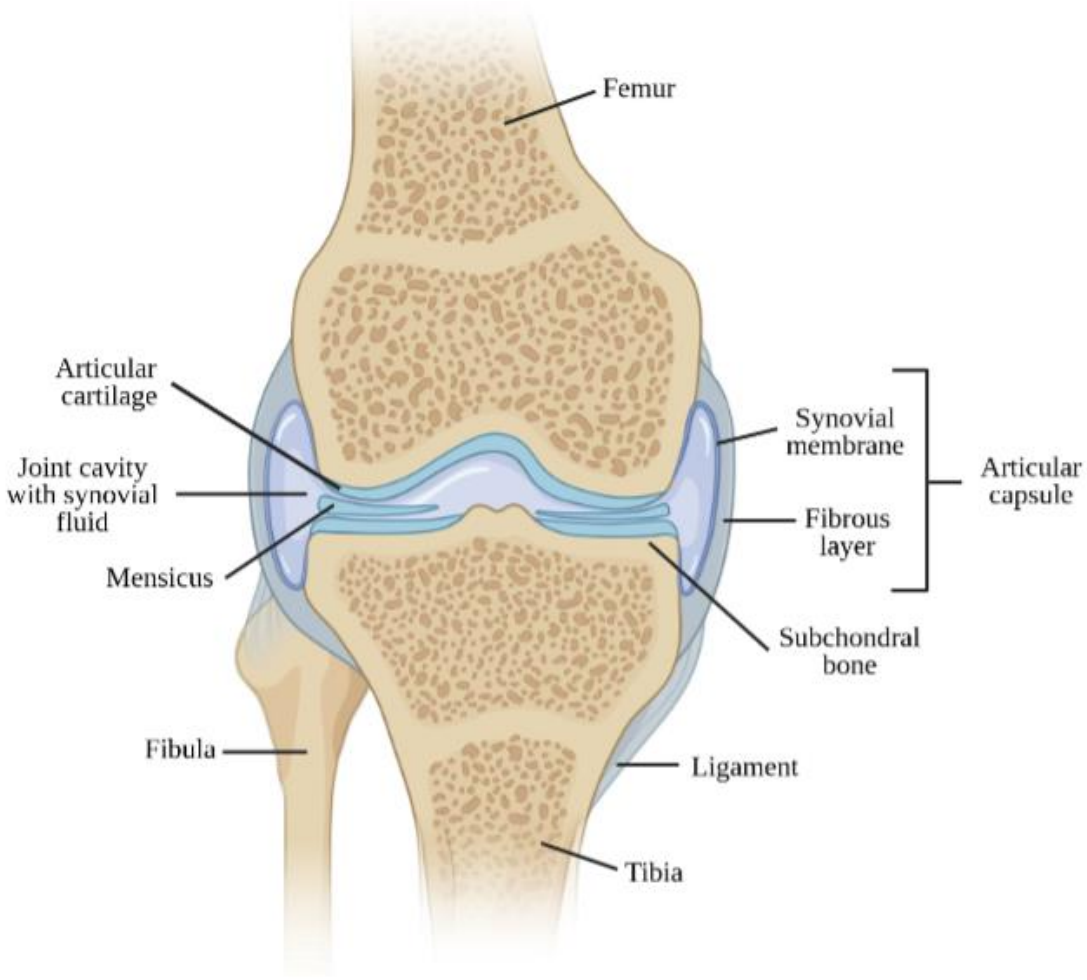

Figure 1.1 Generalized structure of the synovial knee joint. The synovial joint comprises articular cartilage, synovial membrane, intra- and extra-articular joint ligaments (not shown), articular capsule, and subchondral bone, organized into a specialized structure that enables movement and transfers load to prevent fracture to the bone. Diagram modified from Zhang et al., 2015 and created in BioRender.com

1.4.2 Articular cartilage

The articular cartilage is a complex, thin layer of specialized hyaline cartilage covering the ends of articulating bones in the joint. The specialized tissue provides cushion and support for movement and articulation, enabling the transmission of loads (Riemenschneider et al., 2019) while maintaining low friction (McNary et al., 2012) and wear properties (Estell et al., 2021). Articular cartilage has traditionally been considered a non-regenerative organ as it lacks nerves, blood vessels, and lymphatics, thus relying on diffusion for its nutritional supply. However, some research challenges this view due to the likely stem cell-like properties of the superficial zone (Karlsson & Lindahl, 2009). The outer surface of the articular cartilage is attached to a transitional

layer of collagen fibers that transitions into calcified cartilage once it reaches the underlying subchondral bone (Amundsen, 2007). It comprises specialized chondrocytes within a dense extracellular matrix (ECM) – a meshwork of dynamically interconnected macromolecules. Major ECM components are type I and II collagen, proteoglycans (PGs), water, and non-collagenous proteins and glycoproteins (i.e., protein core and glycosaminoglycans) (Karamanos, 2019). About 70-80% of the ECM is aqueous, along with other components, such as collagen, accounting for ~50%, and PGs, accounting for ~ 35% of the ECM dry weight (van Weeren, 2016). The remaining structure includes glycoproteins and other minor components (i.e., minerals, lipids, and cellular components) (Karamanos, 2019; van Weeren, 2016). All components of the ECM are intricately arranged to provide elastic support of articular cartilage for dispersing pressure and stress with joint movement (Becerra et al., 2010). The structure of articular cartilage at a macroscopic level seems homogeneous. However, it is depth-dependent, and changes occur in the collagen architecture as the cartilage surface transitions towards the subchondral bone (Guilak et al., 1994). The structure comprises four zones: the superficial zone, the intermediate (or middle) zone, the deep zone, and the calcified zone – all varying in composition and interactions with other surrounding tissues (Antons et al., 2018). The unique zoning of articular cartilage allows it to absorb moderate mechanical loading; however, overloading may cause ECM composition changes, promoting articular cartilage destruction and potentially triggering OA development (Musumeci, 2016). With pathological conditions such as OA, the physiological balance of anabolic and catabolic processes shifts resulting in an imbalance between chondrocytes breaking down ECM constituents and synthesizing new matrix components (Ströbel et al., 2010), thus promoting the deterioration of articular cartilage.

1.4.3 Synovial membrane

The synovial membrane, or synovium, is a soft tissue lining that envelops the joint, surrounds tendon sheaths, and shapes the bursae lining (Smith et al., 2003; van Weeren, 2016). The synovium comprises 2-3 layers of specialized cells, called synoviocytes, with underlying loose connective tissue consisting of collagen, blood vessels, and adipose cells (O'Connell, 2000; Smith et al., 2003). The essential role of the synovium is to contribute to the synovial fluid composition and maintain joint homeostasis (Levick & McDonald, 1995). The synovium is essentially a semi-permeable membrane that facilitates the diffusion of lubricants (hyaluronic acid,

lubricin) secreted by synoviocyte lining cells from the synovial ECM towards synovial fluid (Kiener et al., 2010). The synovium interacts with the underlying articular cartilage where the tissue folds within the joint space; thus, the articular cartilage and synovium interact to maintain the joint's homeostasis (Bhattaram & Chandrasekharan, 2017; Estell et al., 2021). The normal synovium is distinctive from other barrier membranes. It is comprised of two layers, a subintima (an outer layer) and a continuous surface layer of cells known as the intima (an inner layer) (Smith, 2011). The subintima is comprised of multiple tissue types, such as fibrous (dense collagenous type), adipose, or areolar (loose collagenous type), and is primarily made up of type I and IV collagen with blood vessels, nerve fibers, and lymphatics (Smith, 2011; Stefani et al., 2019). The intima of the synovium is positioned next to the joint cavity. It is comprised of 2-3 layers of synoviocytes, a dominant cell population proposed to produce synovial fluid constituents, absorb fluid from the joint cavity, and perform fluid exchange (Kiener et al., 2010; O'Connell, 2000; Stefani et al., 2019).

Two types of synoviocytes are found within the intima layer of the synovium, macrophage-like (type A or MLS) and fibroblast-like (type B or FLS), with ~90% being FLS and 10% MLS (Stefani et al., 2019; Valencia et al., 2004). MLS have similar characteristics to the macrophage lineage with phagocytic activity and antigen-presenting ability (Bondeson et al., 2006; van Weeren, 2016). FLS produces lubricating constituents (e.g., lubricin, HA) of synovial fluid to aid in protecting the joint from wear and tear and maintaining its typical structure (Antonacci et al., 2012; Elsaid et al., 2005). Due to their residency within the intimal layer, FLS are directly exposed to the mechanical load distribution between the synovium and articular cartilage, and any abnormal load during locomotion may stimulate FLS (Estell et al., 2017; Rattner et al., 2010; Tetsunaga et al. 2011). Moreover, FLS are mechanosensitive, giving them the ability to respond to shear stresses and initiate a cascade of inflammatory cytokines, often contributing to OA progression (Estell et al., 2017). Similarly, frictional interactions between tissues in direct contact with the synovium may provide mechanical stimuli to synovium resident cells (e.g., FLS) (Estell et al., 2021). Thus, frictional interactions in the synovium may trigger the initiation of pro-inflammatory and destructive mediators, which are of great interest in identifying symptoms of OA and studying its progression.

1.4.4 Subchondral bone

The subchondral bone is a supportive structure for the articular cartilage present at synovial joints. The primary role of subchondral bone is to biomechanically attenuate the forces generated by movement and physical activity (van Weeren, 2016). Subchondral bone is typically compact bone positioned adjacent to the calcified articular cartilage and trabecular bone (van Weeren, 2016). The subchondral bone and articular cartilage can function as a single unit since they converge at the osteochondral junction in the joint space, consisting of the calcified cartilage zone and underlying subchondral plate (Lories & Luyten, 2011). Subchondral bone mechanically supports the articular cartilage during locomotion and undergoes modeling and remodeling as it adapts to joint loading (Lories & Luyten, 2011; Madry et al., 2010). The subchondral bone plate and the trabecular bone are two distinctive anatomic units that comprise the subchondral bone (van Weeren, 2016). Mechanical consequences arise with this arrangement considering that the subchondral bone plate provides rigidity support while enabling some flexibility and elasticity from the trabecular component (Lyons et al., 2006). Supportive trabeculae arise from the subchondral bone plate which typically performs shock-absorbing functions and may also contribute to the metabolic needs of the overlying articular cartilage (Brama et al., 2001; Zarka et al., 2019). The biochemical communication between the articular cartilage and the subchondral bone is accomplished by diffusion of small molecules (e.g., growth factors and cytokines) through the calcified cartilage (Pan et al., 2009). The properties of subchondral bone are modified by a cell-mediated balance (i.e., osteoblasts, osteocytes, and osteoclasts) of modeling and remodeling bone tissue. This mechanism may be altered during OA progression, resulting in excessive remodeling and potentially priming the tissue towards bone sclerosis (osteoid deposition) (Li et al., 2019), chondroplastic lesions (Myller et al., 2019), or gross fracture (Zarka et al., 2019). However, some studies hypothesize that bone sclerosis may precede cartilage degradation and loss (Lajeunesse, 2004).

1.4.5 Other soft tissues

Synovial joints comprise other soft tissues, including the articular or joint capsule, ligaments, and menisci. The articular capsule comprises an outer layer (fibrous tissue) and an inner layer, the synovium. This thin, fibrous connective tissue of the outer layer is fastened to extra-

articular structures, i.e., collateral ligaments and epiphyses of the subchondral bone, to structurally support locomotion by keeping bones in their proper positions within the joint (van Weeren, 2016). The articular capsule has several proprioceptive nerve endings that provide information to the brain about joint position and movement (van Weeren, 2016). Intra- and extra-articular ligaments, i.e., anterior cruciate ligament and collateral ligaments, are bands of dense regular connective tissue (collagen type I) that thicken from the articular capsule and stretch the length of the joint to reinforce the articular capsule, limiting movement of the joint (Amundsen, 2007; Beynnon et al., 2020; Wu et al., 2015). Both the articular capsule and ligaments stiffen with age due to increased crosslinks in collagen fibers and decreased proportion of elastic fibers, impacting the quality of movement of the joint (Amundsen, 2007). Another soft tissue important in this context is the articular meniscus, which extends from the articular capsule residing in the synovial joint cavity and consists mainly of a network of collagen fibers (collagen type I), meniscal cells, and ECM (Ribitsch et al., 2018). The collagen fibers of the menisci are arranged in distinctive layers – a thin meshwork of fibrils on the surface, a lamellar layer with outwardly facing fibrils, and a middle layer of circular fibril bundles interconnected with radial bundles (Petersen & Tillmann, 1998; Ribitsch et al., 2018). This intrinsic arrangement is vital for joint biomechanics (e.g., absorbing shock and distributing loads), enhancing stability, and lubricating the articular cartilage surfaces (Fox et al., 2012). Regarding OA joint disease, the articular capsule, in particular, can become stiffer with its progression due to an increasing crosslink formation in collagen fibers, which impacts the joint's quality of movement (Noble et al., 2010). Any insult to soft tissue structures is associated with an increased risk of OA, as the degenerative changes alter homeostasis and contribute to joint instability (Ribitsch et al., 2018). Moreover, there are many soft tissues within the joint, not limited to what has been mentioned in this section, which contributes to the support and articulation of the joint as they indirectly and directly interact with surrounding tissues (i.e., subchondral bone, articular cartilage).

1.4.6 Potential alterations with disease

Synovial joints comprise many specialized tissues, each of which plays a vital role in maintaining the structure and function of the joint. An imbalance in the structural or mechanical aspect of the joint often contributes to the development of conditions like OA. Since OA is a complex condition that comprises the whole joint, the disturbances in physiological relationships

and crosstalk between the tissues are incompletely understood during disease progression. Recent research has unraveled several potential mechanisms in OA's progression, which arise from modifications in joint homeostasis and tissues that interact within the joint space.

1.5 Alteration of joint homeostasis during OA

1.5.1 Potential development of OA

OA often develops following imbalances or shifts in biological and mechanical events that disrupt the normal function of synovial joints, which result in articular cartilage degradation and subchondral bone remodeling. Other alterations that have been observed in OA-affected joints are osteophyte formation, articular capsule thickening with altered peri-articular ligaments and peripheral muscle structure, as well as synovium inflammation (Blom et al., 2004; Nair et al., 2012; Ribitsch et al., 2018). These alterations have been described in various *in vivo* and *in vitro* (cells and tissues) models; thus, OA effects are translatable amongst a variety of models (Kim et al., 2018; Lampropoulou-Adamidou et al., 2014). To date, no models fully mimic the initiation and timeline of OA due to the multi-factorial complexity of the disease that involves the abnormal cross-talk among the tissues in the joint space (Blom et al., 2004; Hayami et al., 2006; Nair et al., 2012). Furthermore, although OA is deemed a disease of the entire joint, many studies focus on a subset or specialized tissue that may participate in the maintenance of joint homeostasis. For example, studies may focus on the articular cartilage, the synovium, and/or the subchondral bone and a better understanding of how they potentially interact and/or individually contribute to OA progression.

1.5.2 Articular cartilage

In a healthy joint, the articular cartilage typically is maintained by a certain degree of natural biomechanical stresses (Antons et al., 2018; Li et al., 2021). However, abnormal stresses may lead to alterations in the articular cartilage’s composition and mechanical properties. For example, the articular cartilage undergoes alterations in the early stages of OA, often initiated by direct, prolonged loading to the synovial joint (Setton et al., 1999). The initial alterations in articular cartilage composition have been characterized as due to loss of proteoglycan (PG) content, disruption of type II collagen fiber content and orientation within the ECM, and the imbalance of

interstitial water content (Hada et al., 2014; Mäkelä et al., 2015). These alterations cause articular cartilage to lose its biomechanical properties (e.g., resilience) and increase its permeability, thus, decreasing its overall structure and stiffness (Mäkelä et al., 2015; Nissinen et al., 2021). Particularly, articular chondrocytes lose the capacity to synthesize new PGs to replace those lost, proliferate, and respond to catabolic and anabolic stimuli. An imbalance between catabolic factors (pro-inflammatory mediators, apoptosis, and degradative enzymes) and anabolic factors (growth factors, enzyme inhibitors, bone morphogenic proteins) leads to ongoing loss and destruction of ECM of the articular cartilage (Alvarez et al., 2014; Sato et al., 2006; Wu et al., 2007). Hence, the cartilage homeostasis is disturbed by an imbalance between the synthesis and degradation of ECM macromolecules, resulting in further degeneration of articular cartilage. The articular cartilage becomes roughened with continued degeneration, causing fissuring and fibrillation that expands through the distinct cartilage zones until reaching the subchondral bone (Faisal et al., 2019; Korhonen et al., 2003). Fibrillation of the articular cartilage changes its mechanical properties, and frictional interactions between the articular cartilage and subchondral bone continue to increase as the tissue degenerates (Estell et al., 2021; Sadeghi et al., 2015). The frictional interactions in areas of direct contact stimulate cells in surrounding tissues due to the generation of cartilage wear particles or endogenous damage-associated molecular patterns (DAMPs) (Estell et al., 2021; Rosenberg et al., 2017). DAMPs originate from ECM degradation (collagen type II, fibronectin fragments), and these products activate both systemic and local inflammation, leading to the secretion of catabolic factors that can cause further damage to the articular cartilage (Rosenberg et al., 2017). The DAMPs are released into the synovial fluid as articular cartilage continues to deteriorate and attach to the synovium, stimulating pro-inflammatory signaling in synovial cells (Estell et al., 2019; Estell et al., 2021). An increase in the concentration of DAMPs within the joint space has been associated with OA pathogenesis (Rosenberg et al., 2017). Ultimately, deteriorating articular cartilage and its ability to promote pro-inflammatory responses in the synovium further contribute to OA's progression. This communication resembles the typical crosstalk among joint tissues but is modified toward the disease pathology (Estell et al., 2017).

1.5.3 Synovial membrane

The articular cartilage and synovium cross-talk to maintain joint homeostasis in standard conditions; however, the effects of OA and how it alters the physiological relationship between

these tissues are incompletely understood (Chou et al., 2020). The cellular constituents of the synovium are somewhat heterogeneous, making it challenging to determine which cell type might be stimulated by the accumulating DAMPs or which mediates the various stages of OA development (Chou et al., 2020; Nair et al., 2012). However, recent evidence suggests that some synovial monocytic and fibroblastic cells (e.g., FLS) can be stimulated via mechanotransduction by the presence of the DAMPs and other wear particles from the deteriorating articular cartilage (Estell et al., 2019; Nair et al., 2012; Rosenberg et al., 2017). DAMPs are detected by a type of pattern recognition receptor (PRR) called toll-like receptor (TLR), located on the outer surface of selective synovium cells. The activation of TLR4, for example, can promote the activation of innate immune responses that consist of pro-inflammatory cytokine and matrix metalloproteinases (MMPs) secretion and the formation of additional DAMPs (Rosenberg et al., 2017). Specifically, TLR4 expression by FLS stimulates the nuclear factor kappa B (NF-κB) signaling cascade, resulting in downstream expression and secretion of IL-1β, TNF-α, and IL-6 (Rosenberg et al., 2017). The synovium inflates, and the imbalance between catabolic and anabolic systems further propagates tissue damage (Kim et al., 2006; Park et al., 2020). These effects can be reversed experimentally and pose an advantage in developing potential therapeutics. Synovium inflammation and its contribution to OA progression are discussed in more detail in Section 1.6.

1.5.4 Subchondral bone

Another alteration occurring in OA-affected joints is remodeling the subchondral bone, particularly in the area adjacent to where the articular cartilage suffered degeneration. Even though much controversy remains regarding the changes in subchondral bone in an OA-affected joint, it is argued that subchondral bone deterioration precedes changes in the articular cartilage (Wei & Bai, 2016; Ziemian et al., 2021). In order to increase stability in response to loading forces between subchondral bone and its neighboring tissues, osteophytes (Blom et al., 2004) and microcracks (Zarka et al., 2019) are formed. Osteophytes are osteocartilaginous outgrowths that usually develop where the synovium connects to the ends of the articular cartilage and combines with the periosteum of the bone. Although osteophyte formation may be an attempted repair mechanism to stabilize deteriorating tissues, it can cause adverse effects, such as loss of movement and pain sensations (Gelse et al., 2003; Zarka et al., 2019). Microcracks are also formed during abnormal joint loading (Burr et al., 1985) and allow the communication between the subchondral

bone and the articular cartilage – providing a stimulus for initiating bone remodeling (Pan et al., 2009; Zarka et al., 2019). During bone remodeling in the regions surrounding microcracks, the turnover of cells and matrix coincides with areas of osteoclastic resorption. In these areas, osteoclasts remove apoptotic osteocytes (Cardoso et al., 2009) and osteoblasts' infilling replaces regions of lost bone (Verborgt et al., 2000). Specifically, apoptotic osteocytes and their debris present cell surface signals (e.g., phosphatidylserine (Fadok & Henson, 2003)) that are used for target removal by osteoclasts (Cardoso et al., 2009; Kennedy et al., 2012). Microcrack formation offers a way for catabolic agents or other small molecules to cross the osteochondral junction and enables the diffusion of pro-inflammatory cytokines and growth factors (Jiang et al., 2021; Kennedy et al., 2012; Pan et al., 2009). Osteocytes stimulate osteoclast differentiation by the expression of cytokines such as RANKL (receptor activator of nuclear factor kappa-B ligand) (Boyce & Xing, 2007; Kennedy et al., 2012). It has been shown that RANKL is secreted from the non-apoptotic osteocytes neighboring the microcracks, not from the osteocytes undergoing apoptosis, and RANKL production is essential to bone remodeling during OA development (Kennedy et al., 2014). Moreover, the production of RANKL is controlled by osteoprotegerin (OPG), which is produced by osteogenic stromal stem cells and osteoblasts to prevent excessive bone resorption by binding to RANKL and blocking its interaction with RANK (receptor of RANKL) (Boyce & Xing, 2007). The RANKL/OPG ratio is essential in maintaining bone mass (Boyce & Xing, 2007), and its imbalance can contribute to further loss of subchondral bone during OA progression. Overall, deteriorating subchondral bone leads to the formation of osteophytes and microcracks in an attempt to stabilize the joint. However, osteophytes and microcracks may adversely impact joint function and further contribute to OA progression.

1.5.5 Mechanisms of action

The progression of OA in synovial joints is overly complex, and it remains challenging to unravel the disease's pathophysiology completely. OA development is complicated further due to the interactions among tissues of the entire joint, including the synovium, the articular cartilage, and the subchondral bone. Some interaction networks among these tissues are represented in Figure 1.2, which shows OA being initiated due to trauma to the joint space (McIlwraith 2013). After an initial trauma (either direct or indirect) to tissue, a network of biological events occurs, involving, but not limited to joint inflammation and articular cartilage degeneration. It is proposed

that the most effective therapeutic targets in treating OA's alterations would ideally reduce inflammation in the synovium, reduce degradation of joint tissues, or improve ECM synthesis to promote articular cartilage repair, shown in green in Figure 1.2 (Eskelinen et al. 2020; McIlwraith 2013). However, targeting an exact pathway in developing therapeutics can be challenging, considering that alterations in one tissue do not necessarily occur independently from the other tissue types in the joint space. OA's complexity makes the development of effective therapeutics a challenging prospect in both human and equine medicine. It is essential to continue discovering and understanding the alterations impacting normal joint homeostasis at an early stage of OA since these changes could potentially be reversed or utilized in developing therapeutic approaches toward the disease.

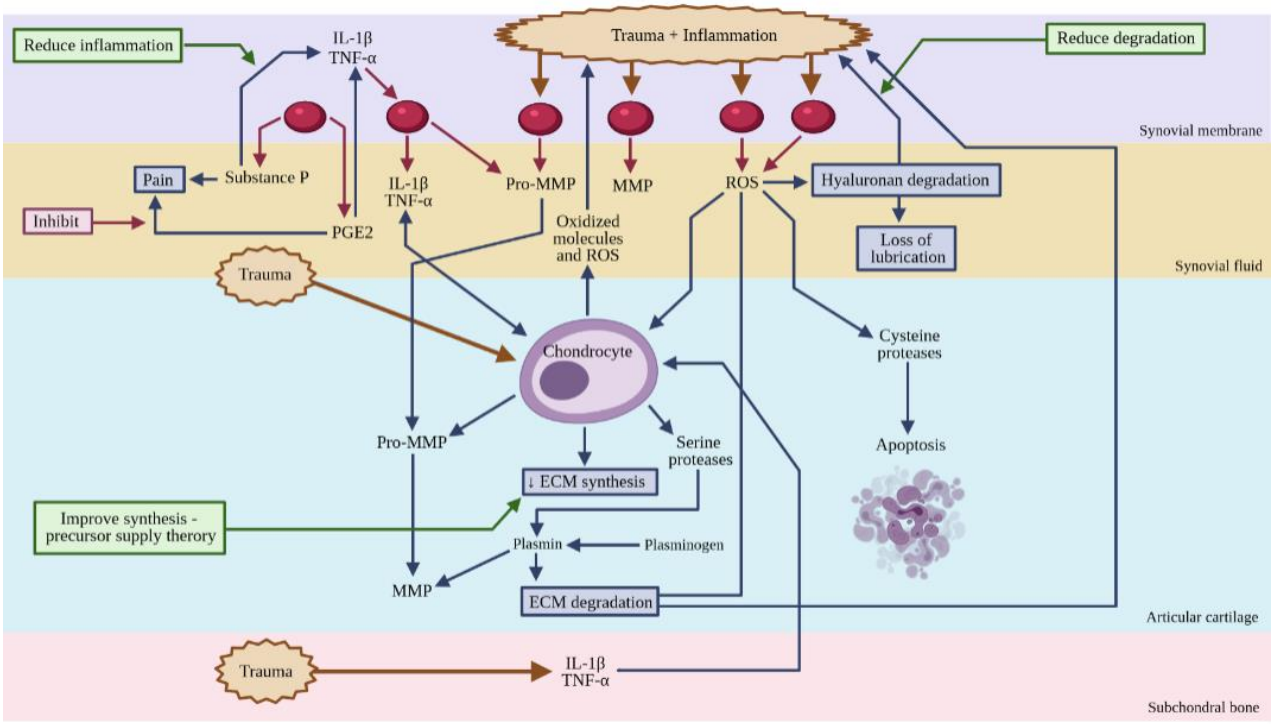

Figure 1.2 Mechanisms of OA development. Schematic outlining the interactions that occur among tissues during osteoarthritis development and the potential mechanisms of action (green) for supplementation or therapeutic interventions to alleviate these processes (e.g., reducing inflammation and cartilage degradation and improving ECM regeneration). Diagram modified from McIlwraith, 2013 and created in Biorender.com.

1.6 Synovium in the pathophysiology of OA

Non-cartilaginous tissues, like the synovium, have become of particular interest in studying the pathophysiology of OA. Early studies deemed OA as a disease predominantly of the articular cartilage and the subchondral bone; however, recent studies suggest that the synovium and its contribution to the inflammatory response are essential in the progression of OA (Bondeson et al., 2006; Harvanova et al., 2022; Huh et al., 2015). Synovial inflammation, clinically called synovitis, contributes to behavioral changes (i.e., production of inflammatory products) among resident synovial cells and neighboring chondrocytes (Bondeson et al., 2006; Ni et al., 2019). The gene expression changes in the synovium result in the secretion of pro-inflammatory cytokines and mediators, which can be identified in the early stages of OA, i.e., prior to macroscopic cartilage degeneration (Huang et al., 2018; Zhao, 2021; Zhu et al., 2012). It has been proposed that synovitis is induced initially by the degradation of ECM that produce cartilage breakdown products, such as DAMPs, following an imbalance between anabolism and catabolism of articular chondrocytes (Estell et al., 2019; Rosenberg et al., 2017). As mentioned in Section 1.5, these products initiate the release of proteolytic enzymes via transcription factor nuclear factor-κB (NF-κB) signaling, for example, and increase the secretion of pro-inflammatory cytokines and other mediators from stimulated FLS (Estell et al., 2019; Silverstein et al., 2017), followed by vascular hyperplasia and immune cell infiltration, contributing to synovial inflammation (synovitis) (Stefani et al., 2019). Thus, the inflammatory cascade initiated by the release of pro-inflammatory cytokines, such as IL-1α (Estell et al., 2017), from FLS causes chondrocytes to produce degradative enzymes, including the upregulation of discoidin domain receptor (DDR)-2 and MMP-13 expression, that further deteriorate articular cartilage and inhibit regeneration of the tissue (Huh et al., 2015; Zhao et al., 2014).

FLS have the primary function of maintaining joint homeostasis by sustaining the composition of both the ECM and synovial fluid (Jones et al., 2021; Thomsen et al., 2017). FLS maintain the synovial ECM by producing and secreting lubricating components of the synovial fluid, such as lubricin, hyaluronic acid, and a series of PGs (Blewis et al., 2010; Kiener et al., 2010). Lubricin, a glycoprotein encoded by the proteoglycan 4 gene, is considered a boundary lubricant and chondroprotective agent within synovial joints (Reesink et al., 2017; Rhee et al., 2005). Hyaluronic acid (HA), a non-sulfated glycosaminoglycan (GAG), facilitates

low-friction lubrication of articular cartilage and gives viscoelastic properties to synovial fluid, along with lubricin and other proteoglycans (e.g., heparan sulfate proteoglycan) (Fasanello et al., 2021; Rosenberg et al., 2017; Schröder et al., 2019). During OA progression, the average concentration of HA is reduced in synovial fluid, forming low-molecular-weight HA, reflecting pro-inflammatory attributes (Band et al., 2015). Also, there is an increase in the covalent crosslinking of HA monomers, adversely affecting the integrity of the articular cartilage (Fasanello et al., 2021). Lubricin regulation is not apparent during OA progression, as its levels have been shown to vary among animal and human models (Reesink et al., 2017; Watkins & Reesink, 2020). Various studies have reported either an increase or no change in lubricin during OA; however, a decrease in lubricin was reported 4 times more frequently (Watkins & Reesink, 2020). Moreover, the supportive (anabolic) role of FLS can be altered to a destructive (catabolic) role with exposure to the imbalances of HA and lubricin (Pap et al., 2020; Schröder et al., 2019). In this catabolic-inducing role, FLS produce diverse matrix-degrading enzymes (MMPs and ADAMs) and other growth factors and destructive tissue components (Pap et al., 2020). Major signaling pathways implicated in synovitis due to FLS involvement are NF-κB and mitogen-activated protein kinase (MAPK) (Huang et al., 2018; Pap et al., 2020). NF-κB is responsible for regulating the innate immune response and has been considered the "holy grail" target for the development of anti-inflammatory drugs (Choi et al., 2019; Haseeb & Haqqi, 2013). Inflammatory responses and other critical cellular functions (e.g., apoptosis) are regulated by the MAPK signaling pathways (Ayroldi et al., 2012; Sun et al., 2017). The signaling downstream of MAPK activates NF-κB in FLS and is triggered by several pro-inflammatory cytokines and mediators, including TNF-α, interleukin (IL)-1β, and IL-6, cellular adhesion molecules, and various chemokines (Lee et al., 2013; Shi & Sun, 2018; Wen et al., 2014). Hence, there are many interactions among transcription factors, cytokines, and other mediators within various signaling pathways – all of which may contribute to the role of FLS in inflammation (Haseeb & Haqqi, 2013).

Various interactions initiate the inflammatory response of FLS; thus, we sought to explore and summarize these interactions by querying *Metascape* (Zhou et al., 2019), a recently developed gene annotation and analysis resource for systems-level datasets. We referred to a recent study by Zahir et al. that analyzed FLS isolated from OA-affected human patients after TNF-α treatment to

uncover unique transcriptional profiles (Zahir et al., 2021). This report compared TNF-α-treated FLS with control untreated cells via NanoString analyses, which confirmed changes in the expression of genes identified by RNA-seq analyses in FLS in the same study. Robust upregulation of inflammation and NF-κB-responsive genes were identified in this study. Our analysis of this publicly available data (GSE157364) (Zahir et al., 2021) yielded 130 genes upregulated at least $\geq$ 1.2-fold with $p < 0.05$. We utilized these upregulated genes in a *Metascape* (Zhou et al., 2019) analysis to better understand pathways mediated by a 24-hour exposure to TNF-α (conditions similar to our studies) on OA FLS. The upregulated genes coincided with several genes we assayed in our study (e.g., IL-1α, IL-1β, TNF-α, and IL-8). The summary from the analysis report shows the critical pro-inflammatory interactions, as represented in Figure 1.3.

The Molecular Complex Detection (MCODE) algorithm by *Metascape* connected at a high level of significance network components of interleukin-1 signaling, cellular response to cytokine stimulus, TNFR1-induced NF-κB signaling, and JAK-STAT/MAPK signaling in the STRING-DB analysis (Figure 1.3A). The MAPK signaling pathway was identified as an enhanced term across the inputted gene profile (Figure 1.3B). A substantial proportion of the upregulated genes showed strong enrichment in the transcriptional effectors RELA/NF-κB and TP53 by TTRUST analysis (Figure 1.3C). These analyses help support the concept that stimulation of FLS *in vitro* with TNF-α or NF-κB-inducing agents (such as LPS) could induce a pro-inflammatory response in FLS. In the following sections, various *in vitro* models utilizing FLS will be further discussed, and the potential of FLS as a therapeutic target for OA.

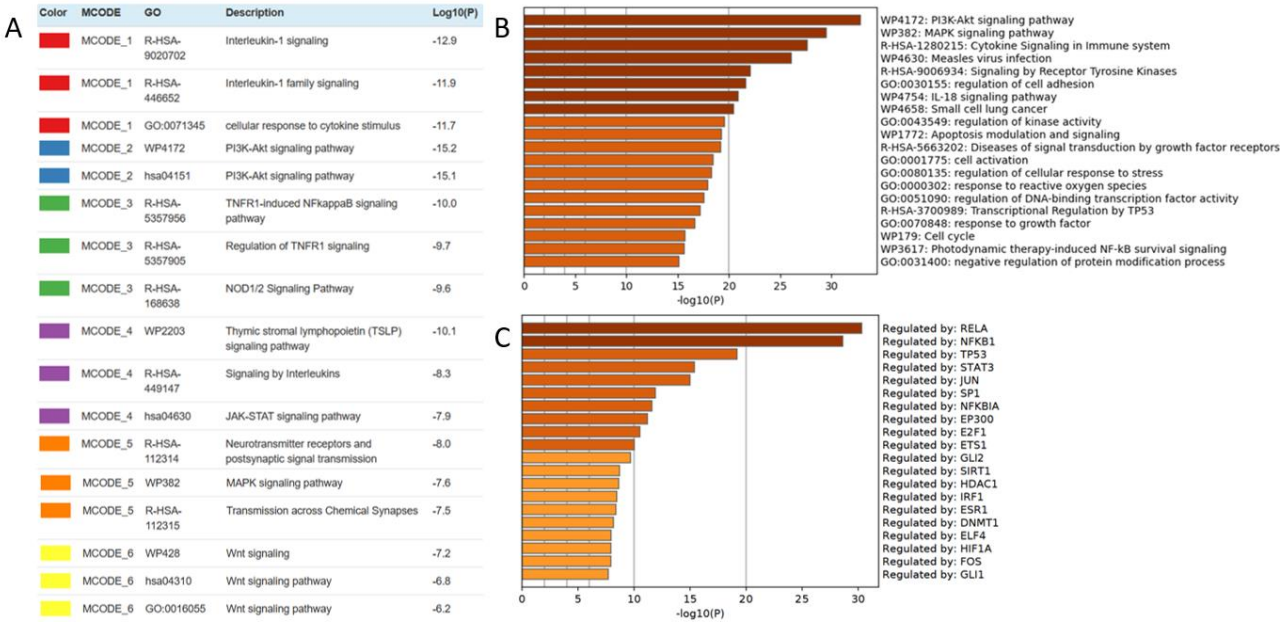

Figure 1.3: Interaction networks identified among inflammatory components associated with OA-FLS. (A) Pathway and process enrichment of MCODE networks with STRING-DB analysis of inputted gene profile. (B) Bar graph of enriched terms across inputted genes, and (C) a summary of TTRUST enrichment analysis for potential transcription factor regulators of the genes. For all panels, analysis by *Metascape* and rankings by p-value (-log10(p)) (Zhou et al., 2019).

1.7 Target-based therapeutics for OA

As discussed in the previous sections, due to the complexity of OA's pathogenesis, there are incompletely effective treatment options accessible to modify degenerative tissue processes or inhibit disease progression. Current treatment options for OA predominantly address symptoms, such as swelling, pain, stiffness, and lack of function (Hunter et al., 2009; Yusuf, 2016). Many non-pharmacological and pharmacological treatment options are currently available, depending on the species and the onset of the disease (McIlwraith et al., 2010; Zhang et al., 2010). Common non-pharmacological approaches toward alleviating the symptoms of OA might include therapeutic exercise or weight management – both applied in human and equine medicine (King et al., 2013; Woods et al., 2017; Zhang et al., 2010). Pharmacological treatment options in human medicine include but are not limited to nonsteroidal anti-inflammatory drugs (NSAIDs), acetaminophen, corticosteroids, opioids, hyaluronic acid, and topical analgesics (Cheng & Visco, 2012; Yusuf, 2016; Zhang et al., 2010). Of these, corticosteroids, hyaluronic

acid, and topical analgesics also are standard in equine medicine, as well as polysulfated glycosaminoglycan and glucosamine (Ferris et al., 2011; Frisbie et al., 2013; Goodrich & Nixon, 2006) . Other compounds that have been reported in equine medicine include dimethyl sulfoxide (DMSO); even if the definitive mechanism of action is not well-understood, studies have suggested some analgesic, anti-microbial, and anti-inflammatory activities (Sotelo et al., 2020). A survey comprised of equine practitioners reported that 18% of its participants use hyaluronic acid, N-acetyl-D-glucosamine, and sodium chondroitin sulfate combination (Polyglycan) for treating horses with OA (Ferris et al., 2011; Frisbie et al., 2013). Over 77% of the survey participants reported using triamcinolone acetonide to treat joints that undergo high motion, and 73% indicated using methylprednisolone acetate for treating low-motion joints in horses (Ferris et al., 2011). Various equine clinics may administer corticosteroids (e.g., triamcinolone acetate, methylprednisolone acetate, or betamethasone esters) in conjunction with NSAIDs (e.g., dexamethasone or phenylbutazone) for the highest effect in reducing inflammation, pain, and restoring mobility (de Grauw et al., 2014; Goodrich & Nixon, 2006; McIlwraith & Lattermann, 2019).

Moreover, the use of non-pharmacological and pharmacological treatments together has provided the best result in treating OA (Brosseau et al., 2014;Yusuf, 2016). For instance, therapeutic exercise (e.g., aquatic therapy) would be combined with a regularly administered NSAID to help alleviate the pain aspect of the disease for both humans and horses (Goodrich & Nixon, 2006; Zhang et al., 2010). An algorithm of when it is appropriate to apply these treatments is often utilized in both human and equine medicine (Hochberg et al., 2012; Zhang et al., 2010). In human medicine, non-pharmacological therapies are first recommended, and then the administration of drugs. Acetaminophen is commonly a first-line drug therapy, followed by the administration of NSAIDs and/or corticosteroids, and then eventual opioid administration with further disease progression (Steinmeyer et al., 2018). Beyond pharmacological treatments, further interventions, such as surgery, may be the next option for addressing ongoing pain and functional disability in human and equine medicine (Goodrich & Nixon, 2006; Zhang et al., 2010). Surgery is an invasive approach to treating OA but is prioritized in the case of refractory pain to improve health-related quality of life (Goldberg & Wera, 2013; Yusuf, 2016). Total joint replacement surgery, osteotomy, joint lavage, and arthroscopic debridement are several

standard practices utilized in human medicine to address an OA-affected joint (Zhang et al., 2010). Total joint replacement surgery is not as common in equine medicine due to its expense, complexity, and high risk of failure (Richardson, 2008) – with the first successful total hip replacement taking place in 2020 at the University of Liverpool in the United Kingdom. Even though all of these approaches may be effective in alleviating symptoms of OA or improving joint function, they act as only a 'bandage' to the long-term impact of OA and may have adverse side effects (Goldberg & Wera, 2013). Thus, there is much-needed attention to developing effective treatments for halting or reversing structural changes within an OA-affected joint.

The change in recent years in our understanding of the OA paradigm from a 'wear and tear' disease to a rather multifactorial etiology that includes age, genetic factors, mechanical overload, among others, has highlighted new opportunities for targeting multiple mechanisms implicated in OA (Harvanova et al., 2022; Yusuf, 2016). Thereby, recent efforts regarding the treatment of OA have been directed at developing therapeutic agents that can reverse, halt or modify the progression of OA (Arra et al., 2020; Fei et al., 2019; Johnson et al., 2012; Wang et al., 2017). Emerging therapies have been described, including disease-modifying osteoarthritis drugs, targeted synovial inflammation mediators, inhibitors of subchondral bone remodeling, and inhibitors of cartilage degeneration (Yusuf, 2016). Synovial inflammation has been suggested as a relevant target for developing therapeutics since this process is critical in initiating and promoting the progression of OA (Bondeson et al., 2006; Mathiessen & Conaghan, 2017; Stefani et al., 2019). Among the cytokines that promotes inflammation in the synovium are IL-1β and TNF-α, which play a central role in inducing downstream expression of several additional pro-inflammatory and catabolic mediators (Aida et al., 2006; Shen et al., 2014). One regenerative therapeutic approach has focused on reducing the degenerative effects of IL-1 by gene and cell delivery of its natural receptor antagonist, the IL-1Ra (Gabner et al., 2018; Nixon et al., 2018). A recent study evaluated the impact of early IL-1Ra (i.e., Anakinra) administration (days 1-7) on the metabolism and biosynthesis of lubricin after a traumatic joint injury in a rat model, finding that intra-articular treatments of IL-Ra reduced chondrocyte apoptosis (Elsaid et al., 2015). Likewise, anti-TNF-α (i.e., adalimumab) has been shown to halt joint damage progression compared to a placebo in an erosive hand OA study (Verbruggen et al., 2012). Another approach used RNA interference to silence IL-1β expression in a rabbit model of post-traumatic arthritis, as well as TNF-α, supporting

the relevance of both molecules as effective targets for therapeutic development (Tang et al., 2015). Additionally, TNF-α neutralizing therapies (TNF inhibitors) have shown clinical benefits in human medicine in reducing the effects of osteoarthritis (Li et al., 2018).

Other promising therapeutic targets have included NF-κB, which has vital roles in promoting the expression of several inflammatory mediators and cytokines, and matrix-degrading enzymes (Marcu et al., 2010). Moreover, the NF-κB mediator can induce inflammation-mediated metabolic shifts in chondrocytes. It influences cells to reprogram toward glycolysis and lactate dehydrogenase production, promoting cartilage degradation through reactive oxygen species (ROS) generation (Arra et al., 2020). ROS can modify lipids and proteins, damage DNA structure, and stimulate other adverse effects in cells (Arra et al., 2020). Elevated levels of ROS in OA modify intracellular signaling, chondrocyte apoptosis, ECM metabolism, inflammatory responses, and subchondral bone dysfunction (Arra et al., 2020; Lepetsos et al., 2019). Recent studies have focused on these roles of NF-κB and how it compares to other signaling cascades, such as the p38 MAPK/c-FOS/AP-1 or JAK/STAT pathways, to understand better the underlying mechanisms of synovial inflammation and degradation of cartilage. These studies have shown that inhibiting NF-κB or p38 MAPK in the joint can halt the progression of OA by preventing the ROS-induced inflammatory response arising from chondrocytes (Arra et al., 2020) resulting in chondroprotective effects from reduced MMP-13 secretion, for example (Lim & Kim, 2011). Most of these studies are preliminary, especially in equine medicine, despite these advancements. Additional work is still necessary to understand the molecular pathways that initiate synovial inflammation and perpetuate cartilage degeneration. Overall, the inhibition of inflammation and its cellular contributors (i.e., FLS) are highly desirable components of developing more effective and safer therapeutics for OA (Chibber et al., 2020). Synoviocytes are discussed in the next section as a potential therapeutic target for developing therapeutics.

1.8 Synoviocytes as a potential target for OA management

Many studies of OA have focused on specific cell populations that take part in synovial inflammation, as the targeting of these cells may represent an opportunity for developing

therapeutic interventions for disease progression. Likewise, FLS have been studied for their ability to respond to inflammatory stimuli by upregulating specific genes that then contribute to further inflammation within OA-affected joints. FLS have been identified as a potential therapeutic target for OA, and assessing their responses to inflammation poses a promising *in vitro* model for studying OA (Harvanova et al., 2022; Huang et al., 2019). In developing an *in vitro* model utilizing FLS, some challenges include the isolation and characterization of FLS since only a few cell-specific markers have been characterized in equine cells, such as FOXO1, PXK, PYCARD, and SAMD9L (Thomsen et al., 2017). Further characterization of FLS markers could help improve the reproducibility and consistency of studies focused on FLS and improve our understanding of the synovium's contribution to the progression of OA.

The field is yet to fully uncover the complexity of how FLS contributes to cytokine production and the development of inflammation within an OA-affected joint. It would be clinically relevant to target the synovium to disrupt their production of pro-inflammatory cytokines, thus halting the initiation of destructive MMP upregulation, among other factors. Current research focuses on priming or stimulating FLS with pro-inflammatory molecules (e.g., lipopolysaccharide (LPS) or TNF-α) that participate in the innate immune response (Andreassen et al., 2015; Harvanova et al., 2022; Ohata et al., 2005). Upon stimulation with pro-inflammatory molecules, changes in FLS gene expression can be detected at various timepoints and characterized to help identify specific inflammatory response biomarkers. Moreover, changes that have been detected in human FLS *in vitro* are the upregulation of TNF-α, IL-6, IL-8, and IL-1β (Nair et al., 2012; Sharma et al., 2020). Equine FLS *in vitro* models have comparable responses, with galectin-1 and galectin-3 expression being additionally recognized (Reesink et al., 2017), although at lower levels than in bone marrow mesenchymal stromal cells.

In summary, *in vitro* models using FLS can enable us to gain novel insights into the molecular signatures contributing to various stages of OA and examine potential therapeutic targets for reducing inflammation or helping reverse the effects of OA. In particular, co-culture models with other cell types or explants could help expand this knowledge gained from FLS culture towards more complex systems such as applicable to joints (e.g., articular cartilage deterioration and subchondral bone remodeling) (Harvanova et al., 2022; Pretzel et al., 2009;

Stefani et al., 2019). Continued research in the development and application of FLS models also is proposed to benefit from the rapidly growing field of modern bioinformatics research in musculoskeletal biology (Chen et al., 2019).

CHAPTER 2. AN *IN VITRO* MODEL FOR TESTING THE POTENTIAL OF NOVEL COMPOUNDS IN REDUCING THE INFLAMMATORY RESPONSE OF EQUINE SYNOVIOCYTES

2.1 Introduction

It has been hypothesized that the secretion of inflammatory cytokines from the synovium induces the release of MMPs, which contribute to ECM degradation, bone remodeling, and synovium inflammation (i.e., synovitis). The phases at which inflammation occurs in OA-affected synovium remain unclear. It is uncertain whether synovitis presents primarily due to a systemic innate immune response or secondary to the catabolic signals from the articular cartilage (Liu-Bryan, 2013; Scanzello & Goldring, 2012). There are various histological signs of synovitis, such as hyperplasia, lymphocyte and macrophage infiltration, fibrosis, and neoangiogenesis (Scanzello & Goldring, 2012). Nevertheless, there is a considerable amount of evidence from the literature focusing on synovitis and its resulting association with the upregulation of several pro-inflammatory cytokines and mediators – contributing to an imbalance in the catabolic and anabolic processes mediated by the articular cartilage (Chou et al., 2020; Pretzel et al., 2009).

The latest insights into OA pathogenesis link mechanical damage and chronic inflammation (Haseeb & Haqqi, 2013; Schröder et al., 2019). Chronic, low-grade inflammation within the joint space has been associated with the induction of innate immune responses intricately involved in activating and perpetuating OA inflammation (Sokolove & Lepus, 2013). The innate immune system recognizes changes within the joint space and detects conserved patterns generated after damage to cellular and cartilage ECM products (Millerand et al., 2020; Silverstein et al., 2017). The detection of these damaged cellular components generates danger-associated molecular patterns (DAMPs) that subsequently activate the responses of the innate immune system (Millerand et al., 2020; Pulai et al., 2005; van Lent et al., 2012). FLS commonly express TLR 1-7 and recognize both pathogen-derived and endogenous factors (PAMPs and DAMPs) (Nair et al., 2012; Rosenberg et al., 2017; Yoshitomi, 2019). Activation of TLRs triggers cellular signals leading to an intermediate immune response, activating surrounding cells to produce and release downstream cytokines and chemokines that mediate inflammation (Kim et al., 2006; Nair et al., 2012). In further detail, the binding of LPS to cells is known to cause TLR-4 receptor

dimerization, resulting in the activation of downstream effectors, including the transcription factor NF-κB (Abella et al., 2016; Miguel et al., 2007; Nair et al., 2012). NF-κB is typically bound to the cytoplasmic protein IκB, remaining in its inactive state until the phosphorylation of IκB occurs, which then permits NF-κB dimers to translocate to the nucleus (Bondeson et al., 2006; Choi et al., 2019). DNA binding by NF-κB activates the transcription of several pro-inflammatory genes, resulting in the production and secretion of cytokines (e.g., TNF-α, IL-1β, and IL-6), chemokines, reactive oxygen and nitrogen species, and enzymes (Figure 2.1) (Choi et al., 2019; Gupta et al., 2010; Pulai et al., 2005; Shen et al., 2014). Therefore, upon activation of an innate immune response program, NF-κB induces catabolic gene transcription and significantly stimulates inflammatory mediators through a positive feedback loop – constituting a promising target in developing effective therapeutic agents (Choi et al., 2019; Ding et al., 2019).

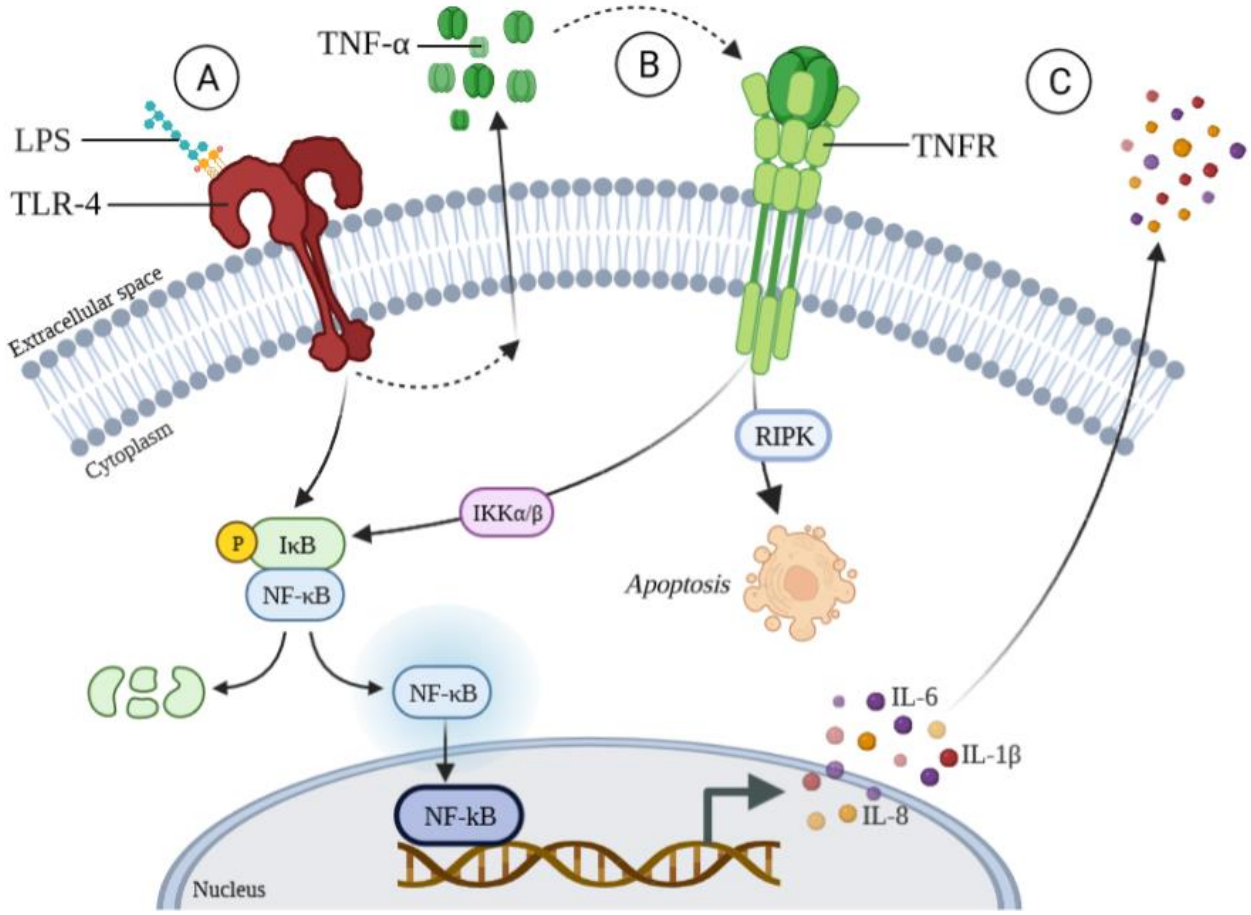

Figure 2.1 Diagram of innate signaling pathways after stimulation of FLS with LPS. The innate immune system is initiated with stimulation (e.g., LPS) (A). The initial stimulation then signals the cell to release tumor necrosis factor (TNF), which binds to its receptor, TNFR, downstream in the signaling pathway (B). Next, the cell releases pro-inflammatory cytokines, such as interleukin (IL)-6, IL-1β, and IL-8 (C). This cascade promotes the generation and propagation of inflammatory signals in the joint space. Diagram created in BioRender.com.

Multiple studies suggest that other signaling pathways also contribute to regulating genes that impact the progression of OA, such as the TGF-β (Zhen et al., 2013), the AMPK/SIRT-1/PGC-1α (Li et al., 2020), the p38 MAPK/c-FOS/AP-1 (MAPK) (Lim & Kim, 2011), and the JAK2/STAT1/2 (JAK/STAT) pathways (Qiao et al., 2019). A majority of these signaling pathways are triggered by IL-1β-stimulated chondrocytes or FLS, and recent studies have shown that both the MAPK and the JAK/STAT pathways contribute to the production of MMPs (Lim & Kim, 2011). Thus, blocking the NF-κB transcription factor and other pathways may be necessary to inhibit FLS-mediated inflammation and further degeneration of articular cartilage.

FLS are mainly studied in RA for their production of chemokines and cytokines that attract various types of immune cells (e.g., lymphocytes and monocytes) into the synovium, inducing chondrocytes to secrete and stimulate ECM-degrading enzymes (Bottini & Firestein, 2013). In RA, and now also proposed in OA, FLS can migrate (Corrigall et al., 2001) and interact with surrounding tissues, i.e., occupy the articular cartilage and secrete cartilage matrix-degrading enzymes, or attack the underlying subchondral bone and initiate osteoclast-mediated bone resorption and ECM degradation processes (Bottini & Firestein, 2013; Tu et al., 2020). Overall, research from several types of arthritis implicates a role for FLS in inflammatory signaling within the synovium, making this cell type a candidate of interest for developing an *in vitro* model in which to characterize their response to novel therapeutic compounds, particularly for representing some of the early signaling and/or stages of OA development.

In vitro models of OA can be beneficial in better understanding the initial causes of the disease, as these models are more cost-effective relative to *in vivo* models and less complex; thus, they may provide more reproducible data (Grenier et al., 2014; Haltmayer et al., 2019; Harvanova et al., 2022). The primary purpose of these models is to mimic some of the factors and conditions that initiate OA progression in synovial joints (Chan et al., 2022; Haltmayer et al., 2019; Singh et al., 2021). These models can help dissect signaling pathways or other mechanisms that trigger disease progression and are beneficial for screening and testing novel candidate therapeutics. Several temporal and concentration effects of compounds can be explored in a much

simpler environment utilizing *in vitro* models than *in vivo* and enable the selection and prioritization of compounds for future preclinical applications. Since inflammation is considered a hallmark in OA-affected joints, recent studies have focused on uncovering mechanisms to develop interventions to reduce or halt its impact on degenerating or poorly repairing (hypertrophic chondrocytes) joint tissues (Allas et al., 2020; Harvanova et al., 2022). Several pro-inflammatory stimuli can be considered candidates for inducing OA-related FLS signaling changes (e.g., TNF-α, IL-1β, as well as LPS) (Andreassen et al., 2015; Liu et al., 2019). FLS transcribe many genes encoding pro-inflammatory cytokines and mediators downstream of NF-κB activation and other signaling pathways participating in the innate immune response (Chen et al., 2019; Chow & Chin, 2020). Therefore, establishing an *in vitro* model of an FLS-mediated pro-inflammatory response using different stimuli (LPS, TNF, among others) may enable the development of therapeutics that may encompass several connecting proinflammatory pathways relevant to either early or late stages of OA.

In developing our *in vitro* model of inflammation, the endotoxin LPS or the cytokine TNF-α were used as stimuli for promoting specific pro-inflammatory characteristics in FLS that mimic signaling pathways elicited in the OA-affected joint. Numerous studies have utilized cytokines TNF-α and IL-1β to initiate inflammatory responses in FLS (Harvanova et al., 2022; Liu et al., 2019; Shen et al., 2014). LPS stimulation also has been used to promote inflammation (RA or OA) via TLR recognition of both endogenous factors and pathogens in FLS (Ding et al., 2019; Jin et al., 2016; Schwarzbach et al., 2019). TLR-3 and TLR-7 recognize single- and double-stranded RNA, and the TLR2/TLR4 heterodimer recognizes proteins and other low molecular weight molecules, such as LPS (Nair et al., 2012), with downstream NF-κB activation (Rosenberg et al., 2017). Thus, both LPS or TNF-α-stimulated FLS would activate NF-κB and MAPK signaling pathways and promote increases in gene expression for pro-inflammatory cytokines. Although these stimuli are most studied in RA-focused models, establishing a pro-inflammatory response of FLS using these agents in an *in vitro* setting would allow for preliminary testing of potential therapeutic agents toward OA.

Many studies have utilized inflammatory *in vitro* models to test the efficacy of potential therapeutic agents, like sulforaphane, hyperoside, lactate dehydrogenase A, or other novel agents undergoing early investigation (Arra et al., 2020; Davidson et al., 2014; Sun et al., 2021). Similarly, in collaboration with Dr. Herman Sintim, our laboratory recently developed a series of novel compounds incorporated in an *in vitro* model utilizing stimulated FLS to study inflammatory responses, further discussed in this chapter. This drug discovery project began with an *in-silico* approach that targeted a small interface where a portion of Pigment Epithelium Derived Factor (PEDF) interacted with one of its receptors, the non-integrin Laminin Receptor 1 (LAMR1) (Umbaugh et al., 2018). This study identified the compound "C3" – proposed to mimic the effects of a portion of PEDF (peptide p18) in binding the LAMR1. PEDF is also recognized as SERPINF1 or EPC1 and is a 50-kDa multifaceted glycoprotein with various properties, such as anti-inflammatory, anti-angiogenic, anti-oxidative, and anti-tumorigenic, thus of much interest as a therapeutic candidate (Bernard et al., 2009; Ma et al., 2021; Wen et al., 2017). Studies have shown that PEDF interacts through different receptors, including LAMR1 (also known as RPSA), a newer established receptor now known to mediate the effects of PEDF (Bernard et al., 2009). The binding of PEDF and LAMR1 has been a topic of several investigations, considering that modulating this interaction with a peptide mimic or a drug could lead to the development of therapeutic targets for various diseases (e.g., cancer, arthritis, and PCOS), depending on whether the LAMR1 is inhibited or activated (Belkacemi & Zhang, 2016; Nakamura et al., 2017; Silber et al., 2020). For example, a study treating myeloma cells with a LAMR1 antagonist suppressed the ability of PEDF to bind to this receptor, reducing myeloma cell viability (Matsui et al., 2014). Hence, the function of PEDF is flexible depending on the targeting of agonist or antagonist domains of its receptor, LAMR1.

Studies focusing on inflammation (in various diseases) showed that increases in PEDF reduce the levels of pro-inflammatory cytokines (IL-1β, IL-17A, IL-6, and TNF-α) through the inhibition of MAPK p38 and JNK (Ma et al., 2021; Matsui et al., 2013). The exact functions of the PEDF/LAMR1 interactions in different cell systems are incomplete due to their involvement in complex signaling pathways. However, several reports indicate the signaling involves MAPK and JNK cascades (Gong et al., 2014; Ma et al., 2021) and also NF-kB inhibition (Ide et al., 2010). An analysis of the available literature describing the effects of PEDF or LAMR1 on signaling

relating to anti-inflammatory processes followed by *Metascape* (Zhou et al., 2019) visualization yielded the diagrams shown in Figure 2.2. Figure 2.2A suggests that there may be a significant role for TNF-α and NFκB1 in mediating the effects of PEDF/LAMR1 pathways. For PEDF/SERPINF1, the literature relating to its anti-inflammatory properties yielded downregulation in 25 genes or cytokines (Lu et al., 2014; Matsui et al., 2014; Zhou et al., 2009), with the impact on IL-10 remaining unclear with PEDF treatment (Yang et al., 2010; Zamiri et al., 2006). For LAMR1/RPSA, the literature relating to its anti-inflammatory properties yielded 7 reported gene or cytokine expression changes (Kane et al., 2019; Matsui et al., 2014). PEDF is connected to reduced expression of a cluster of angiogenic/ECM molecules and reducing a network of inflammatory molecules, including TNF, NF-κB, and IL-1β, for example. LAMR1 also reduced the expression of several of the central inflammatory molecules connected through the serine-threonine receptor-interacting protein kinase-1 (RIPK1) in our analysis results (Figure 2.2A). Interestingly, RIPK1 is a crucial mediator of TNF-mediated apoptosis and inflammatory pathways (Yatim et al., 2015), and its downregulation can help alleviate osteoarthritis (Liang et al., 2019). Moreover, Figure 2.2B shows the top 20 pathways enriched in the *Metascape* analysis, and Figure 2.2C shows the transcription factors predicted as regulators of the genes inputted. In combination, these analyses suggest that PEDF and LAMR1 each or in combination can impact the regulation of several inflammatory or ECM-related pathways, with a potential focus on reduced NF-κB signaling. Additionally, the network is centered on the pro-inflammatory molecules TNF-α/IL1b/NFkB, although there may be contributions from other anti-inflammatory mechanisms such as increased IL-10 signaling and/or decreased CXCL8, CCL2, and IL18. The primary regulators suggested by the analysis in Figure 2.3 were NFkB/RelA, yet other regulators may also be implicated, such as JUN, SP1, or STAT1/3.

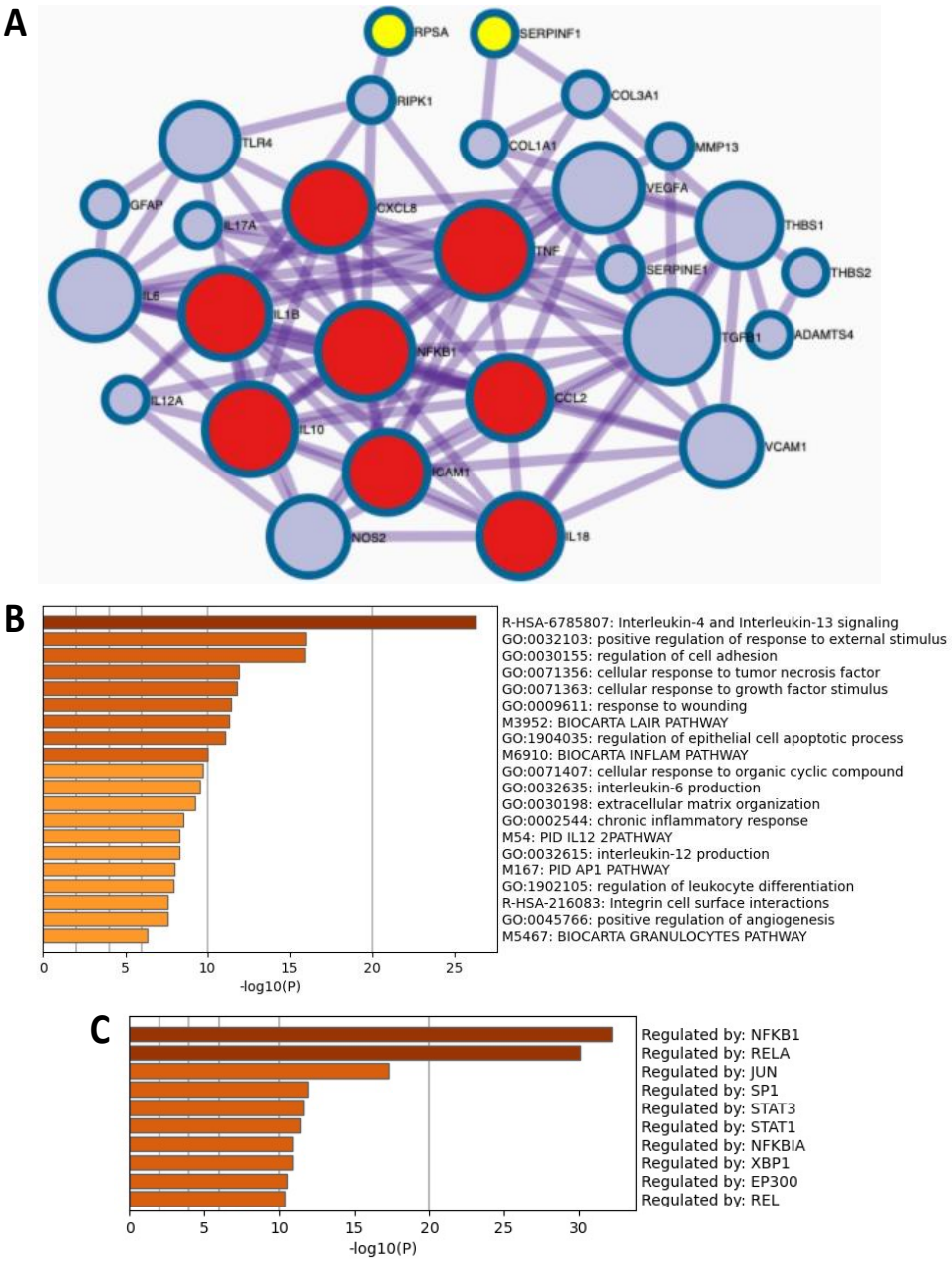

Figure 2.2 Network interactions of PEDF/LAMR1 signaling pathway constituents. (A) Interaction networks using Metascape with STRING-DB analysis after inputting genes and cytokine expression changes from our work and the literature on PEDF and LAMR1. *Yellow*, LAMR1/RPSA, and PEDF/SERPINF1. *Red*, the subnetwork highlighted by the Molecular Complex Detection (MCODE1) algorithm analysis, highlighting the *IL-10 signaling* and *Cellular Response to Lipopolysaccharide* pathways; (B) the top 20 enriched pathways detected by Metascape and ranked by *p*-value. (C) The top 10 enriched transcription factors predicted to regulate the expression of the genes inputted (TTRUST analysis) detected by Metascape and ranked by p-value. Diagrams created using Metascape.org (Yingyao Zhou et al., 2019).

As our lab has sought to develop small molecules that can mimic the interaction between PEDF and LAMR1 for arthritis therapy, we have begun to characterize the impact of a series of compounds based on the initially described compound C3. The novel C3 has been predicted to interact with Histidine-169 of the 37 kDa form of LAMR1 (37 LR) by a hydrogen bond, the known binding region of PEDF (Umbaugh et al., 2018). The interaction of C3 with LAMR1 has been proposed to modulate the overall activity of LAMR1 and mimic the effects of PEDF. Hence, it is assumed that the binding of C3 to LAMR1 allows PEDF to affect its role as an anti-inflammatory molecule. Additionally, recent work in the lab has shown that C3 has the potential for reducing angiogenesis (Umbaugh et al., 2018) and inflammatory gene expression (i.e., IL-1β) in human macrophages (THP-1) (Haffner et al., 2017), as well as for promoting upregulation of chondrogenic genes (e.g., COL2A1, among others) and reducing hypertrophic chondrocyte-related gene expression (e.g., COL10, among others) in differentiating eqMSC and hMSC 3D cultures (Keating et al., 2019). These preliminary studies support a role for C3 and related molecules under development as potential therapeutics for controlling inflammation and helping to promote cartilage repair.

Building on these recent laboratory preliminary studies, it was of interest in this work to utilize C3 for its potential anti-inflammatory activity in equine FLS-based models. C3 may be relevant to a future clinical application as the target LAMR1 is expressed on FLS (Konttinen et al., 2000) and has the potential to stimulate chondrocyte differentiation (Keating et al., 2019). Furthermore, second-generation compounds have been developed based on the C3 parent compound. Among these compounds, the II-09/02-09 analog (Figure 2.3) was the most promising in the pilot experiments, showing a ~3-fold improved affinity for LAMR1 compared to C3 and improved activity in various cell types (Haffner et al., 2017; Keating et al., 2019). However, a significant barrier to translating C3 or 02-09 to a clinical study is their current micromolar activity level (~10 μM is the 50% effective concentration, EC50) in cell-based assays. For clinical intra-articular delivery in horses, one needs to have a compound with high activity at low doses to reduce production costs, increase efficacy, and have fewer off-target effects (Evans et al., 2014). These compounds have been utilized in several studies within our laboratory and are currently included in a patent assigned to the Purdue Research Foundation (Diaz-Quinones et al., 2011; Umbaugh et al., 2018).

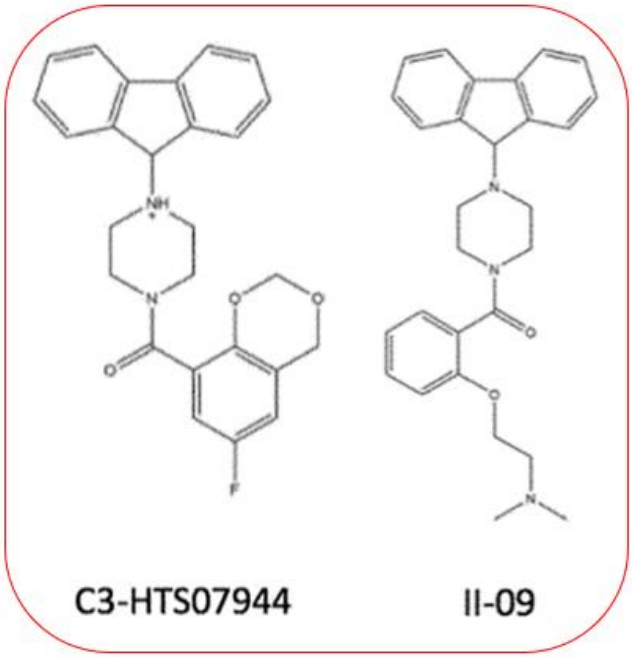

Figure 2.3 Chemical structures of C3 and 02-09. C3, or HTS07944, from the Maybridge high-throughput screening (HTS) collection for drug discovery (Thermo Fisher) (left), was utilized as a parent molecule initially discovered from an *in-silico* screen (Umbaugh et al., 2018). C3 inspired the development of a series of derivative compounds tested in a pilot project (Haffner et al., 2017; Keating et al., 2019) (Haffner et al., 2017) with potential anti-inflammatory activity for OA treatment. II-09, also known as 02-09 (right), is the derivative compound developed from C3 using medicinal chemistry approaches in collaboration with Dr. Herman Sintim.

Therefore, in the present work, we aimed to develop an *in vitro* model of OA to test the efficacy of our novel compounds in reducing the pro-inflammatory activity of stimulated FLS. First, we utilized LPS or TNF-α as stimuli to achieve a pro-inflammatory response in equine FLS (eqFLS) to examine the anti-inflammatory potential of compounds C3 and 02-09. This *in vivo* inflammation model would potentially be useful for evaluating the anti-inflammatory potential of a more extensive series of therapeutic compounds, ultimately allowing us to improve drug activity at lower effective concentrations. Following various study designs and gene expression analyses, we characterized a model that induced OA-related gene expression changes in eqFLS and assessed novel therapeutic agents for their ability to counteract the inflammatory response of eqFLS. These novel compounds have the potential for future development into therapeutic agents for reducing inflammation and potentially promoting cartilage repair (studied by the lab in another project that utilizes MSCs) to treat equine OA.

2.2 Materials and Methods

2.2.1 Cell isolation

Equine fibroblast-like synoviocytes (eqFLS) were isolated from the synovial membrane of the carpal (knee) and stifle joint of an 11-year-old gelding (show horse), euthanized for reasons unrelated to this study, in collaboration with Dr. Timothy Lescun (VCS). The synovial membrane was minced into 3-4 mm pieces with sterile scalpels or fine scissors. The tissue pieces were washed once with 30 mL Hank's Balanced Salt Solution (HBSS) (1X) containing calcium and magnesium (+Ca+Mg) (Thermo Fisher Scientific, Waltham, MA) and placed into a T-75 flask (Corning Incorporated, Corning, KY) for the next steps. The tissue solution was treated with 10 mL/g of dissociation digest media consisting of 1.52 mg/mL Collagenase II (Worthington, CLS-2, 290U/mg dry weight, Lot # 45D15718) in 1xHBSS +Ca+Mg. The tissue solution was incubated at 37^{o}C for 4 hours on a rocker platform, where the digest was also supplemented with 3 mM $CaCl_2$ (Lee et al., 2013). Cells were then dispersed by passing through a 70 μm nylon mesh under sterile conditions, and remaining tissue fragments were disaggregated by gently use of forceps. The solution was centrifuged at 1,500 rpm for 5 minutes and washed with 30 mL HBSS +Ca+Mg. The cell pellet was resuspended in 12 mL Dulbecco's modified Eagle's medium (DMEM) (Gibco, Gaithersburg, MD) with 10% Fetal Bovine Serum (FBS) (Hyclone Laboratories, Logan, UT) and 1% Pen-Strep (Gibco). Cells were seeded at 6 x 10^5 per well of a 6-well plate (Corning) in 2.5-3 mL media each well and expanded at low passage number (P1-3), passaging at a split ration 1:3. The low passages were collected and prepared with 1.0 x 10^6 cells/cryovial and 500 μL of Bambanker Serum-Free Freezing Medium (Thermo Fisher Scientific) and then preserved at -80^{o}C until further use.

2.2.2 Cell culture

For experiments using eqFLS, the cells were expanded from the cryopreserved vials on 100 mm culture dishes (Corning) until reaching passages between 4 and 12 (P4-12) in a complete growth medium consisting of DMEM (Gibco), 10% FBS (Hyclone), and 1% Antibiotic-Antimycotic (Anti-Anti) (Gibco). Cells were incubated at 37^{o}C in a controlled CO_2 atmosphere to 70-80% confluence with media changes every 3-4 days. At confluence, cells were washed with Dulbecco's Phosphate-Buffered Saline (DPBS) (Thermo Fisher Scientific), harvested using 0.25%

Trypsin-EDTA solution (Gibco), and counted using a Scepter 2.0 Handheld Cell Counter (Millipore Sigma, Saint Louis, MO). eqFLS were seeded at 1.2 x 10^6 cells/well in 6-well plates (Corning Incorporated) and incubated for 24 hours at 37ºC in a controlled CO_2 atmosphere to allow adherence of cells overnight. The culture media conditions varied in some experiments, as noted in other methods and results.

2.2.3 Pro-inflammatory stimulation

eqFLS were seeded at 1.2 x 10^6 cells/well in 6-well plates and incubated for 24 hours at 37ºC in a controlled CO_2 atmosphere to allow adherence of cells. After 24 hours, the complete growth medium was removed, and cells were stimulated with either lipopolysaccharide (LPS) (1 mg/mL) (Cat. #: 50-571-26; 3P LPS E Coli O111:B4, Millipore-Sigma, St Louis, MO) or recombinant equine tumor necrosis factor-alpha (TNF-α) (25 ng/mL) (R & D Systems) diluted in Opti-MEM Reduced-Serum Medium (Gibco) to a final concentration of 10 ng/mL. The dilutions were added to designated wells to a final volume of 2.5 mL in each well and incubated for 24 hours at 37ºC in a controlled CO_2 atmosphere. After 24 hours, eqFLS were examined for cell viability and either harvested for gene expression or further treated with vehicle control or novel compounds (Section 2.2.5). Unstimulated cells were used as the negative control.

2.2.4 Novel molecule treatment

Control and novel compounds were tested for their ability to function in counteracting the pro-inflammatory response of eqFLS. Dimethyl sulfoxide (DMSO) (0.1%) was used as a vehicle control baseline in all samples. The compound P18 (1 μM) as a positive control PEDF peptide mimic; novel compounds C3 (10 μM), a PEDF/LAMR interaction mimic, and 02-09 (10 μM), a derivative to C3 with varying chemical groups predicted to augment drug-like interactions with LAMR1. The final concentrations of these compounds were diluted with Opti-MEM Reduced-Serum Medium (Gibco) and then directly added to designated wells for 24 hours with or without the initial stimulation of TNF-α (10 ng/mL) or LPS (10 ng/mL). After 24 hours, eqFLS were washed with Dulbecco's Phosphate-Buffered Saline (DPBS) (Thermo Fisher Scientific), harvested using 0.25% Trypsin-EDTA solution (Gibco), and counted using a Scepter 2.0 Handheld Cell Counter (Millipore Sigma). Cell suspensions of each sample were collected and

centrifuged at 1,500 rpm for 5 min. to obtain a cell pellet. Cell pellets were stored at -80^{o}C until further analysis of gene expression (Section 2.2.7)

2.2.5 Characterizing eqFLS inflammation response

Three study designs were utilized to characterize the inflammatory response of eqFLS. Study Designs A and B (Figure 2.2) consisted of first stimulating eqFLS for 24 hours with either LPS or TNF-α as mentioned in Section 2.2.4. For all studies, the media used was Opti-MEM Reduced-Serum Medium (Gibco) with 1% Anti-Anti (Gibco), and the compounds were diluted to a final concentration mentioned in Section 2.2.4. For study design A, the initial stimulation was removed after 24 hours, the cells were washed with DPBS (Thermo Fisher Scientific), and then the control and novel compounds were added to the designated wells. The initial stimulation was not removed for study design B, and the control and novel compounds were added directly to designated wells. For study design C, eqFLS were first treated for 24 hours with control or novel compounds and then stimulated with either LPS or TNF-α for an additional 24 hours before sample collection. All study designs consisted of collecting cell suspensions by harvesting the cells using 0.25% Trypsin-EDTA solution (Gibco), washing with DPBS, to a final product of a cell pellet by centrifugation at 1500 rpm for 5 min. The cell pellet was then stored at -80^{o}C until further processing for gene expression analysis. eqFLS that remained unstimulated or untreated were used as a negative control (Section 2.2.7).

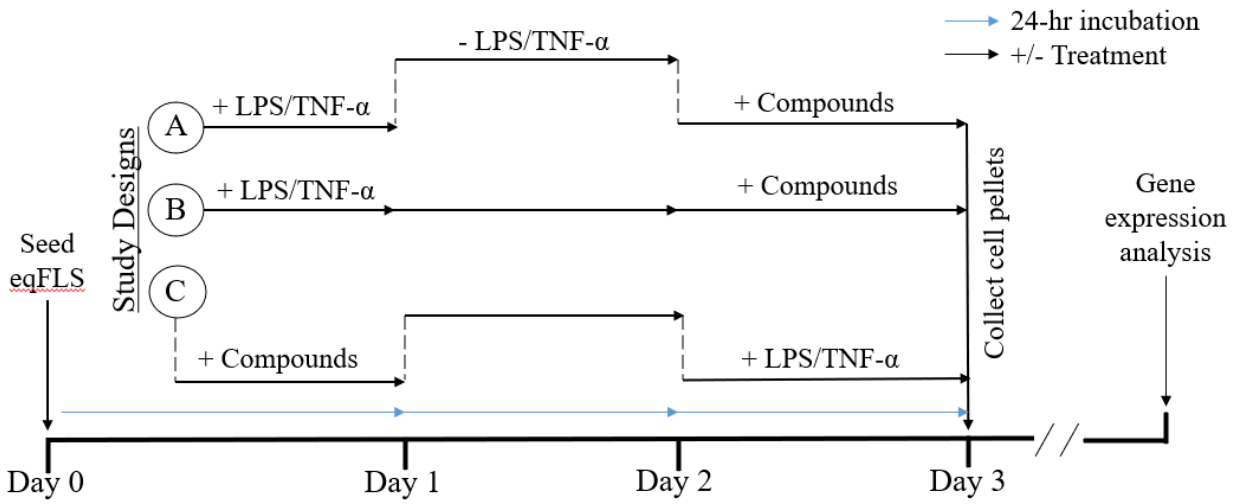

Figure 2.4 Study designs utilized to characterize the inflammatory response of eqFLS. Various study designs were used to achieve the best model for eqFLS contribution to OA inflammation. Study Design A and Study Design B are similar, with eqFLS seeded in 24-well plates at 5 x 10^4 cells/well, incubated overnight to allow adherence, stimulated with LPS or TNF-α, incubated another 24 hours, and then novel and control compounds were added. The cell samples were collected after 24 hours. Study Design A consisted of washing the plate before adding the control and novel compounds to the wells. Study Design C consisted of adding the control and novel compounds prior to stimulating the eqFLS with LPS or TNF-α; all other steps are like the other study designs.

2.2.6 Cell viability screen

eqFLS were seeded in 96-well plates at 5 x 10^3 cells/well using the Scepter 2.0 Handheld Automated Cell Counter (MilliporeSigma). eqFLS were stimulated with either LPS (0.1 µg/mL) or TNF-α (10 ng/mL) and treated with vehicle control (DMSO at 0.1% or 1.0%), or compounds, C3, 02-09, or P18 at concentrations of 1 µM, 5 µM, 10 µM, 50 µM, or 100 µM for 60 hours Cell viability was measured using the Cell Counting Kit-8 (CCK-8) (Dojindo Molecular Technologies, Rockville, MD) according to the manufacturer's instructions. Absorbance was quantified at 450 nm using a GloMax Reader (Promega, Fitchburg, WI). A baseline plate reading at 0 hours was obtained to normalize for variations in cell seeding. Additional plate readings were obtained at 72 hours and 120 hours. Then the relative cellular viability was calculated by dividing corrected absorbance values by the untreated control readings to obtain a % cell viability. The average % viability values and standard deviation were calculated from triplicates per plate using Microsoft Excel.

2.2.7 Gene expression analysis

Frozen cell pellets were processed with RNeasy (Qiagen, Valencia, CA), as per the manufacturer's instructions, to isolate RNA. The nucleic acid content was determined spectrophotometrically using NanoDrop One Microvolume UV-Vis (Thermo Fisher Scientific). RNA was reverse transcribed into complementary DNA (cDNA) using the amfiRivert cDNA Synthesis Platinum Master Mix (GenDEPOT, Katy, TX), according to the manufacturer's instructions. Relative gene expression levels were determined by real-time quantitative polymerase chain reaction (RT-qPCR) with each sample containing 1 μL cDNA template, 2X SYBR Green reagents (Roche Diagnostics, Indianapolis, IN), and 20 μM of forward and reverse primer nucleotide sequences (Table 2.1). All real-time PCR assays were prepared in triplicates and performed using the ViiA7 Real-Time PCR System (Applied Biosystems, Foster City, CA) using 40 cycles of 95^{o}C for 3 minutes, 95^{o}C for 3 seconds, 60^{o}C for 30 seconds, and 72^{o}C for 19 seconds. All expression levels were normalized to the control glyceraldehyde 3-phosphate dehydrogenase (GAPDH). Fold changes were determined using the delta-delta C(T) method while comparing gene expression to baseline. The baseline was equal to the expression of eqFLS cultured in a complete medium without novel compounds or initial stimulation (Rao et al., 2013).

Table 2.1 Equine-specific gene primers used for RT-qPCR. Primers were used to amplify gene expression in stimulated/non-stimulated and treated/non-treated eqFLS. Interleukin 6, 1β, 8, 1α (IL-6, -1β, -8, -1α), ADAM Metallopeptidase with Thrombospondin Type 1 Motif 4 (ADAMTS4), Matrix Metalloproteinase 13 (MMP-13), tumor necrosis factor-α (TNF-α), cluster differentiation 90, 44 (CD90, CD44), Sterile Alpha Motif Domain Containing 9 Like (SAMD9L), and PX Domain Containing Serine/Threonine Kinase Like (PXK), and glyceraldehyde 3-phosphate dehydrogenase (GAPDH) as the housekeeping gene control.

Gene Name	Forward Sequence *(5'→3')*	Reverse Sequence *(5'→3')*
IL-6	CCTGGTGATGGCTACTGCTTTC	GGATGTACTTAATGTGCTGTTTGGTT
IL-8	CTTTCTGCAGCTCTGTGTGAAG	GCAGACCTCAGCTCCGTTGAC
IL-1α	CAATATCTTGCGACTGCTGCATTAA	CTCTTCTGATGTATAAGCACCCATGT
IL-1β	GAGCCCAATCTTCAACATCTATGG	ATACCAAGTCCTTTTACCAAGCCTG
ADAMTS-4	GCTGGGCTACTATTATGTGCTG	GCTGGGCTACTATTATGTGCTG
MMP-13	GTCCCTGATGTGGGTGAATAC	ACATCAGACCAAACTTTGAAGG
TNF-α	TTCTCGAACCCCAAGTGACAAG	GCTGCCCCTCGGCTT
CD90	TCTCCTGCTGACAGTCTTGC	GGACCTTGATGTTGTACTTGC
CD44	TTCATAGAAGGGCACGTGGT	GCCTTTCTTGGTGTAGCGAG
SAMD9L	GAACCGGAAAACGTCTGTGT	GGGAGAAAGTCGGTGCATTA
PXK	CATTACCTCCACCTCCTCCA	GATCACAGGTTTCGGCTTTC
GAPDH	GGGGCTGCCCAGAACATC	GACTGACACGTTAGGGGTGG

2.2.8 Statistical analysis

All assays were performed in triplicates ($n = 3$) with values expressed as the mean ± standard deviation (SD), and statistical analysis was performed using comparisons among groups with a 2-tailed t-test of the data, which utilized the delta-delta C(T) method to obtain gene expression changes relative to a housekeeping control gene, using Microsoft Excel. Statistical significance was defined as $p < 0.05$, and specific significance values are stated in the figure with an asterisk (*) representing significance to the untreated controls and a hashtag (#) representing significance ($p < 0.05$) relative to the DMSO vehicle-treated groups.

2.3 Results

2.3.1 The fibroblast-like synoviocyte (FLS) cell type was characterized in samples isolated from equine carpal joints

The fibroblast-like synoviocytes (FLS) utilized for this study were isolated from the synovial membrane of a horse's equine carpal and stifle joints and maintained under the designation of equine FLS (eqFLS) in our laboratory. It was of interest to better characterize

eqFLS by culturing passage 0 until 70-80% confluence. eqFLS were cultured under specific protocols we adapted from several references specifically for FLS isolation, as mentioned in Section 2.2.2, and analyzed for common morphological characteristics of FLS which agreed with the literature on these cells, such as the presence of a relatively large nucleus (arrows in Figure 2.5A) and a distinctive endoplasmic reticulum distributed throughout the cytoplasm. These features are typical of Type B but not Type A (monocytic) cells (Iwanaga et al., 2000). FLS presented more as spindle cells (Iwanaga et al., 2000) and became in our cultures the predominant adherent cell type after 10 days; we believe any suspension cells (i.e., monocyte/macrophage-like cells) were lost as the passage number increased with further culturing, a finding supported by other groups' observations (Harvanova et al., 2022; Hatakeyama et al., 2017; Liu et al., 2019). Additionally, eqFLS formed sheet-like structures in culture following 10 days that suggested they may have some ability to form a lining-like layer *in vitro* (Figure 2.5B), as indicated by other groups (Kiener et al. 2006).

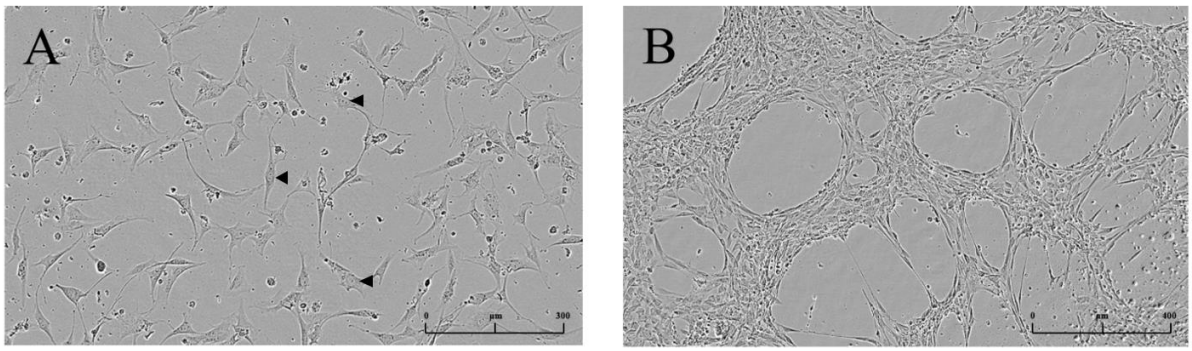

Figure 2.5 Morphology and appearance of eqFLS in culture. A. Culture of eqFLS after 3 days of expansion shows the characteristics of long protrusions from the cell body, large nucleus (darkened arrows), and distinctive endoplasmic reticulum. B. eqFLS form a lining-like layer in extended (> 10-day) culture. Cells were seeded in 96-well plates at 2.0 x 10^4 cells/well and imaged using the IncuCyte Live-Cell Analysis System (Sartorius) under the phase contrast channel.

2.3.2 Stimulation of eqFLS with LPS for 24 hours resulted in an upregulation of pro-inflammatory genes

It was of interest to establish an *in vitro* eqFLS pro-inflammatory condition to test novel compounds with potential anti-inflammatory activity. We wanted to establish an ideal stimulus to elicit an inflammatory response from eqFLS. We initially selected LPS and used it at a final

10 ng/mL concentration, following the protocol mentioned in Section 2.2.3. After stimulating eqFLS with LPS for 24 hours, the samples were collected and processed for gene expression analysis. We observed significant upregulation of IL-6 and a trend towards increased ADAMTS-4 gene expression. However, IL-1β and others did not significantly change in this pilot experiment (Figure 2.6). This pilot data provided the basis for exploring the development of a pro-inflammatory model using LPS-stimulated-eqFLS.

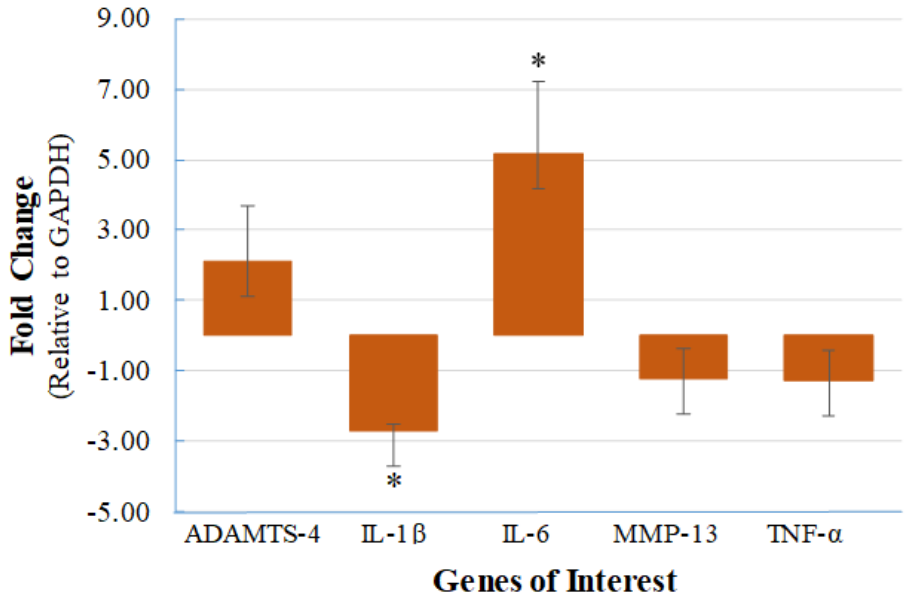

Figure 2.6 eqFLS gene expression after LPS stimulation. eqFLS were stimulated with LPS for 24 hours to achieve a pro-inflammatory response. Gene expression levels were analyzed using RT-qPCR and compared to a baseline control GAPDH (Table 2.1). As described in Materials and Methods, statistical analysis (*) indicates a significant difference at $p < 0.05$ relative to DMSO control.

2.3.3 Optimizing the concentration of vehicle (DMSO) that would not detrimentally affect eqFLS viability

DMSO was selected as a solvent or vehicle for our compounds since these drugs are under development and typically have poor solubility in water. The disadvantage is that DMSO can have toxic effects on cells' viability and normal morphology (Lee & Park, 2019). A reference suggested that a final vehicle concentration greater than 1% DMSO might reduce eqFLS cell viability (Chen & Thibeault, 2013). Our novel compounds, C3 and 02-09, and the positive control peptide mimic of the PEDF/LAMR interaction (P18), were delivered in DMSO

concentrations at or below the 1% DMSO mark. We investigated the influence of DMSO on eqFLS viability using a Cell Counting Kit-8 (CCK-8), as mentioned in Section 2.2.6. We evaluated the effects of two different concentrations of DMSO, 0.1 % and 1.0 % of the total media volume, on the cell viability of eqFLS and found significant differences relative to untreated control for both effects. We observed that a higher concentration of DMSO (1.0 % of media volume) significantly impacted cellular viability during a 120-hour assay (a ~ 40% reduction). The relative value (%) of eqFLS viability was significantly higher for the lower DMSO concentration (0.1 % of media volume) at both 72 and 120 hours, suggesting the 0.1% DMSO should be selected for further studies, as it does not seem to impact eqFLS viability detrimentally. These findings were consistent with the literature, although it was surprising that our cells were more sensitive to the impact of 1% DMSO than prior reports.

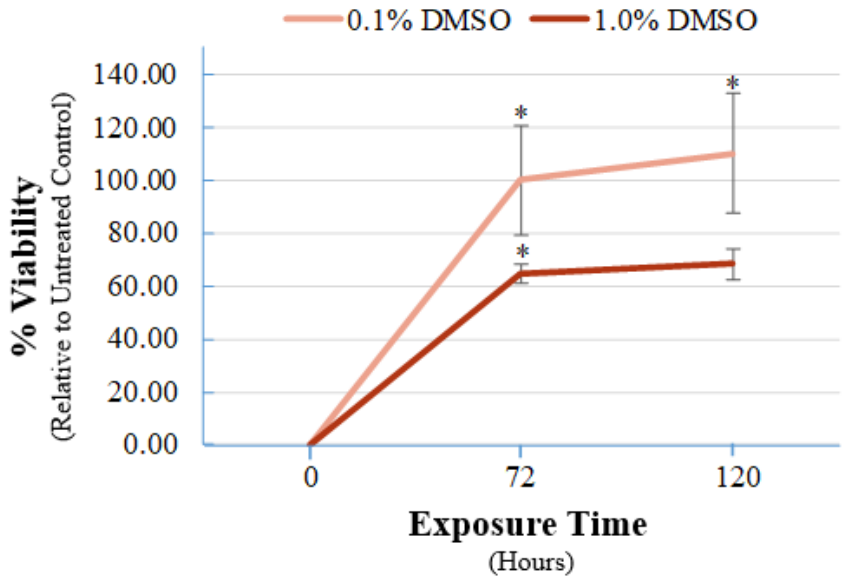

Figure 2.7 Effect of DMSO on eqFLS viability. CCK-8 assay results at 0, 72, and 120 hours cultured with complete growth media. A baseline plate reading at 0 hours was obtained to normalize for variations. Microsoft Excel was utilized for analysis with a significance of $p < 0.05$, and both DMSO groups ($n = 3$, mean ± SEM) were compared to cells-only control. Statistical analysis as described in Materials and Methods, where (*) indicates a significant difference at $p < 0.05$.

2.3.4 Novel compounds did not significantly reduce cell viability of eqFLS

Considering that the novel compounds, C3 and 02-09, and positive control, P18, were dissolved in DMSO and the interaction of the vehicle and the compounds is unknown, we

wanted to investigate the impact of these compounds on eqFLS viability relative to DMSO alone. Using the CCK-8 assay, we found that the novel compounds did not dramatically impact the overall cellular viability on Days 3 and 5. Different concentrations of the compounds either enhanced or slightly reduced the viability of eqFLS. Several concentrations enhanced the viability of eqFLS under these normal culture conditions (non-inflammatory). The viability of eqFLS remains close to the same for P18 at 5 μM for Days 3 and 5, with the highest viability % among the other P18 concentrations, indicating that higher concentrations of P18 may impact eqFLS viability. Based on other prior work from the lab indicating promising effective concentrations of 10-25 μM for C3 and 02-09 for other cell lines, we selected a concentration of 10 μM for using the control and novel compounds in future study designs and the favorable viability date (Figure 2.8).

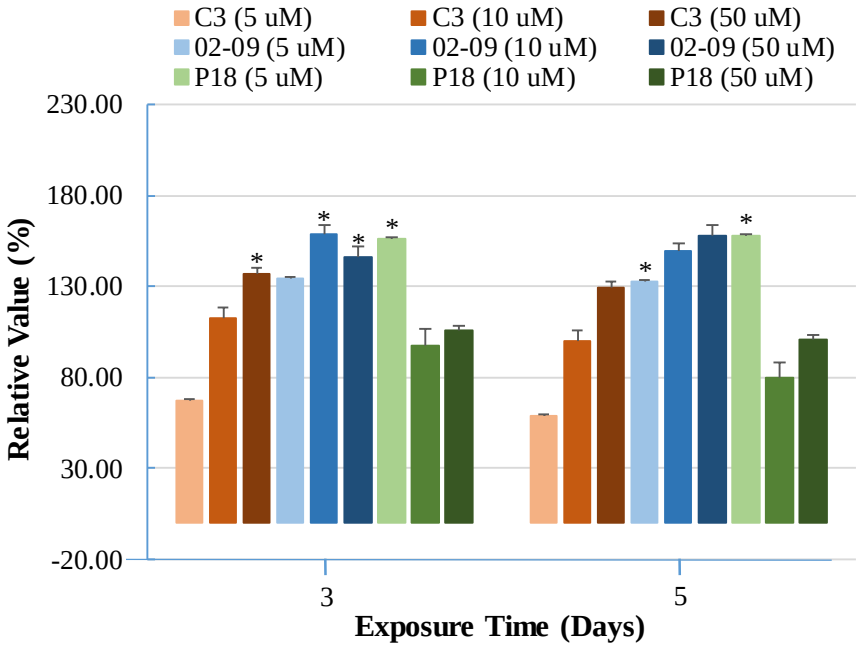

Figure 2.8 eqFLS viability following treatment with novel compounds. CCK-8 assay results at day 3 and day 5 post-seeding and cultured in complete growth media. A baseline plate reading at 0 days was obtained to normalize for variations, and treatment groups (n = 3, mean ± SEM) were compared to cells-only control. Statistical analysis as described in Materials and Methods, where (*) indicated a significant difference at $p < 0.05$.

2.3.5 Novel compounds C3 and 02-09 demonstrated similar downregulation of inflammatory response as DMSO control in Study Design A

Study Design A, mentioned in Section 2.2.5, was utilized as an initial *in vitro* model to test the effectiveness of the novel compounds against the inflammatory response of LPS-stimulated eqFLS. A comparison of -/+ LPS in the control sample showed an upregulation of IL-6 expression in eqFLS upon LPS stimulation. Thus, LPS appeared successful in promoting a pro-inflammatory response in eqFLS. However, the DMSO vehicle appeared to dampen the IL-6 inflammatory gene expression induced by LPS. Interestingly, the literature suggests some anti-inflammatory activity for DMSO in equine joints (Brien et al., 2008). The compound C3 significantly reduced IL-6 relative and DMSO, although this was significantly different (#, $p < 0.05$) in LPS-stimulated eqFLS (Figure 2.9). The fold change among the groups was so similar (~1.34-1.69 ± 0.03-0.08), indicating that the DMSO either reduced the LPS stimulation of IL-6 in this design or Study Design A was likely not a good model for examining the compound performance relative to the vehicle in downregulating IL-6. However, P18 significantly decreased IL-6 relative to the control.

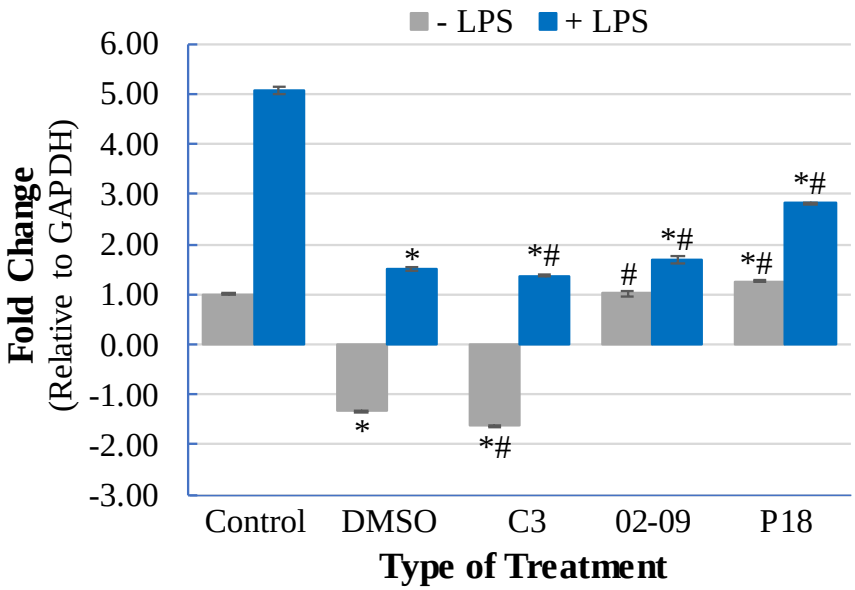

Figure 2.9 IL-6 gene expression utilizing Study Design A with LPS. Expression of IL-6 cytokine from eqFLS cells using Study Design A consisting of washing the wells before +/- LPS stimulation and treatment with novel compounds, C3 and 02-09 at 10 μM, compared to DMSO control and normalized to GAPDH (n = 3, mean ± SEM). A delta-delta C(T) method was used for calculating gene expression changes and statistical analysis as described in Materials and Methods, where (*) indicates a significant difference at $p < 0.05$ relative to control and (#) represents a significant difference relative to DMSO with $p < 0.05$.

2.3.6 The derivative compound 02-09 showed a promising ability to downregulate the eqFLS inflammatory response in Study Design B

Study Design B, mentioned in Section 2.2.5, was utilized next as an *in vitro* model to test the effectiveness of the novel compounds against the LPS-mediated eqFLS inflammatory response. A comparison of the effect of -/+ LPS in the control sample showed upregulation of IL-6 expression in eqFLS. In this design, LPS appeared to induce a pro-inflammatory response in eqFLS, as seen by an upregulation in IL-6 levels; however, the levels reached were more modest than with Study Design A. DMSO appeared not to attenuate the LPS-induced IL-6 gene expression in this design. C3 with LPS stimulation did not show a promising trend among the treatment groups. Its fold change (2.15 ± 0.06) was close to both DMSO and P18, making it ineffective in downregulating the inflammatory response of eqFLS (Figure 2.10). C3 and 02-09 appeared to reduce IL-6 gene expression without LPS stimuli. However, 02-09 with LPS stimulation further (though slightly relative to 02-09 lacking LPS) downregulated IL-6 with a fold change of -3.31 ± 0.02. Considering that 02-09 was significantly downregulated compared to the controls, we proposed that Study Design B was a potential model for downregulating the inflammatory expression of LPS-stimulated eqFLS. 02-09 is an analog to C3, so this may also indicate that the second generation of the compounds is becoming more efficient in controlling the inflammatory response of LPS-stimulated cells. This study design was more representative of more complex *in vivo* conditions, considering that the inflammatory stimulation is present throughout the entire study, rather than being removed, as in Study Design A.

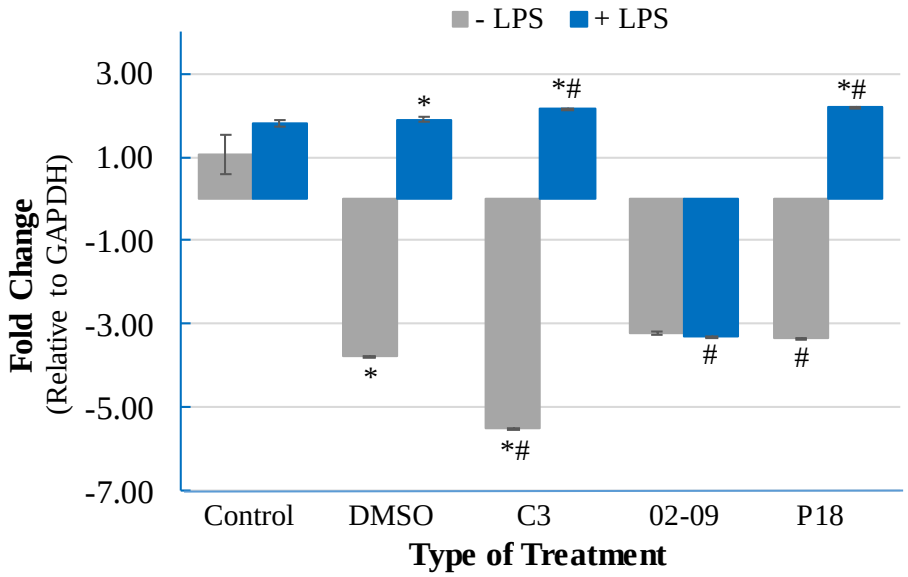

Figure 2.10 eqFLS IL-6 gene expression utilizing Study Design B with LPS. The expression of IL-6 cytokine from eqFLS cells using Study Design B consisted of +/- LPS stimulation and treatment with novel compounds, C3 and 02-09 at 10 μM, compared to DMSO control normalized to GAPDH (n = 3, mean ± SEM). A delta-delta C(T) method was used for calculating gene expression changes and statistical analysis as described in Materials and Methods, where (*) indicates a significant difference at $p < 0.05$ relative to control and (#) represents a significant difference relative to DMSO with $p < 0.05$.

2.3.7 The expression trends were not substantial between non-stimulated and LPS-stimulated eqFLS in Study Design C

Study Design C, mentioned in Section 2.2.5, was utilized as an *in vitro* model to test the effectiveness of the novel compounds for reducing gene expression representing the inflammatory response of LPS-stimulated eqFLS. The LPS control had a robust and significant fold change (284.37 ± 3.38) relative to the control without LPS (1.00 ± 0.05), validating that eqFLS can upregulate pro-inflammatory genes at elevated levels when stimulated with LPS. The gene expression of key inflammatory mediator IL-6 with C3 and 02-09 was our primary response investigated in LPS-stimulated eqFLS. The compounds effectively downregulated the IL-6 in eqFLS; however, there were no significant differences among the groups (Figure 2.11). The IL-6 expression fold changes for C3 (13.49 ± 0.15) and 02-09 (11.87 ± 0.36) were similar to the DMSO control (13.14 ± 0.15), suggesting Study Design C was not ideal for studying the inflammatory response of eqFLS.

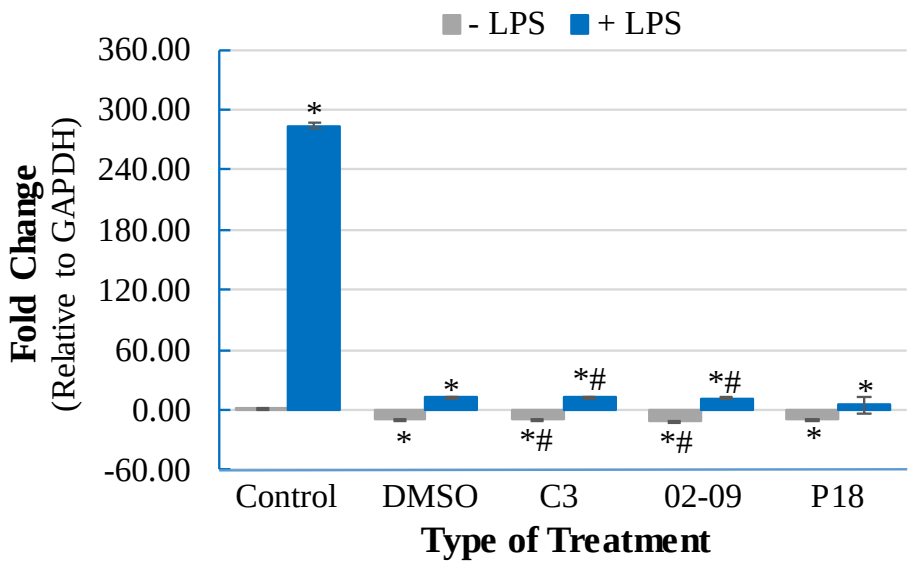

Figure 2.11 eqFLS IL-6 gene expression utilizing Study Design C with LPS. Expression of IL-6 cytokine from eqFLS cells using Study Design C consisting of treatment with novel compounds, C3 and 02-09 at 10 μM, and then +/- LPS stimulation, compared to DMSO control and normalized to GAPDH (n = 3, mean ± SEM). A delta-delta C(T) method was used for calculating gene expression changes and statistical analysis as described in Materials and Methods, where (*) indicates a significant difference at $p < 0.05$ relative to control and (#) represents a significant difference relative to DMSO with $p < 0.05$.

2.3.8 IL-6 gene expression was the best marker for assessing the pro-inflammatory activity of eqFLS in response to TNF-α

We next wanted to investigate whether TNF-α could replace the use of LPS as stimulation in initiating the pro-inflammatory response of eqFLS (Figure 2.12). We stimulated eqFLS with TNF-α for 24 hours and analyzed the gene expression of various pro-inflammatory cytokines and mediators selected from literature for TNF-α stimulation of both human and equine FLS. All the analyzed genes were upregulated to such a high extent that we present the fold changes on a logarithmic ($\log_{10}$ base) scale. The IL-6-fold change was 113.02 ± 0.46, and IL-8 had a fold change of 146.54 ± 1.97. The fold change of IL-1α was the lowest value at 1.15 ± 0.07. We established that TNF-α was effective in initiating the pro-inflammatory response of eqFLS, and it elicits fold changes greater than with LPS stimulation for a similar incubation time. Thus, TNF-α was utilized in the studies to establish a model that represented a relatively more robust inflammatory response of eqFLS.

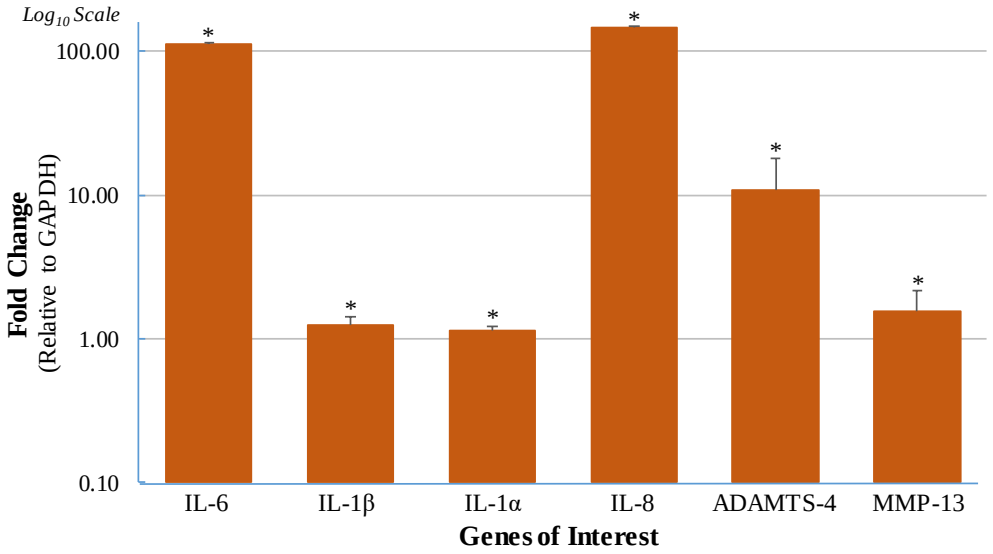

Figure 2.12 eqFLS gene expression after TNF-α stimulation. eqFLS were stimulated with TNF-α for 24 hours to achieve a pro-inflammatory response relative to control. Gene expression levels were analyzed using RT-qPCR and compared to a baseline control GAPDH (Table 2.1). The fold change was presented on a $\log_{10}$ base scale. Statistics were as described in Materials and Methods, and significant differences represented with (*) at $p < 0.05$.

2.3.9 Stimulation of eqFLS with TNF-α promoted a higher and more reliable upregulation of IL-6 expression as compared to LPS stimulation

We established that IL-6 gene expression was the best marker among those assayed for detecting the pro-inflammatory response of eqFLS when stimulated with LPS; however, we wanted to confirm if the same would be true for TNF-α stimulation. We evaluated TNF-α at a 10 ng/mL concentration, following the protocol mentioned in Section 2.2.3, and compared its effects on gene expression relative to LPS stimulation. After stimulating eqFLS with either LPS or TNF-α, we observed a significant upregulation of IL-6 with TNF-α relative to LPS (Figure 2.13). At 24 hours, IL-6 expression was increased by 113.55 ± 7.61-fold with TNF-α, whereas LPS mediated an IL-6-fold change of only 4.65 ± 1.07. The IL-6 expression fold change gap increased at 72 hours, and fold change extensively increased at 72 hours, with TNF-α at 720.41 ± 132.26 and LPS at 673.02 ± 12.45. IL-6 gene expression was maintained at significantly higher levels at 72 hours for TNF-α. Thus, this result characterized that TNF-α has a stronger influence on initiating the pro-inflammatory response of eqFLS than the LPS stimulus at the earlier (24h or 48h) timepoints, although both can sustain their expression for the period assayed.

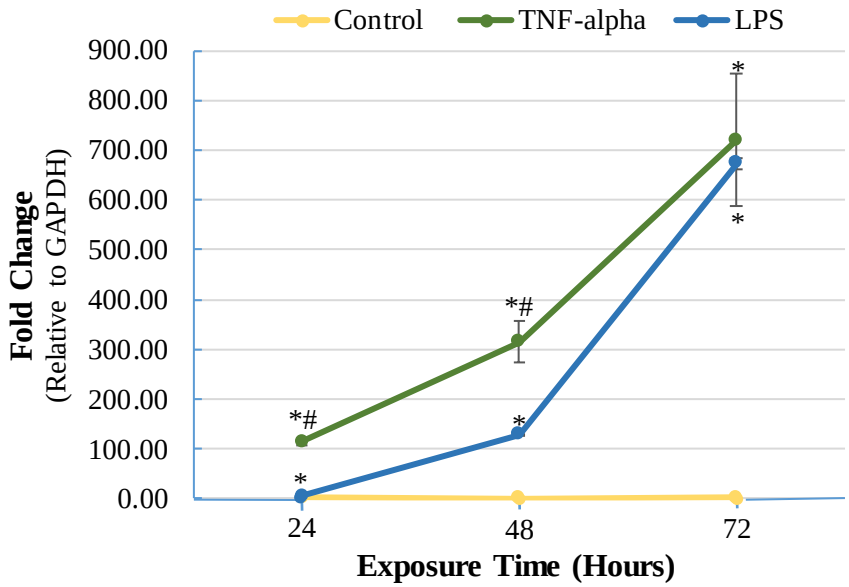

Figure 2.13 eqFLS IL-6 gene expression with TNF-α or LPS stimulation. eqFLS were stimulated with LPS or TNF-α for a duration of 72 days to assay for IL-6 expression, a pro-inflammatory response. IL-6 gene expression levels were analyzed using RT-qPCR and compared to a baseline control GAPDH (Table 2.1). Statistics were described in Materials and Methods, where (*) indicates a significant difference at $p < 0.05$ relative to control and (#) represents a significant difference relative to LPS with $p < 0.05$.

2.3.10 Study Design B with TNF-α stimulation might be the best model for inducing a pro-inflammatory response of eqFLS that can be used to test anti-inflammatory compounds.

Study Design B, mentioned in Section 2.2.5, was utilized as an *in vitro* model to test the effectiveness of the novel compounds against the TNF-α-stimulated inflammatory response of eqFLS. TNF-α alone upregulated IL-6 expression of eqFLS by a small amount (control -/+ TNF-α; Figure 2.14), where the cells treated with TNF-α showed only a 13% increase in gene expression. Interestingly, in the DMSO vehicle, TNF-α successfully reproduced a pro-inflammatory response in eqFLS as assessed by a significant increase in IL-6 expression (~12-fold). However, C3 was inefficient in preventing TNF-α-stimulated IL-6 upregulation among the treatment groups. However, 02-09 and the P18 (positive control) were efficient in reducing or maintaining IL-6 expression at levels like that of control in the presence of TNF-α stimulation.

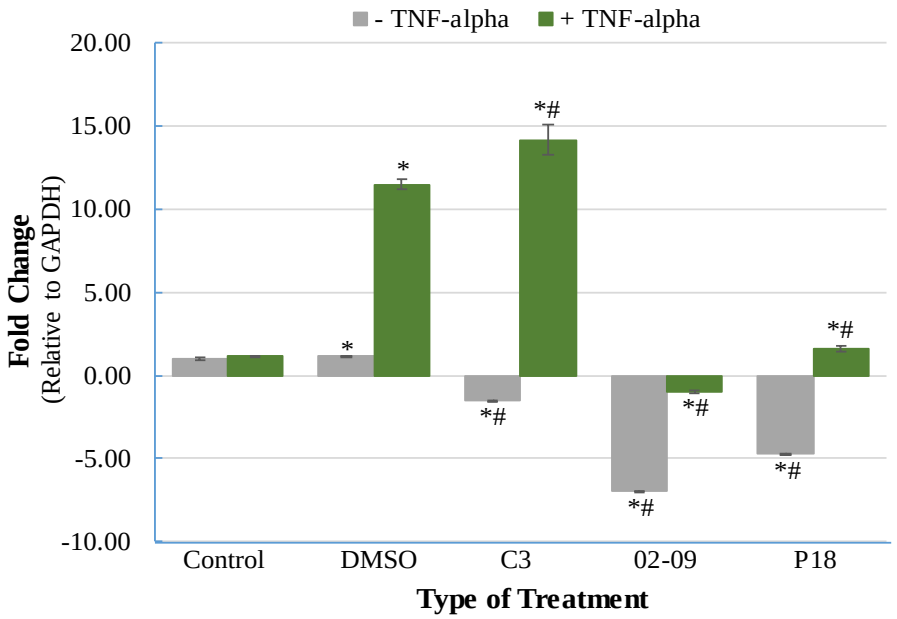

Figure 2.14 eqFLS IL-6 gene expression utilizing Study Design B with TNF-α. Expression of IL-6 cytokine from eqFLS cells using Study Design B consisting of +/- TNF-α stimulation and treatment with novel compounds, C3 and 02-09 at 10 μM, compared to DMSO control and normalized to GAPDH (n = 3, mean ± SEM). A delta-delta C(^{T}) method was used for gene expression analysis. Statistics were as described in Materials and Methods and significant differences where (*) indicates a significant difference at $p < 0.05$ relative to control and (#) represents a significant difference relative to DMSO with $p < 0.05$.

2.3.11 Novel C3-derivative compound, 02-09, seems promising in downregulating pro-inflammatory cytokines and mediators

Study Design B was utilized, as mentioned in Section 2.2.5, which stimulated eqFLS with TNF-α for 24 hours, treated with control and novel compounds, and then collected the cell samples for further processing and gene analysis. A heatmap with a color-coding system was developed to represent the up- and downregulation of the various pro-inflammatory cytokines and mediators (i.e., IL-1β, IL-1α, ADAMTS-4, MMP-13, IL-6, and IL-8) across multiple experiments. The heatmap enabled a quick visualization of all groups. The red color represented an upregulation in gene expression (fold change relative to the GAPDH housekeeping gene). The green color represented a downregulation in gene expression relative to GAPDH (Figure 2.15). This representation illustrated that C3 was not as effective as 02-09 in downregulating or reducing the inflammatory response of eqFLS to TNF-α. The expression of pro-inflammatory cytokine IL-1β was the most downregulated when 02-09 was used relative to C3. This pattern

matched that of the positive control, P18, although limitations to this data have included downregulation of genes also being detected at times in -TNF groups.

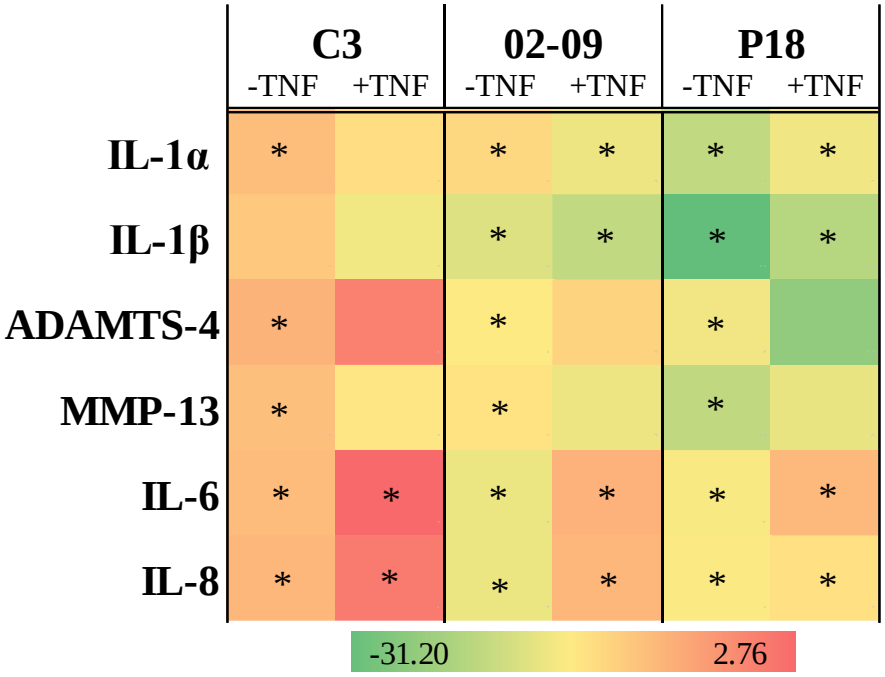

Figure 2.15 Heatmap representing gene expression changes in response to compound treatment and corrected to vehicle (DMSO) control utilizing Study Design B. The heatmap represents the up-and downregulation of the pro-inflammatory cytokines and mediators +/- TNF stimulation for 24 hours. Upregulation is signified with red with the highest fold change reaching 2.76, and downregulation is signified with green with the lowest fold change reaching -31.20. This map was generated using Microsoft Excel, and delta-delta C(T) method was used for gene expression analysis. *, $p < 0.05$ relative to DMSO control

2.4 Discussion

Cells were initially isolated from the synovial membrane of equine joints utilizing published protocols, and these cells appear to be morphologically eqFLS. From the literature, we know that the synovium comprises a heterogeneous cell population (i.e., Type A and B cells, macrophages, fibroblasts) with Type B cells, or FLS, making up almost 90% of the population (Stefani et al. 2019; Valencia et al. 2004). Our cell cultures are consistent with an FLS morphology, where the cells have a larger nucleus, a distinctive ER distributed throughout the cytoplasm, and spindle-like protrusions from the cell body, as compared to the physical appearance of normal fibroblasts, Type A cells (MLS), and MSCs (Shikichi et al. 1999). This

cell population should be enriched for adherent cells consistent with eqFLS since monocytic cells would have been removed from the cultures when expanding into 100 mm plates. Thus, passages of 4 and no greater than 12 (P4-P12) were utilized for experimentation to ensure the cultures comprised FLS and that their maintained viability. FLS are also known to form a network or sheet-like structure when cultured over 10 days with a complete growth medium supply. This supports a recent study that suggested that FLS have the intrinsic capacity to form a lining-like layer *in vitro,* reminiscent of their roles in the synovium as components of a synovial membrane structure that supply constituents to the articular cartilage ECM (Prado et al., 2015; Shikichi et al. 1999).

To help characterize the FLS cell population in the samples, we sought to analyze common surface markers. We analyzed the relative gene expression of surface markers thought to be specific to FLS from human cell studies (SAMD9L and PKX) in comparison to surface markers specific to MSCs (CD90 and CD44), as well as inflammatory markers (IL-6 and IL-8). This experiment consisted of expanding eqFLS, equine bone marrow-derived MSCs (eqBM-MSCs), and equine adipose-derived MSCs (eqASC). Once the three different cell populations reached 70-80% confluence, they were harvested and processed for gene expression analysis using RT-qPCR. From this experiment, the trends were not as expected; however, we did observe that eqBM-MSCs and eqASCs showed a higher gene expression of CD44 and CD90 than eqFLS. The FLS did not express surface markers PXK and SAMD9L as expected, but this could be due to them not being ideal markers for eqFLS compared to human FLS. This data was not shown but instead used as a reference for better classifying FLS to be an independent cell type within the isolated samples. Future directions may involve characterizing the eqFLS population isolated here in more detail using flow cytometry to confirm or discover FLS-unique equine markers.

We next investigated the inflammatory response of eqFLS in an *in vitro* model that attempted to mimic factors and conditions which may initiate inflammation in OA. We initially utilized lipopolysaccharide (LPS) to induce an inflammatory response in eqFLS, effective in previous studies with human FLS (Jin et al., 2016). We found that LPS-stimulated eqFLS showed a significant upregulation of IL-6 and ADAMTS-4 by RT-qPCR. From the literature, we know that IL-6 is expressed in strong association with inflammation (Choi et al. 2010; Schröder

et al. 2019), and this was an inflammatory phenotype confirmed by this experiment. However, other pro-inflammatory cytokines and mediators (i.e., IL-1β, MMP-13, and TNF-α) also expected to be upregulated showed downregulation of gene expression in this setting, reflecting the timing or pattern of expression differences between humans and equine for the LPS stimulus.

Once we established that LPS was effective in at least activating an inflammatory response in eqFLS that could be detected via IL-6 upregulation, we wanted to test the efficacy of our novel compounds in suppressing the inflammatory response. These novel compound series, which included C3 and 02-09, started being developed in 2018 in our laboratory (Umbaugh et al., 2018) and have shown promising effects in reducing inflammation and promoting cartilage regeneration in other pilot projects using equine or human cells (Haffner et al., 2017; Keating et al., 2019). These compounds have initially been tested in the context of LPS as a stimulus for human macrophages (Haffner et al., 2017). However, for eqFLS, we needed to examine study design variations to enhance the effect of LPS on inflammatory gene expression to enable us to detect any therapeutic impact of suppression of inflammation (by C3 and 02-09). Before developing an in vitro model that encapsulates these effects, we considered many variations. There is no data shown, but we found that for eqFLS, the utilization of 6-well plates was necessary for optimal RNA concentration yields relative to 24-well plates. We also found that Opti-MEM Reduced-Serum Medium (Gibco) was better suited for experimentation, considering it did not influence the growth rate or morphology of eqFLS. The effects of Opti-MEM were likely due to its reduced serum content but may indicate a positive impact of several supplements within the media, including insulin, transferrin, hypoxanthine, and thymidine.

It was also of interest to analyze the impact that the control compounds DMSO (- Ctrl) and P18 (+ Ctrl) and the novel compounds (C3 and 02-09) could have on the viability of eqFLS by utilizing a cell viability screen. This assay allowed us to determine an effective compound concentration range that would not impact the normal viability and function of eqFLS. Thus, we found that a lower concentration of DMSO (0.1 % media volume) did not significantly harm the viability of eqFLS over a 120-hour assay. We also found that the compounds did not significantly reduce the cellular viability on Days 3 and 5, which was favorable since these were

non-inflammatory conditions (i.e., the therapeutics may not harm normal cells). Finally, the cellular viability at 10 μM was the lowest concentration that significantly enhanced viability when using derivative compound 02-09; thus, a standardized concentration of 10 μM was utilized for control and novel compounds in future study designs.

We established a model that would induce inflammation in eqFLS with LPS and allow us to detect reduced pro-inflammatory gene expression by the novel compounds (C3 and 02-09). We developed and tested three study designs (A, B, and C). Study Design A represented a "treatment" approach, where eqFLS were initially stimulated with LPS and then treated with novel compounds. However, this design removed the stimulus (LPS) before adding the control and novel compounds, making Study Design A less relevant relative to *in vivo* models of OA. Nonetheless, it allowed us to compare the novel compounds' impact on counteracting the initial LPS stimulation. From Study Design A, we learned that LPS effectively stimulated eqFLS, although the compounds were not quite efficient in downregulating IL-6 expression. On the other hand, Study Design B was more likely to be relevant as a "treatment" design. The LPS stimulus was not removed after 24 hours; eqFLS were stimulated for the duration of the experiment, which better represented the occurrence of inflammation in an OA-affected joint. In Study Design B, C3 with (+) LPS-stimulated eqFLS did not show a promising trend; however, 02-09 significantly downregulated IL-6 compared to C3 and the DMSO and P18 controls. Thus, Study Design B was a promising model for downregulating the inflammatory response of LPS-stimulated eqFLS. It also supported some prior data from the lab (Keating et al., 2019; Haffner et al., 2017) that the second-generation compound, 02-09, could be more effective than C3. Study Design C represented a "preventative" approach, as eqFLS were exposed to the novel compounds prior to LPS stimulation. The magnitude of IL-6 upregulation was higher in this design, but, in Study Design C, there were no significant differences among any of the groups, making it suboptimal for studying the inflammatory response of eqFLS. Therefore, among the three study designs, we found that Study Design B was the most promising in allowing us to obtain an inflammatory response in LPS-stimulated eqFLS.

Even though we determined that Study Design B seemed promising as an *in vitro* model of OA inflammation, we wanted to investigate the effects of an alternative stimulus that could

elicit more robust gene expression changes for testing the impact of the novel compounds. For this purpose, we selected tumor necrosis factor-alpha (TNF-α) for inducing an inflammatory response of eqFLS. TNF-α has been implicated in joint degeneration and is one of the most prominent cytokines in the acute OA stages (Kamm et al., 2010). We were first interested in examining its impact on eqFLS by utilizing a cell viability screen, finding that TNF-α had less impact than LPS on cellular viability. We noted that 24 hours would be a good exposure time to accomplish an inflammatory response of eqFLS. By using TNF-α as an alternative stimulus to LPS, we found a significant upregulation (~10-fold change) of all pro-inflammatory cytokines and mediators assayed (i.e., IL-6, IL-1β, IL-1α, IL-8, ADAMTS-4, and MMP-13), suggesting that TNF-α might more uniformly promote the NF-κB pathway and its target genes to stimulate inflammation responses in FLS (Ding et al., 2019). With TNF-α stimulation, the IL-6 gene expression was also an excellent marker for detecting the inflammatory response of eqFLS, with TNF-α inducing a 10-fold increase relative to LPS at 24 hours. Once we discovered that TNF-α could be a more uniform and robust inflammatory stimulus in FLS, we applied it in Study Design B. We observed that TNF-α could initiate a ~13% increase in pro-inflammatory gene expression in eqFLS relative to untreated control, but not in vast amounts compared to previous designs. C3 was inefficient in preventing TNF-α stimulated IL-6 upregulation among the treatment groups. However, 02-09 and the P18 PEDF mimic peptide (+ Ctrl) were efficient in reducing or maintaining IL-6 expression at levels like control in the presence of TNF-α stimulation, although limitations to this data have included downregulation of genes also being detected at times in -TNF groups.

We expanded the gene expression analysis, utilizing Study Design B with TNF-α, and represented the data with a heatmap that illustrated that the pro-inflammatory cytokine IL-1β was the most downregulated when 02-09 was used relative to C3. This pattern matched that of the positive control, P18. Also, 02-09 was promising at downregulating most of the genes of interest assayed (i.e., IL-1α, IL-1β, IL-6); either due to the 02-09's compound derivative structure having a higher affinity for binding with LAMR1 or an ability to induce more potent effects at the same effective concentration (10 μM) via additional targets.

In closing, we have thus far established a preliminary yet novel, eqFLS-based *in vitro* model with flexible designs that can induce various pro-inflammatory genes in response to LPS or TNF-α, which can be examined for testing the efficacy of novel compounds such as 02-09 by gene expression changes. However, it is challenging to fully understand the inflammatory response of eqFLS and how different signaling pathways come into play, considering that this model only captures inflammatory marker expression at specific time points rather than analyzing cellular activity in real-time. Chapter 3 of this thesis explores an IL-1β promoter cell-based drug screen that would provide a better understanding of the inflammatory response in eqFLS, at least in what pertains to the IL-1β mediator expression, and how effective our novel and future series of molecules can be in counteracting the inflammatory response in FLS.

CHAPTER 3. DEVELOPMENT OF AN IL-1B PROMOTER-GFP CELL-BASED DRUG SCREEN FOR REAL-TIME REPORTING ON THE INFLAMMATORY RESPONSE OF EQUINE SYNOVIOCYTES

3.1 Introduction

As discussed in Chapters 1 and 2, FLS have shown to be vital for the joint-destructive process seen in OA and participate by secreting abundant inflammatory cytokines and promoting inflammatory cell infiltration (macrophages) that contribute to local and systemic inflammation (Moradi et al., 2015; Nair et al., 2012; Qiao et al., 2020; Stefani et al., 2019). TNF-α and IL-1β are increased in OA-affected joints (Kamm et al., 2010; Shen et al., 2014), and both contribute to the increased activity observed in the NF-κB and MAPK signaling pathways (Sharma et al., 2020; Shen et al., 2014; Wang & He, 2018). The intermediates of the NF-κB and MAPK pathways, in turn, upregulate the expression of MMPs, cyclooxygenase-2 (COX-2), prostaglandins, and nitric oxide synthase (iNOS), promoting cartilage degradation and further increases in joint inflammation (Haseeb & Haqqi, 2013; Viana et al., 2020). These inflammatory and degradative processes can be modulated with recently described therapeutics (Wang et al., 2016). There is a promise for continued research into therapeutics that could help reduce the impact of TNF or IL-1β during OA development.

Past and recent studies of OA have concentrated on the role of the pro-inflammatory cytokine IL-1β, as it is known to exacerbate damage to articular cartilage once signaling through its pathway is initiated (Ji et al., 2016). IL-1β is produced and secreted by various cells, including FLS, as a 31 kDa precursor (pro-IL-1β) in response to specific molecular motif patterns, such as recurring protein folding or debris of cellular components (Lopez-Castejon & Brough, 2011). The process of IL-1β secretion is complex, considering that there are multiple mechanisms, including regulation by cyclophilin A (Yang et al., 2022), but each contributes to IL-1β-dependent inflammation (Lopez-Castejon & Brough, 2011). The mechanism of IL-1β secretion may influence the level of the inflammatory stimulus (e.g., TNF-α); for example, the IL-1β concentration must be relatively high to initiate an inflammatory response (Lopez-Castejon & Brough, 2011). Hence, detecting and monitoring the activity of IL-1β in a cellular

model (i.e., FLS) could help give insights into the type of influences (and thresholds) that activate its expression and how its secretion might be reduced. In the current work, we sought to use IL-1β expression to monitor the inflammatory response in FLS following pro-inflammatory stimuli treatment. Future studies could also aim to incorporate systems that would monitor its secretion.

Since we proposed monitoring IL-1β expression in a live cell-based screen, we chose to utilize transfection as a method for FLS gene modification. Typically, genetic material can be introduced into eukaryotic cells via various strategies, including cationic lipids such as Lipofectamine 2000 Transfection Reagent (Thermo Fisher Scientific) and physical electroporation such as the Neon Transfection System (Thermo Fisher Scientific). We sought to compare the transfection efficiency of FLS with plasmid DNA containing an IL-1β promoter driving expression of a marker gene, Green Fluorescent Protein (GFP), using two transfection techniques. These transfection methods have been utilized to study the activation of various signaling pathways and their downstream regulators. The novelty of our approach lies in utilizing an IL-1β promoter for querying in real-time the inflammatory response (or reduction thereof) in FLS cells.

Several methods exist to analyze cells post-transfection (i.e., flow cytometry, luminometry, fluorometry, microscopy). Fluorescent microscopy enables us to directly visualize positively transfected cells to analyze genetic material encoding for GFP expression. A fluorescent microscope can examine any differences among the groups qualitatively; however, quantitative analysis of transfection efficiency requires extensive cell counting and analysis, which is a daunting prospect with many replicates. It is thus desirable to use an image analysis software capable of counting positive cells over time to streamline the image collection and analysis. The IncuCyte Live-Cell Analysis System (Sartorius, Bohemia, NY) is an innovative system that enables visualization and quantification of cell marker gene expression or behavior over time by automatically gathering and analyzing images in real-time within a standard laboratory incubator (Figure 3.1).

We were interested in developing a screen-based analysis to detect IL-1β expression upon stimulation and monitor its expression in a real-time setting compared to previous studies. We obtained some insights into the biological impact of our novel therapeutic molecules on reducing

the inflammatory response of eqFLS. Consistent with our previous study design, it was interesting to monitor the inflammatory response of equine FLS (eqFLS) in a real-time analysis following TNF-α stimulation (100 ng/mL) and/or exposure to novel compounds, C3 and 02-09. Initially, we sought to obtain a promoter element that could be translatable between equine cells and human cells for potentially screening drugs with promise for treating inflammation in OA. The IL-1β promoter was chosen as this gene upregulation promotes increased levels of IL-1β, a classical central mediator of several inflammatory processes in the joints of both species. Interestingly, a recent paper (Chou et al., 2020) with human OA single-cell RNA sequencing (scRNA-seq) characterization indicated that the most prevalent pathogenic synoviocyte in humans is monocytic, with crucial contributions also from synovial fibroblast (FLS) populations. IL-6 was widely expressed in synoviocytes, including FLS, whereas TNF-α and IL-1β were expressed in 60% of acquired cells, including chondrocytes. Another interesting observation was that > 55% of crucial OA-related cytokines (e.g., TNF-α, IL-1β, IL-1α, and IL-6) were produced by synoviocytes (Chou et al., 2020). Thus, this screen concept could also be extrapolated to other promoters active in FLS, monocytic cells, and/or chondrocytes for drug screening in either species.

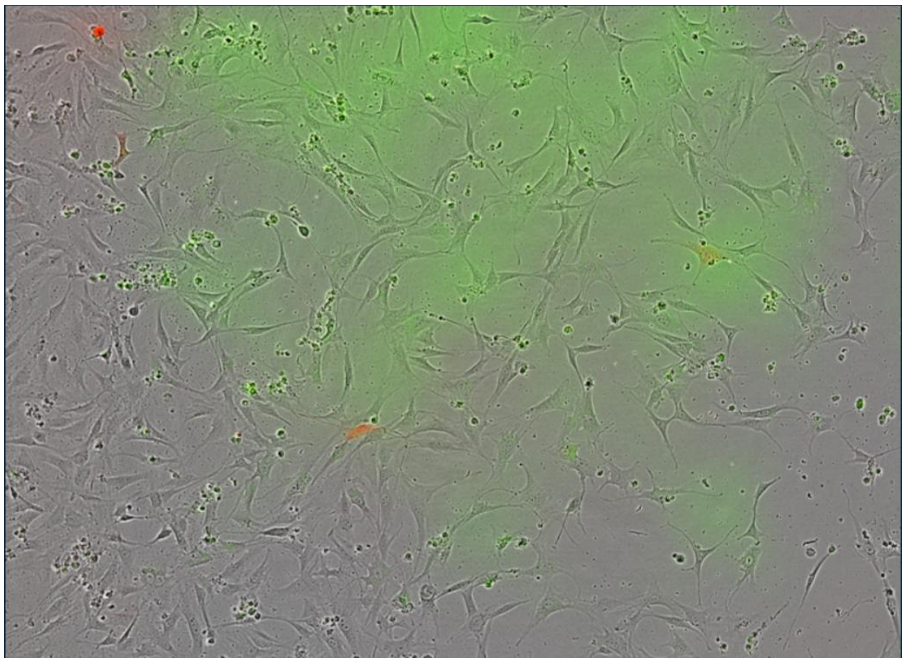

Figure 3.1 Unprocessed image from IncuCyte Live-Cell Analysis System (Sartorius) An image was obtained from the IncuCyte Live-Cell Analysis System (Sartorius) to show the appearance of images before analysis, in which the green background would be removed using 'spectral unmixing' and adjustment of other parameters on the software were performed before obtaining graphical representations.

3.2 Materials and Methods

3.2.1 Cell culture

eqFLS were isolated following the protocol described in Section 2.2.1. Before experimentation, eqFLS were expanded on non-coated 100 mm culture dishes (Corning) at passages no higher than P12 in the complete growth medium, consisting of 500 mL high glucose DMEM (Gibco), 50 mL of FBS, and 5 mL of Antibiotic-Antimycotic solution (Gibco) and incubated at 37^{o}C in a controlled CO_2 atmosphere until 70-80% confluence with media changes every 3-4 days. At confluence, the cells were harvested using 0.25% Trypsin-EDTA (Gibco) and, dependent on the experiment, seeded in a 96-well plate at no less than 2.5 x 10^4 cells/well. The culture media conditions varied in some experiments, as noted in other methods and results.

3.2.2 DNA plasmid information

Three different DNA plasmids were utilized: a control plasmid, pDr5.GFP2 (Invivogen, San Diego, CA) was initially used to test for the transfection efficiency of eqFLS. pDr5.GFP2 is

a DNA plasmid with the composite mCMV-hEF1-HTLV promoter sequence and features a GFP reporter cDNA sequence for monitoring promoter activity. The strength of the promoter was assessed qualitatively by using the Olympus 1X71 Inverted Fluorescence Microscope (Olympus Life Science Solutions, Waltham, MA). The second plasmid, pIL-1βp.GFP was designed by us and cloned by GeneCopoeia (Rockville, MD), using the human promoter region for the IL-1β gene. This promoter was determined to share a high homology both in sequence (75.6% by BLASTN) and in crucial transcription factor binding sites (PU.1 and CEBPA/B) using *Tfbind* software (Tsunoda and Takagi 1999). The equine IL-1β promoter was obtained from *e-Ensembl* (Cunningham et al. 2022) (e-Ensembl, 2022) using the sequence EquCab3.0:15:16416738: 16446697:1. This DNA plasmid would ideally serve as a reporter of IL-1β gene expression in real-time. It could be applied to screen a more considerable number of medium to high throughput compounds for the inflammatory response of eqFLS. The pIL-1βp.GFP plasmid consists of a pEZX-PF02.1 vector backbone with the hIL-1β promoter region driving a green fluorescence protein (GFP) cDNA expression. The third plasmid, pmCherry.N1 (Clontech, Mountain View, CA), was utilized as a cotransfection control marker for characterizing transfection efficiency transfected with pIL-1βp.GFP. pmCherry.N1 is a mammalian expression vector that can create fusion proteins with the mCherry on the N-terminus. However, we only used it for its red fluorescence properties as a transfection control (~2-5% of total plasmid DNA).

3.2.3 Transfection with Lipofectamine 2000 Transfection Reagent

eqFLS were at 70-80% confluence on the day of transfection. eqFLS were collected and counted to a cell density no less than 2.5 x10^4 cells/well for each transfection reaction. Lipofectamine 2000 Transfection Reagent (Thermo Fisher Scientific) was utilized for transfection and performed per the manufacturer's instructions. pIL-1β.GFP was transfected at 0.2 μg/well with pmCherry.N1, a cotransfection marker, calculated as 5% of the pIL-1βp.GFP concentration. The complexes were added to designated wells within the 96-well plate and then incubated at 37^{o}C in a controlled CO_2 atmosphere for 18-48 hours prior to testing expression for DNA plasmids under fluorescence detection methods.

3.2.4 Transfection with the Neon Transfection System

eqFLS were at 70-80% confluence on the day of transfection, with each transfection consisting of cells at a density no less than 2.5 x10^4 cells/well. eqFLS were prepared and transfected using the Neon Transfection System (Thermo Fisher Scientific), performed as per manufacturer's instructions. An optimization protocol was performed with a control plasmid containing a constitutive promoter (not inflammation-responsive), pDr5.GFP2, to test the transfection efficiency in eqFLS using this method. The optimization parameters used are shown in Table 3.1. The pIL-1β.GFP plasmid was transfected at 0.5 μg/well with pmCherry.N1, a cotransfection marker, was used at 5% of the pIL-1βp.GFP concentration. After transfection, eqFLS were directly transferred into a 96-well plate with 100 μL/well of pre-warmed DMEM (Gibco) media consisting of 50% FBS without antibiotics. eqFLS were incubated at 37ºC in a controlled CO_2 atmosphere to allow adherence before adding designated conditions to the wells. Testing expression for DNA plasmids was conducted immediately under fluorescent methods of analysis.

Table 3.1 Optimization of parameters of the Neon Transfection System. Using the Neon Transfection System, various parameters were utilized to optimize the transfection efficiency of eqFLS transfected with plasmid DNA. Protocol #5 from the manufacturer's guidelines for the Neon Transfection System was most successful in transfecting eqFLS with a transfection efficiency > 72%.

Optimization Number	Pulse Voltage (V)	Pulse Width (ms)	Pulse Number
#5	1,700	20	1
N/A	1,000	40	2
#16	1,400	20	2
#22	1,400	10	3
#24	1,600	10	3

3.2.5 Qualitative analysis of plasmid DNA transfection of eqFLS

eqFLS were transfected using either the Lipofectamine 2000 Transfection Reagent (Section 3.2.4) or the Neon Transfection System (Section 3.2.5), depending on the experiment. Expression levels of DNA plasmids, pDr5.GFP2, IL-1βp.GFP and mCherry.N1 were analyzed using the Olympus 1X71 Inverted Fluorescence Microscope (Olympus Life Science Solutions,

Waltham, MA). Data were collected as raw images from the Olympus cellSens Software, and qualitative analysis was performed to determine plasmid expressions. Quantitative analysis of pIL-1βp.GFP expression was further discussed in Sections 3.2.7 and 3.2.8.

3.2.6 Developing a method to screen eqFLS pro-inflammatory response

eqFLS were transfected as described in Section 3.2.2 and incubated at 37°C in a controlled CO_2 atmosphere in the IncuCyte Live-Cell Analysis System (Sartorius) to allow adherence and initial analysis of cell viability after transfection. eqFLS were stimulated (+/-) TNF-α or LPS at concentrations of 10, 50, 100, or 200 ng/mL and incubated for 24 hours. The pro-inflammatory response of eqFLS was assessed by detecting fluorescence signals from the pIL-1βp.GFP plasmid. The expression levels of pIL-1βp.GFP and pmCherry.N1 control were analyzed for up to 5 days to capture the inflammatory activity of eqFLS. Each sample condition was prepared in triplicates, and the average expression levels of IL-1βp.GFP was exported from the IncuCyte Live-Cell Analysis System (Sartorius) into Microsoft Excel for statistical analysis (Section 3.2.9).

3.2.7 Assaying the anti-inflammatory potential of compounds with eqFLS imaging

eqFLS were transfected following the methods in Section 3.2.5. After the incubation period, eqFLS were stimulated with TNF-α (100 ng/mL) for 24 hours and then exposed to control compounds DMSO (0.1%) or P18 (1 μM), and novel compounds C3 (10 μM) or 02-09 (10 μM) for an additional 24 hours. The expression levels of pIL-1βp.GFP and pmCherry.N1 were detected using the IncuCyte Live-Cell Analysis System (Sartorius). The expression of pIL-1βp.GFP was evident as green fluorescence, and the expression of pmCherry.N1 as red fluorescence signals. The expression levels of pIL-1βp.GFP and pmCherry.N1 control were analyzed for 5 days according to the conditions defined in Section 3.2.6. Each sample condition was prepared in triplicates, and the average expression levels of IL-1βp.GFP has been exported from the IncuCyte Live-Cell Analysis System (Sartorius) software into Microsoft Excel for statistical analysis (Section 3.2.9). Figure 3.2 shows the screening methodology for the anti-inflammatory response of novel compounds on eqFLS.

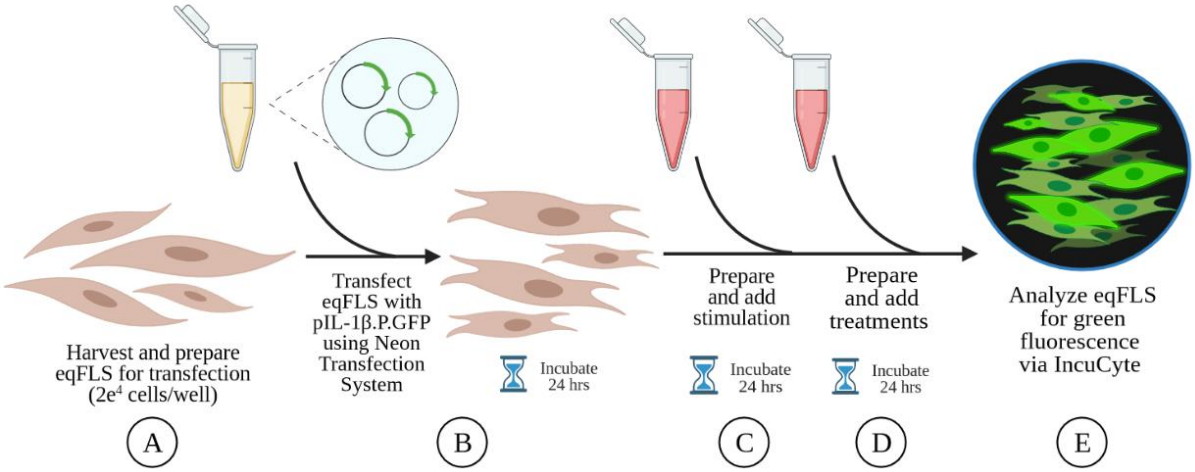

Figure 3.2 Methodology of the screen of eqFLS inflammatory response. eqFLS were harvested as mentioned in Section 3.2.1 and prepared for transfection (A). eqFLS were transfected with pIL-1.P.GFP plasmid and control vector pmCherry.N1 using the Neon Transfection System, directly transferred into a 96-well plate at a final concentration of 2.0 x 10^4 cells/well, and then incubated for 24 hours to allow adherence (B). eqFLS were stimulated with TNF-α (C), and then novel compounds or controls were added (D). The IncuCyte Live-Cell Analysis System (Sartorius) was used to detect the expression of the IL-1βp.GFP plasmid I. Diagram was created on BioRender.com.

3.2.8 Statistical analysis

All assays were performed using technical triplicates ($n = 3$) with values expressed as the mean ± standard deviation (SD), and statistical analysis was performed using the IncuCyte Live-Cell Analysis System (Sartorius) and exported into Microsoft Excel for the development of graphical representations. Comparisons among groups were analyzed using a 2-tailed *t*-test. A one-way ANOVA analysis defined statistical significance to compare across the groups using the mean and SD, with (*) indicating $p < 0.04$ (Girden 1992).

3.3 Results

3.3.1 The Lipofectamine 2000 Transfection Reagent was successful in transfecting plasmid DNA into eqFLS

eqFLS were transfected with plasmid DNA using the lipid-based reagent, Lipofectamine 2000 Transfection Reagent (Invitrogen), as mentioned in Section 3.2.3. A control plasmid, pDr5.GFP2 was applied at a final concentration of 0.2 ng/mL to evaluate the efficiency of this transfection method in eqFLS. We seeded at four different cell densities (10,000; 20,000; 30,000; and 40,000 cells/well) with four different Lipofectamine 2000 dilutions (0.2, 0.3, 0.4, and 0.5

μL) in Opti-MEM Reduced-Serum media (Gibco). The various groups were qualitatively analyzed using a fluorescent microscope (Section 3.2.5). We observed that a cell density of over 3,000 cells/well performed poorly regarding the negative transfection efficiency and viability of eqFLS. The 0.3 and 0.4 μL dilutions of the Lipofectamine 2000 reagent appeared to be more effective in the transfection protocol than 0.2 and 0.5 μL. It is evident that the Lipofectamine 2000 Transfection Reagent successfully transfected eqFLS; however, we were interested in trying various transfection methods to attain the highest transfection efficiency in eqFLS (Figure 3.3).

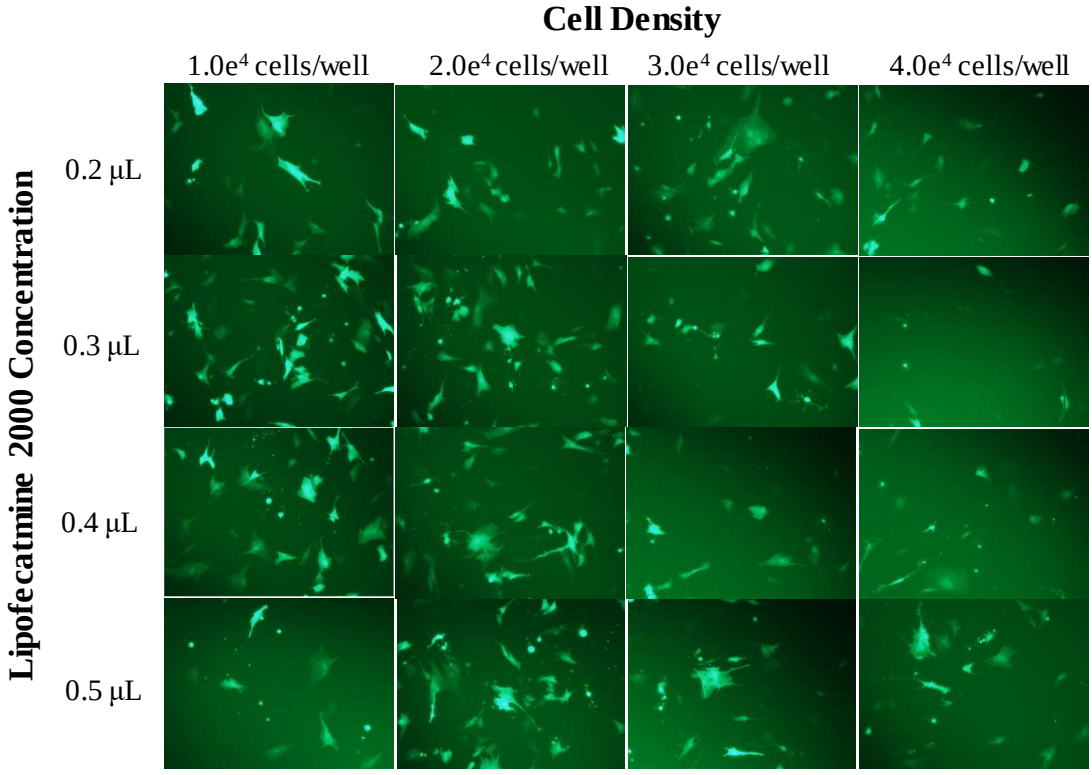

Figure 3.3 Transfection of eqFLS with Lipofectamine 2000 Transfection Reagent. eqFLS were transfected with control plasmid DNA, pDr5.GFP2, to determine the transfection efficiency among groups with 0.2, 0.3, 0.4, or 0.5 μL Lipofectamine 2000 reagent per transfection and cell densities of $1x10^4$ ($1.0e^4$), $2.0e^4$, $3.0e^4$, or $4.0e^4$ per well. Data was collected as raw images from the Olympus cellSens Software, and qualitative analysis was performed to determine the percent GFP+ to indicate transfection efficiency among the groups.

3.3.2 Optimization of parameters within the Neon Transfection System protocol revealed the most effective method for transfecting plasmid DNA into eqFLS

eqFLS were transfected with plasmid DNA using an electroporation transfection method, the Neon Transfection System, as mentioned in Section 3.2.4. eqFLS were prepared at a cell density of 2,000 cells/well and a control plasmid, pDr5.GFP2 was applied at a final concentration of 0.5 ng/mL to test the transfection efficiency of this transfection method. Various parameters were optimized in the initial transfection of eqFLS (Table 3.1). The expression level of the plasmid and the transfection efficiency among all groups were qualitatively compared using a fluorescent microscope (Section 3.2.5). It was evident that the plasmid was expressed with all the protocols, except in the control. Protocol number #5, shown in Figure 3.4B, appeared to be the most effective in transfecting pDr5.GFP2 into eqFLS, as its expression was detectable in virtually all eqFLS within the collected image. The transfection efficiency of protocol #5 using the Neon Transfection System was also compared to the Lipofectamine 2000 Transfection Reagent, shown in Figure 3.3. We observed that protocol #5 using the Neon Transfection System was the most efficient method of transfecting eqFLS with plasmid DNA compared to the Lipofectamine 2000 Transfection Reagent. Notably, the expression of pDr5.GFP2 was more prominent with protocol #5 using the Neon Transfection System than the Lipofectamine 2000 Transfection Reagent. The Neon Transfection System was a more efficient process of maintaining cellular count per transfection and allowed immediate analysis of plasmid expressions.

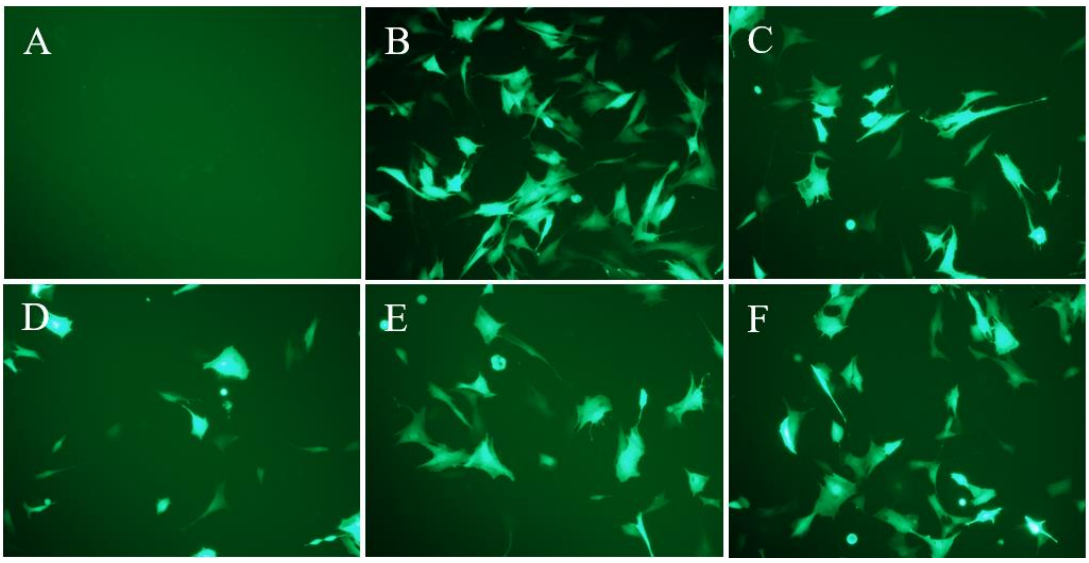

Figure 3.4 Optimizing parameters of transfecting eqFLS with the Neon Transfection System. eqFLS were transfected with plasmid DNA (pDr5.GFP2) at a 0.5 μg/well concentration using the Neon Transfection System. Various parameters were optimized to reveal the highest transfection efficiency with this transfection method: (A) control with no transfection, (B) transfection with optimization #5, (C) transfection with an unnumbered optimization protocol, (D) transfection with optimization #16, (E) transfection with optimization #22, and (F) transfection with optimization #24 (Table 3.1).

3.3.3 TNF-α stimulation showed more significant induction of IL-1βp.GFP expression relative to LPS stimulation

Once we established a method with the Neon Transfection System that matched the Lipofectamine 2000 Transfection Reagent and successfully transfected eqFLS with plasmid DNA, we moved forward with transfecting the plasmid for our inflammatory screen, pIL-1βp.GFP, with its cotransfection control marker, pmCherry.N1. It was of interest to analyze the effectiveness of LPS and TNF-α stimuli on initiating an inflammatory response in eqFLS assayed as changes in expression of the pIL-1βp.GFP plasmid. We qualitatively compared the expression levels of IL-1βp.GFP and mCherry.N1 between LPS and TNF-α stimulated eqFLS at various concentrations of inflammatory stimulus (50, 100, and 150 ng/mL) (Section 3.2.6). The mCherry.N1 plasmid was expressed among all the groups, suggesting the transfection method could be successful – the IL-1βp.GFP expression was not detected among the LPS stimulated groups, as shown in Figure 3.5. However, its expression was detectable after TNF-α stimulation at 50 and 100 ng/mL. This data provided us with the information that TNF-α was likely a better pro-inflammatory stimulus for promoting the expression of IL-1βp.GFP compared to LPS.

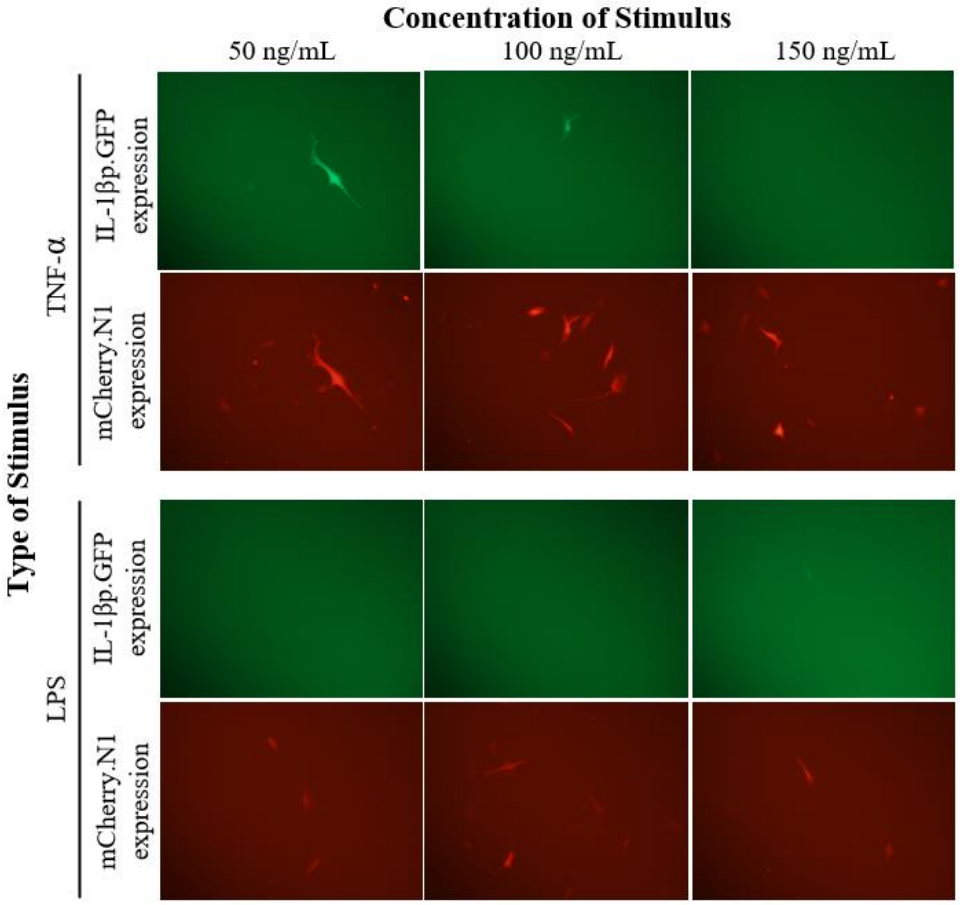

Figure 3.5 Expression of mCherry.N1 and IL-1βp.GFP after stimulation with LPS or TNF-α eqFLS were transfected with IL-1βp.GFP and pmCherry.N1 (Section 3.2.5) and stimulated with either LPS or TNF-α at various concentrations (50, 100, and 150 ng/mL). Images were obtained using the Olympus 1X71 Inverted Fluorescence Microscope. Data was collected as raw images from the Olympus cellSens Software, and groups were qualitatively analyzed for plasmid expressions.

3.3.4 TNF-α at a 100 ng/mL concentration promoted higher levels of IL-1βp.GFP expression relative to other concentrations

It was of interest to determine the most effective concentration of TNF-α to stimulate the expression of IL-1βp.GFP. eqFLS were stimulated with various concentrations of TNF-α (10, 20, 50, and 100 ng/mL (Section 3.2.7) and the expression of the IL-1βp.GFP plasmid was compared among all groups, as shown in Figure 3.6. Day 2 showed the first 24 hours at which the eqFLS were exposed to TNF-α, the expression of IL-1βp.GFP seemed to remain close to 0 and then increased on Day 3 to 100 ng/mL. After Day 3, IL-1βp.GFP expression significantly increased for TNF-α at 100 ng/mL and remained constant for 10, 20, and 50 ng/mL. IL-1βp.GFP

showed its greatest expression with TNF-α at a 100 ng/mL concentration, even though it showed an unexplainable pattern of reduced expression from Day 1 to Day 3, as do all the expression levels among these groups. From this, we can conclude that TNF-α at a 100 ng/mL concentration was promising for reaching the most significant and consistent expression increase with IL-1βp.GFP.

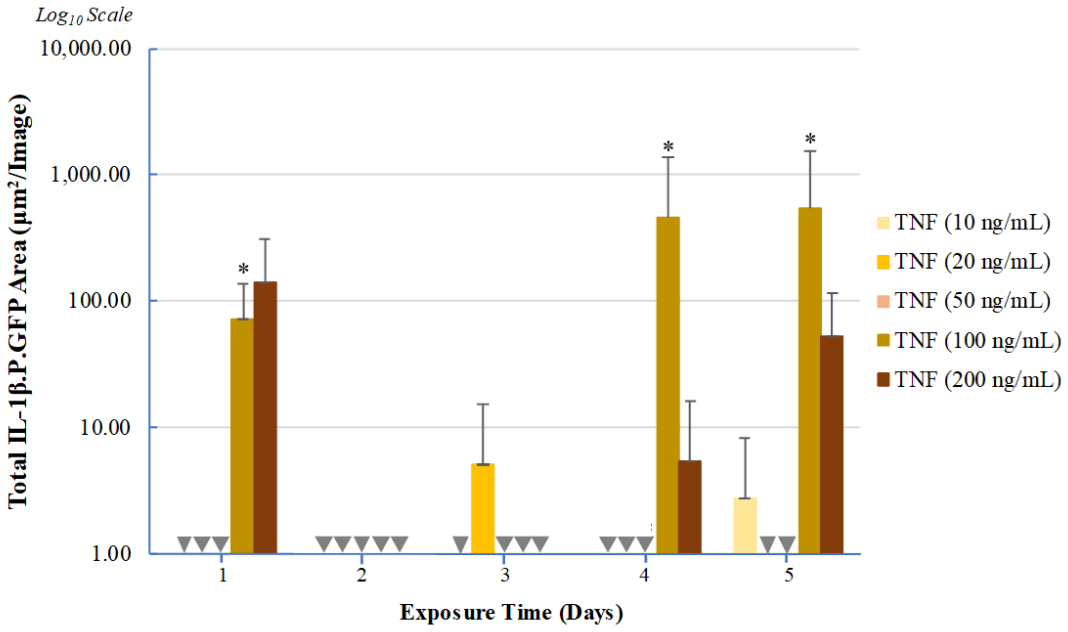

Figure 3.6 Expression levels of IL-1βp.GFP after stimulation with TNF-α at various concentrations. eqFLS were transfected with IL-1βp.GFP and pmCherry.N1 (Section 3.2.5) and then stimulated with TNF-α at various concentrations (10, 20, 50, 100, 200 ng/mL). A screen of IL-1βp.GFP expression (Section 3.2.7) was performed using the IncuCyte Live-Cell Imaging software and quantitatively analyzed using Microsoft Excel. A one-way ANOVA was used using the mean and SD, with (*) indicating $p < 0.04$ relative to either day 1 (TNF200), day 4 (TNF100), or day 5 (TNF100) groups.

3.3.5 Stimulation of IL-1βp.GFP with TNF-α at 100 ng/mL revealed a promising expression pattern over 6 days

Once establishing that 100 ng/mL was the most effective concentration of TNF-α, we wanted to investigate the expression pattern of IL-1βp.GFP over a period. The stimulus was added on Day 1, and the expression levels were analyzed over 6 days. The control group lacking plasmid or TNF-α (-IL-1βp.GFP/-TNF; Figure 3.7, red line) had only baseline expression. The group with plasmid alone (+IL-1βp.GFP/-TNF; Figure 3.7, blue line) mainly showed baseline expression until Day 6, when there was an increasing trend in IL-1βp.GFP upregulation, but this

was not significant relative to control. We believe that future optimizations would have to correct data to the proliferation rate of cells in culture. The third group, containing both plasmid and TNF-α (Figure 3.7, green line), showed the highest expression levels from the IL-1β promoter as detected by higher than control GFP signals, which were significant on Days 3 and 6. The overall trend shown by +IL-1βp.GFP/+TNF was promising since the expression of the IL-1β promoter was significantly activated at least by 3 days post-stimulation with TNF-α. Although not significant, a trend of IL-1β promoter activation could be detected as early as 24 hours (150 μm^2/Image), considering that eqFLS were incubated with TNF-α prior to the data represented in Figure 3.7. The concentration of TNF-α (100 ng/mL) was successful in promoting IL-1β expression in eqFLS.

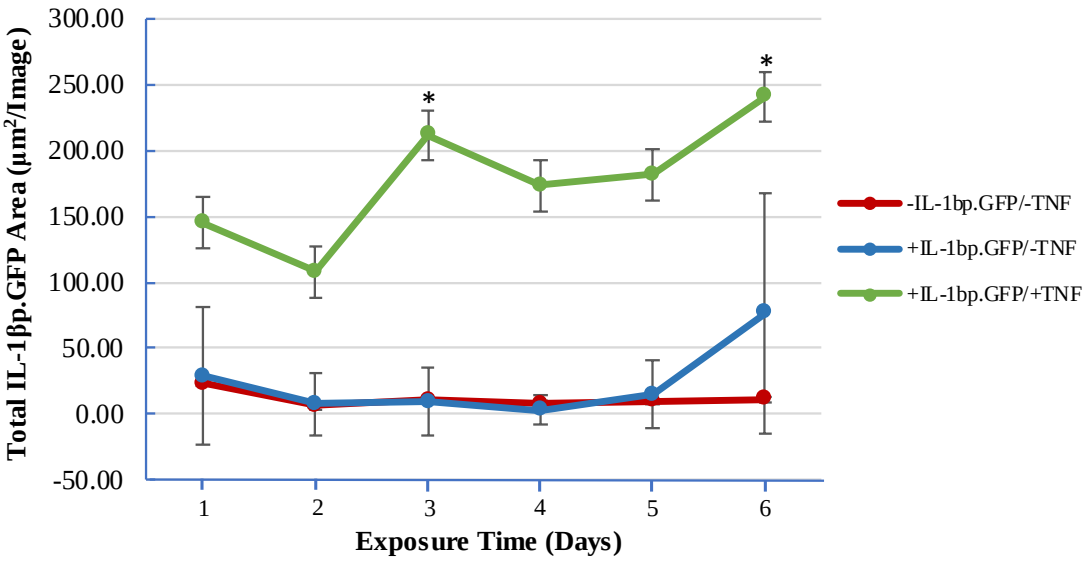

Figure 3.7 Expression level of IL-1βp.GFP after stimulation with TNF-α. eqFLS were transfected with IL-1βp.GFP and pmCherry.N1 (Section 3.2.5) and then stimulated with TNF-α (100 ng/mL). A screen of IL-1βp.GFP expression (Section 3.2.7) was performed using the IncuCyte Live-Cell Imaging software and quantitatively analyzed using Microsoft Excel. A one-way ANOVA was used using the mean and SD, with (*) indicating $p < 0.04$ for that group relative to the other groups on either Day 3 or Day 6.

3.3.6 Novel compounds, C3 and 02-09, reduced IL-1β promoter-driven GFP expression following initial stimulation with TNFα

In parallel with Study Design B mentioned in Chapter 2, we wanted to develop a model that would capture the inflammatory response of eqFLS in real-time. We utilized TNF-α (100 ng/mL) as the stimulus and evaluated the effectiveness of the novel compounds, C3 and 02-09, against the inflammatory response of TNF-α-stimulated eqFLS assessed by IL-1βp.GFP. This pilot screen showed promise for compounds C3 on Day 3 and 02-09 on Day 5 if compared to the DMSO+TNF control. However, there was high variability in the results collected, likely due to an impact of TNF on cell viability or cell seeding variability, and this approach will undoubtedly have to be optimized in future studies. These results were contrary to those expected since the IL-1β promoter was upregulated in the DMSO -TNF control relative to DMSO +TNF on Days 3 and 5, and the same pattern was repeated for C3 and P18 on Day 5.

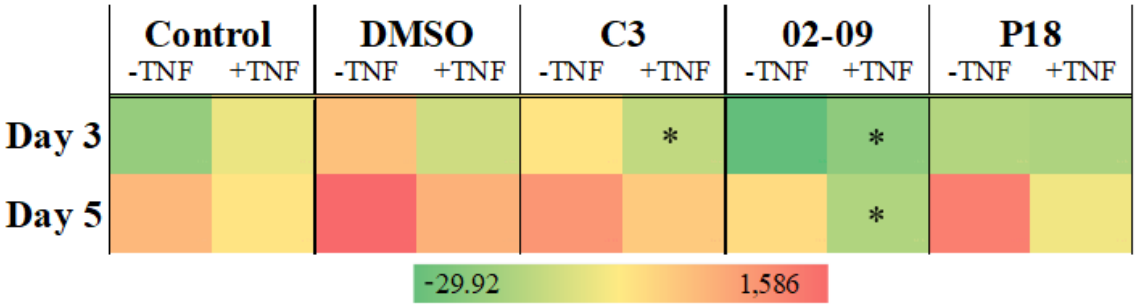

Figure 3.8 Heatmap of expression levels of IL-1βp.GFP after stimulation with TNF-α and treatment with novel or control compounds. eqFLS were transfected with IL-1βp.GFP and pmCherry.N1 (Section 3.2.5) and then stimulated with TNF-α (100 ng/mL). A screen of IL-1βp.GFP expression (Section 3.2.7) was performed using the IncuCyte Live-Cell Imaging software and quantitatively analyzed using Microsoft Excel. Upregulation is signified with red with the highest expression of IL-1β promoter (total area – μm^2/image) reaching 1,586, and downregulation is signified with green with the lowest expression of IL-1β promoter (total area – μm^2/image) reaching -29.92. This map was generated using Microsoft Excel, and a one-way ANOVA was used using the mean and SD, with (*) indicating $p < 0.05$ for C3 or 02-09+TNF relative to the other +TNF groups at Days 3 or 5.

3.4 Discussion

IL-1β is a downstream regulator of the NF-κB signaling pathway and is considered a suitable candidate for mediating the inflammatory response of eqFLS. To examine the real-time IL-1β activity in eqFLS, we chose our best previously established study design and utilized a DNA plasmid containing an IL-1β promoter driving GFP expression, or pIL-1βp.GFP. In designing this

experiment, the availability of an equine IL-1β promoter was limited from GeneCopoeia; thus, we designed the vector with the human promoter. We analyzed the sequence of the promoters between the two species, and due to relatively high sequence homology, we determined that the human IL-1β promoter would be compatible for expression by eqFLS.

Since the literature is scarce on transfecting eqFLS with plasmid DNA, it was critical to establish an effective method. We utilized pDr5.GFP2 to establish a transfection method to achieve high transfection efficiency and cellular viability. The pDr5.GFP2 plasmid contains a promoter region that is continuously expressed without stimulation, which allowed us to qualitatively analyze the efficiency of these two transfection methods. In a pilot, we transfected eqFLS utilizing Lipofectamine 2000 (Thermo Fisher Scientific). We observed that a cell density of over 30,000 cells per well in a 96-well plate reduced the transfection efficiency of eqFLS. Optimization led to a cell density of 2,000 cells/well for future experimentation. We found this transfection method to be successful in transfecting eqFLS. However, due to some cell toxicity (estimated at ~ 45% with 0.5 μL of Lipofectamine 2000), we chose to explore the Neon Transfection System (Thermo Fisher Scientific) as a transfection method to enable more efficient DNA uptake.

Supporting literature for transfecting eqFLS with the Neon Transfection System was limited. Thus, it was of interest to optimize its parameters (i.e., pulse voltage, pulse width, number of pulses) and troubleshoot the manufacturer's protocol. To reveal the most effective protocol for eqFLS transfection, we experimented with five different parameters and the number of transfections prepared per "batch" — mentioned in the manufacturer's protocol as the number of transfections prepared collectively in a single 1.5 mL tube. We found protocol #5 (pulse voltage (V): 1,700; pulse width (ms): 20; pulse number: 1) to be the most effective in transfecting pDr5.GFP, as its expression was successfully detected in virtually all eqFLS within the well. Using a hemocytometer and cell counting using the method of Trypan Blue exclusion (Thermo Fisher Scientific, 2022), we also found that transfection efficiency and viability were greater when transfection was carried out in smaller (3 transfections/batch) than in larger batches (15 transfections/batch). The smaller batches showed 73.53 % cell viability compared to 37% viability for larger batches (data not shown). Overall, comparing these findings to the Lipofectamine 2000 Transfection Reagent, we concluded that the Neon Transfection System using protocol #5 was the

most efficient method of transfecting eqFLS with plasmid DNA and virtually all cells were transfected.

We used the Neon Transfection System to transfect the IL-1βp.GFP plasmid with a cotransfection control, pmCherry.N1 – a common approach to control transfection variability and/or efficiency, where the cotransfection control represents ~1-5% of the total plasmid transfected. Considering that IL-1βp.GFP is a promoter sequence that would respond to inflammatory stimuli (inducible); we compared the pro-inflammatory stimuli LPS and TNF-α. The initial investigation compared the expression of IL-1βp.GFP after stimulation with LPS or TNF-α at the concentrations of 50, 100, and 150 ng/mL. Using qualitative analysis (microscopy), we found that GFP expression was not detected among any LPS stimulated groups. TNF-α stimulation was more promising in stimulating GFP expression from the plasmid at 50 and 100 ng/mL.

In our preliminary study comparing LPS and TNF-α stimulation, we utilized 50, 100, and 150 ng/mL concentrations. We found that the IL-1β promoter could be activated with 50 and 100 ng/mL with TNF-α stimulation. We found that LPS was ineffective in inducing the expression of the IL-1β promoter, considering the expression of GFP was lacking by qualitative analysis. This experiment allowed us to compare qualitative and quantitative analyses and gave us insight into investigating these findings utilizing a quantitative analysis approach. Using the IncuCyte Live-Cell Imaging equipment and software (Sartorius), we detected the promoter expression following stimulation with various concentrations of TNF-α (10, 20, 50, and 100 ng/mL). The expression pattern of the IL-1β promoter was slightly reduced between Days 1 and 2 after seeding; it is proposed that there is a lag time likely related to attachment and adaptation to the culture surface. When cells were stimulated with TNF-α, the promoter expression level substantially increased from a total area value of 0 to 500 with a TNF-α, but at a relatively high 100 ng/mL concentration. The expression of mCherry.N1 was consistent from Day 1 to Day 5, suggesting transfection could be efficient and that there were viable eqFLS cells. Thus, we observed that TNF-α, at 100 ng/mL, was the most promising concentration for reaching significant expression levels of the IL-1β promoter relative to control (-IL-1βp.GFP/-TNF; Figure 3.7, red line) over a 6-day analysis. This experiment provided us with an understanding of the pro-inflammatory activity that eqFLS displayed after being stimulated. When eqFLS were transfected but unstimulated, it was evident

that expression of the promoter did not occur, supporting the idea that the IL-1β promoter must be activated by pro-inflammatory stimuli to drive reporter gene expression (GFP). The expression of the IL-1β promoter showed a promising trend after stimulation with TNF-α. However, it underwent a lag phase, then increased on Day 2 (24 hours after TNF-α stimulation) and maintained its expression for at least 6 days. Future studies could examine more extended periods to determine the upper limit of maintenance of expression.

We thus developed the basis for a model providing real-time activity that can be used in a future medium- to high-throughput drug discovery screens for identifying molecules that could counteract inflammation in eqFLS. We hypothesized that at least one of our novel molecules, C3 and/or 02-09, could reduce the inflammatory activity of eqFLS, as assessed by this screen. Ideally, we wanted to see that the IL-1β promoter was activated in the control groups receiving TNF-α (as assessed by increased GFP levels) and not expressed or significantly reduced (GFP reductions) in the C3 and/or 02-09 treatment groups. TNF-α exposure successfully initiated IL-1βp.GFP expression relative to the control lacking TNF-α, and this was an expected result. C3 and 02-09 significantly reduced the expression of IL-1βp.GFP relative to DMSO+TNF-α control after Day 4 (Figure 3.8). Although interesting, these results should be interpreted cautiously, as they are preliminary. This pilot screen showed some promise for compounds C3 on day 3 and 02-09 on Day 5 if compared to the DMSO+TNF control. However, there was high variability in the results, likely due to an impact of TNF on cell viability or cell seeding variability, and will undoubtedly have to be optimized in future studies. Nevertheless, this screen appears promising for future screening of the next-generation compounds and/or novel drugs that could inhibit the inflammatory activity of eqFLS. The screen so far reports on the TNF-α activation stimulus but can be further expanded to other inflammatory stimuli. Additional troubleshooting of the transfection protocol and variations in cell culture (i.e., Poly-L-Lysine coating of 96-well plates to augment cell attachment) will be critical to enhancing the application of this screen to capture the real-time inflammatory activity of eqFLS.

Exploring an IL-1β promoter cell-based drug screen provided some dynamic information on ‘how’ and ‘when’ eqFLS begin activating a pro-inflammatory gene in real-time, which was possible with the transfection of a novel DNA plasmid. We detected and tracked eqFLS response

to the simulation and some promising initial responses to the exposure to the novel compounds. Overall, this screen allowed us to detect an inflammatory gene expression pattern upon stimulation and monitor its expression in a real-time setting and began to provide an insight into the biological impacts of our novel therapeutic molecules on reducing the inflammatory response of eqFLS.

CHAPTER 4. LIMITATIONS, CONCLUSIONS, AND FUTURE DIRECTIONS

4.1 Limitations

We wanted to acknowledge some limitations that may influence the conclusions possible from the research conducted in this thesis. We identified several limitations to the methodology that could be refined in future studies; for instance, we had complications with low cell viability during the cell-based screen experiments presented in Chapter 3. Sample size also could have been a limitation in gene expression analyses presented in Chapter 2 and the expression of IL-1βp.GFP is described in Chapter 3. Additionally, only one donor was used for the eqFLS isolation, and future studies should reproduce these results in primary cells from an independent donor. During experiments described in Chapters 2 and 3, we had challenges reproducing the same gene expression levels in eqFLS following TNF-α stimulation and/or exposure to our novel compounds. Some technical factors that may have contributed to the challenges in reproducibility included some equipment malfunctions, which limited some data acquisition with the IncuCyte Live-Cell Analysis System (Sartorius). Some of these challenges were overcome, whereas others remain for further studies to refine with increased sample size numbers and experiment repetitions.

One of the methodological limitations we encountered was the low viability of eqFLS. We propose eqFLS viability was influenced by numerous factors, including the combined processes of transfection and stimulation with TNF-α. Most mammalian cell lines are vulnerable to losses in viability following transfection (Maeß et al., 2014). We obtained a higher transfection efficiency (~ 72%) when we transfected eqFLS using the Neon Transfection System (Thermo Fisher Scientific); however, we observed some physical damage that still contributed to some loss in cellular viability. We also suspect that stimulating eqFLS with TNF-α could have influenced the overall loss of viability. The concentration of TNF-α is critical considering that high concentrations trigger cell death, whereas low concentrations could promote cell survival. We evaluated various concentrations of TNF-α to achieve significant changes in the expression of our IL-1β promoter in eqFLS. We determined 100 ng/mL to be the most effective concentration in eliciting a response from the IL-1β promoter. We hypothesize that the high cytokine level was necessary since it was a human promoter activated in equine cells, thus having incomplete compatibility in transcription

factors or complexes that might be necessary for the most efficient equine-specific transcription. The level of cytokine necessary could render it toxic to eqFLS, and further studies should re-make the construct with an equine promoter or assay differently made cytokines. For instance, the TNF-α utilized in our experiments was obtained from R & D Systems as a recombinant protein produced in *Escherichia coli* (*E. coli*). Thus, it lacks eukaryotic post-translational modifications (PTMs) with potential essential roles in modulating physiological functions. The lack of PTMs (i.e., residue 81 glycosylation or other lipidation sites) (Gaudet et al. 2011) could have influenced the higher concentration of TNF-α needed to activate the IL-1β promoter we had to use higher-than-endogenous levels to reach a similar activity.

The sample size was another limitation we propose that may have impacted the conclusions possible from experiments described in Chapters 2 and 3. We obtained low RNA concentrations (< 50 ng/μL) in the initial pilot experiments and had issues with low cell counts. We had to troubleshoot culturing protocols until we could achieve reliable RNA concentrations to move forward with RT-qPCR. During the cell-based screen experiments, we propose that a refinement to detecting statistically significant differences among averages of different conditions could include designs where more samples are added per condition (> triplicates). The sample size and potential toxicity of TNF-α or novel compounds limited reproducibility, which was evident in gene expression variability after stimulation. The same issue was encountered when analyzing the results from the cell-based screen. The expression levels of the IL-1β promoter varied across similar experiments, limiting the conclusions possible from the current data. We propose that DMSO and novel compounds may have off-target effects on eqFLS in both sets of experiments, even though the compounds were developed against the crystal structure of LAMR1. This is not completely surprising since DMSO, the vehicle or negative control for C3 and 02-09, has been shown to induce alterations in miRNA levels and some epigenetic effects (e.g., changes in mitochondrial pathways) that may hinder basal cell metabolism. Future studies would aim to alter compounds by medicinal chemistry to have them soluble in other, more biocompatible aqueous vehicles.

Data collection using different equipment and software might have also limited the possible conclusions across different experiments. For example, we had to utilize a fluorescent microscope

to identify IL-1βp.GFP expression due to the unexpected repair of our IncuCyte Live-Cell Analysis System (Sartorius); thus, for some time, we were unable to quantitatively analyze our results, which impacted our ability to choose the best method of transfecting eqFLS (i.e., Lipofectamine 2000 or Neon Transfection System) and limited our ability to precisely identify the expression levels of the IL-1β promoter after stimulating with LPS or TNF-α at concentrations of 50, 100, or 150 ng/mL.

We must acknowledge these limitations to be addressed in future studies. The present studies gave the following insights, which can be used to refine and improve the future experiments in this project. First, to avoid the issue of low viability of eqFLS after transfection and/or stimulation with TNF-α, it would be beneficial to continue troubleshooting and optimizing the transfection protocol using the Neon Transfection System and utilize a TNF-α concentration that induces the expression of the IL-1β promoter but does not significantly impact cell viability. Second, in refining these models, it would also be beneficial to use lower passages of eqFLS during experimentation. A lower passage number would decrease the odds of eqFLS changing their phenotype and genotype characteristics during experimentation. Third, using flow cytometry with antibody markers specific to FLS (e.g., CD11b, CD106/VCAM-1, and CD45/ICAM-1) would allow us to characterize our population of eqFLS better. Fourth, it would be beneficial to utilize a greater sample size per condition (> triplicates) when planning future experiments with biological replicates and a higher number of technical replicates (Lazic et al., 2018). A greater sample size per condition during the cell-based screen experiment would have assisted in eliminating influences from a low cell count, for example. Overall, we have identified some limitations that we propose have impacted the conclusions possible from the results presented. It is essential to acknowledge these limitations to better design future experiments to continue this study.

4.2 Conclusions

The work in this thesis examines the aspects of an *in vitro* model that was developed to induce OA-like inflammatory signaling in equine fibroblast-like synoviocytes (eqFLS). Candidate therapeutic compounds were examined in this model by characterizing their impact on reducing pro-inflammatory cytokine gene expression (Chapter 2) and by their performance in a novel screen (Chapter 3) that utilized an IL-1β promoter to enable real-time detection of changes in green

fluorescent protein expression as a response to therapeutics. Moreover, this model provided an understanding of the inflammatory activity of eqFLS and insight into inflammation as a therapeutic target in reducing or reversing the effects of equine OA.

In Chapter 2, we developed an *in vitro* model for testing the potential of novel compounds in reducing the inflammatory response of eqFLS. We classified our collected samples from equine joints to be predominantly FLS by light microscopy, which we called eqFLS. eqFLS showed distinctive morphological characteristics in cell culture, such as having a unique endoplasmic reticulum, a relatively large nucleus, and long elongated spindles from the cell body. As mentioned by other groups, these cells also formed a lining layer *in vitro* (Kiener et al. 2006). However, limitations to this approach include the absence of specific markers assessed in these cultures. Future characterization could involve flow cytometry or other methods for detecting FLS-specific protein expression in this cell population.

The literature and previous studies suggested that eqFLS were promising candidates in studying OA-related inflammation, as they play a pivotal role in OA's early and late stages. We utilized LPS as the initial stimulus to achieve a pro-inflammatory response of eqFLS. We found that eqFLS displays immunomodulatory properties in response to LPS stimulation after 24 hours (Figure 2.6), thus resulting in the upregulation of pro-inflammatory cytokines and mediators (e.g., ADAMTS-4, IL-1β, IL-6, MMP-13, and TNF-α). The limitations of this approach were that we assayed gene expression changes; thus, in some cases may not match protein level changes. Future studies could examine the respective changes in secreted molecules using techniques such as ELISA.

Once we accomplished a preliminary pro-inflammatory model, we were interested in examining the efficacy of our novel compounds in reducing the initial inflammatory response of eqFLS. We wanted to ensure that the control and novel compounds would not reduce the viability of eqFLS and observed that DMSO (vehicle) should be utilized at a lower concentration (0.1 % of media volume), as eqFLS can be sensitive to its exposure. This cell viability assay showed that the novel compounds, C3 and P18, did not significantly impact eqFLS viability, also uncovering 10 μM to be an ideal effective concentration for the follow-up experiments. We utilized three different

study designs, A, B, and C. In doing so, we determined that Study Design B was the most promising in capturing the inflammatory response of eqFLS after treatment with compounds C3 and 02-09. We chose to enhance the magnitude of gene expression modulated by the inflammatory stimulus and thus reduce some of the variability from LPS-stimulated gene expression by investigating the effects of an alternative stimulus, TNF-α. TNF- α promoted greater eqFLS viability and upregulated pro-inflammatory cytokines to a greater extent, particularly for common inflammatory marker IL-6 (a ~10-fold increase relative to LPS stimulation). We utilized Study B with TNF-α stimulated eqFLS and found promising trends in this model, with 02-09 downregulating the initial inflammatory response of eqFLS (Figure 2.10). Overall, we were able to develop a preliminary *in vitro* model that provided us with some understanding of the role of eqFLS in inflammation and an ability to assay the efficiency of our novel compounds in reducing the inflammatory response. Still, examining gene expression changes in larger culture sizes (needed to obtain enough RNA for analyses) was not amenable to high-throughput drug screening. We wanted to develop a screen where we could more dynamically examine gene expression over time and potentially test multiple compounds in a second or third-generation series simultaneously.

In Chapter 3, we developed a dynamic screen to detect the inflammatory response of eqFLS in real-time. The literature was minimal on transfection conditions for eqFLS, and the plan involved introducing a plasmid into these cells to detect a pro-inflammatory gene promoter driving a reporter gene (GFP). Thus, much of our work was novel and entailed many optimizations to achieve sufficient transfection efficiency for GFP detection. We first investigated the ability of eqFLS to be transfected by using a control vector, pDr5.GFP2, in two transfection methods, chemical: Lipofectamine 2000 Transfection Reagent, or physical: Neon Transfection System. We transfected IL-1βp.GFP to detect the inflammatory responses of eqFLS when stimulated with TNF-α and/or the novel compounds. A range of TNF-α concentrations was compared, with 100 ng/mL achieving the highest IL-1βp.GFP expression. Moving forward with this real-time screen, we expected that the IL-1βp.GFP would express at its highest after stimulation with TNF-α relative to wells lacking TNF-α, and this pattern was achieved successfully. Our primary interest was to examine if our molecules could successfully reduce inflammation. The real-time screen, utilizing the IncuCyte Live-Cell Imaging software, was promising in providing this information as the novel compounds effectively reduced the IL-1β promoter expression in the presence of TNF, at least by

Day 5 and for the 02-09, C3, and P18 groups relative to DMSO control. Overall, we successfully screened for the pro-inflammatory activity of eqFLS after stimulation with TNF-α and analyzed the efficacy of our novel compounds in real-time, showing promising trends in reducing a common pro-inflammatory biomarker, the IL-1β promoter.

4.3 Future Directions

In the future directions of this project, it will be of interest to test the efficacy of newer-generation compounds based on the parent C3 and its first-generation derivative, 02-09, by utilizing the recently established models. Second-generation novel compounds are currently being developed, collaborating with Dr. Herman Sintim, with modifications designed toward achieving a higher affinity for the LAMR1 and enabling dissolution in more aqueous solvents, thus enhancing their chance of translation in therapeutic settings. These novel compounds have been shown to reduce inflammation in previous studies, this one included, and have shown promise in promoting chondrogenic differentiation of MSCs into chondrocytes in previous pilot studies by the lab. In a therapeutic setting, these novel compounds or the next generation derivatives could serve as an anti-inflammatory and pro-chondrogenic agents, as diagrammed in Figure 4.1. These combined properties would be beneficial since, thus far, therapies are not available to inhibit structural deterioration of articular cartilage effectively, or that can effectively reverse its existing structural defects. Thus, even though only preliminary data has been collected thus far for these novel compounds, they have the exciting potential to mitigate structural changes in an OA joint by reducing inflammation (i.e., innate immune response) that leads to tissue deterioration and potentially also promote chondrogenesis.

We propose that these novel compounds have a high potential for future development into therapeutic agents for OA in equine and other species. In preclinical or clinical application, it might be interesting to utilize C3-related compounds to promote therapeutic synergy with steroids, potentially helping to reduce steroid doses commonly administered to treat diseases like OA. Other current therapeutics focus on TNF and IL-1β inhibition and have several disadvantages, including a high cost and a lack of an ability to promote articular cartilage regeneration. Thus, utilizing our novel compounds as therapeutic agents and hyaluronic acid and/or doses of steroids that are lower than those currently used could be a potential avenue for treating OA-affected joints.

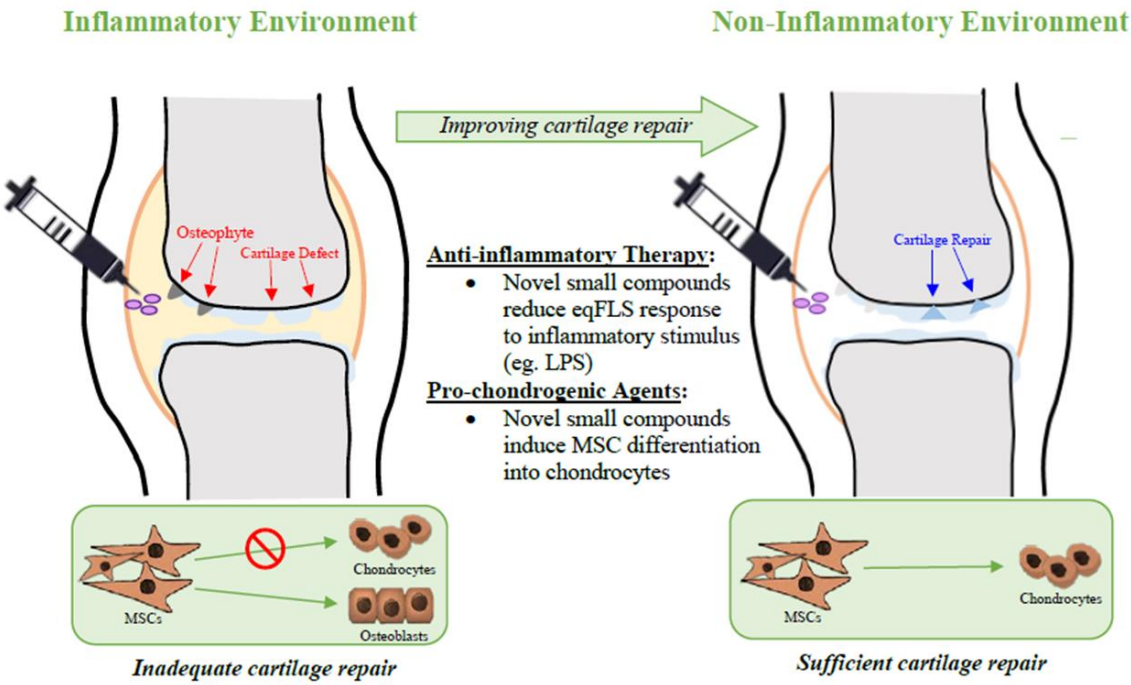

Figure 4.1 Representation of *in vivo* future direction of study. Novel compounds would be utilized as therapeutics that would be administered directly to the joint space with the goal of the compounds to reduce the inflammatory response within the synovium and promoting articular cartilage regeneration by initiating MSCs to differentiate into chondrocytes within the articular cartilage.

REFERENCES

Abella, V., Scotece, M., Conde, J., López, V., Pirozzi, C., Pino, J., … Gualillo, O. (2016). The novel adipokine progranulin counteracts IL-1 and TLR4-driven inflammatory response in human and murine chondrocytes via TNFR1. *Scientific Reports, 6,* 20356. doi: 10.1038/srep20356

Aida, Y., Maeno, M., Suzuki, N., Namba, A., Motohashi, M., Matsumoto, M., … Matsumura, H. (2006). The effect of IL-1beta on the expression of inflammatory cytokines and their receptors in human chondrocytes. *Life Sciences, 79*(8), 764–771. doi: 10.1016/j.lfs.2006.02.038

Allas, L., Rochoux, Q., Leclercq, S., Boumédiene, K., & Baugé, C. (2020). Development of a simple osteoarthritis model useful to predict in vitro the anti-hypertrophic action of drugs. *Laboratory Investigation*, *100*(1), 64–71. doi: 10.1038/s41374-019-0303-0

Alvarez, K., de Andrés, M. C., Takahashi, A., & Oreffo, R. O. C. (2014). Effects of hypoxia on anabolic and catabolic gene expression and DNA methylation in OA chondrocytes. *BMC Musculoskeletal Disorders*, *15*, 431. doi: 10.1186/1471-2474-15-431

Amundsen, L. R. (2007). Effects of age on joints and ligaments. In *Geriatric Rehabilitation Manual* (pp. 17–19). Elsevier. doi: 10.1016/B978-0-443-10233-2.50011-0

Andreassen, S. M., Berg, L. C., Nielsen, S. S., Kristensen, A. T., & Jacobsen, S. (2015). mRNA expression of genes involved in inflammation and haemostasis in equine fibroblast-like synoviocytes following exposure to lipopolysaccharide, fibrinogen and thrombin. *BMC Veterinary Research*, *11*, 141. doi: 10.1186/s12917-015-0448-z

Antonacci, J. M., Schmidt, T. A., Serventi, L. A., Cai, M. Z., Shu, Y. L., Schumacher, B. L., … Sah, R. L. (2012). Effects of equine joint injury on boundary lubrication of articular cartilage by synovial fluid: role of hyaluronan. *Arthritis and Rheumatism, 64*(9), 2917–2926. doi: 10.1002/art.34520

Antons, J., Marascio, M. G. M., Nohava, J., Martin, R., Applegate, L. A., Bourban, P. E., & Pioletti, D. P. (2018). Zone-dependent mechanical properties of human articular cartilage obtained by indentation measurements. *Journal of Materials Science. Materials in Medicine*, *29*(5), 57. doi: 10.1007/s10856-018-6066-0

Arra, M., Swarnkar, G., Ke, K., Otero, J. E., Ying, J., Duan, X., … Abu-Amer, Y. (2020). LDHA-mediated ROS generation in chondrocytes is a potential therapeutic target for osteoarthritis. *Nature Communications, 11*(1), 3427. doi: 10.1038/s41467-020-17242-0

Ayroldi, E., Cannarile, L., Migliorati, G., Nocentini, G., Delfino, D. V., & Riccardi, C. (2012). Mechanisms of the anti-inflammatory effects of glucocorticoids: genomic and nongenomic interference with MAPK signaling pathways. *The FASEB Journal, 26*(12), 4805–4820. doi: 10.1096/fj.12-216382

Bailey, C. J., Reid, S. W., Hodgson, D. R., & Rose, R. J. (1999). Impact of injuries and disease on a cohort of two- and three-year-old thoroughbreds in training. *The Veterinary Record*, *145*(17), 487–493. doi: 10.1136/vr.145.17.487

Band, P. A., Heeter, J., Wisniewski, H. G., Liublinska, V., Pattanayak, C. W., Karia, R. J., … Kraus, V. B. (2015). Hyaluronan molecular weight distribution is associated with the risk of knee osteoarthritis progression. *Osteoarthritis and Cartilage*, *23*(1), 70–76. doi: 10.1016/j.joca.2014.09.017

Becerra, J., Andrades, J. A., Guerado, E., Zamora-Navas, P., López-Puertas, J. M., & Reddi, A. H. (2010). Articular cartilage: structure and regeneration. *Tissue Engineering. Part B, Reviews*, *16*(6), 617–627. doi: 10.1089/ten.TEB.2010.0191

Belkacemi, L., & Zhang, S. X. (2016). Anti-tumor effects of pigment epithelium-derived factor (PEDF): implication for cancer therapy. A mini-review. *Journal of Experimental & Clinical Cancer Research*, *35*, 4. doi: 10.1186/s13046-015-0278-7

Bendele, A. M. (2001). Animal models of osteoarthritis. *Journal of Musculoskeletal & Neuronal Interactions*, *1*(4), 363–376. PMID: 15758487.

Bernard, A., Gao-Li, J., Franco, C.-A., Bouceba, T., Huet, A., & Li, Z. (2009). Laminin receptor involvement in the anti-angiogenic activity of pigment epithelium-derived factor. *The Journal of Biological Chemistry*, *284*(16), 10480–10490. doi: 10.1074/jbc.M809259200

Bertoni, L., Jacquet-Guibon, S., Branly, T., Legendre, F., Desancé, M., Mespoulhes, C., … Audigié, F. (2020). An experimentally induced osteoarthritis model in horses performed on both metacarpophalangeal and metatarsophalangeal joints: Technical, clinical, imaging, biochemical, macroscopic and microscopic characterization. *Plos One*, *15*(6), e0235251. doi: 10.1371/journal.pone.0235251

Beynnon, B. D., Fiorentino, N., Gardner-Morse, M., Tourville, T. W., Slauterbeck, J. R., Sturnick, D. R., … Imhauser, C. W. (2020). Combined injury to the ACL and lateral meniscus alters the geometry of articular cartilage and meniscus soon after initial trauma. *Journal of Orthopaedic Research*, *38*(4), 759–767. doi: 10.1002/jor.24519

Bhattaram, P., & Chandrasekharan, U. (2017). The joint synovium: A critical determinant of articular cartilage fate in inflammatory joint diseases. *Seminars in Cell & Developmental Biology*, *62*, 86–93. doi: 10.1016/j.semcdb.2016.05.009

Blewis, M. E., Lao, B. J., Jadin, K. D., McCarty, W. J., Bugbee, W. D., Firestein, G. S., & Sah, R. L. (2010). Semi-permeable membrane retention of synovial fluid lubricants hyaluronan and proteoglycan 4 for a biomimetic bioreactor. *Biotechnology and Bioengineering*, *106*(1), 149–160. doi: 10.1002/bit.22645

Blom, A. B., van Lent, P. L. E. M., Holthuysen, A. E. M., van der Kraan, P. M., Roth, J., van Rooijen, N., & van den Berg, W. B. (2004). Synovial lining macrophages mediate osteophyte formation during experimental osteoarthritis. *Osteoarthritis and Cartilage*, *12*(8), 627–635. doi: 10.1016/j.joca.2004.03.003

Bondeson, J., Wainwright, S. D., Lauder, S., Amos, N., & Hughes, C. E. (2006). The role of synovial macrophages and macrophage-produced cytokines in driving aggrecanases, matrix metalloproteinases, and other destructive and inflammatory responses in osteoarthritis. *Arthritis Research & Therapy*, *8*(6), R187. doi: 10.1186/ar2099

Bottini, N., & Firestein, G. S. (2013). Duality of fibroblast-like synoviocytes in RA: passive responders and imprinted aggressors. *Nature Reviews. Rheumatology*, *9*(1), 24–33. doi: 10.1038/nrrheum.2012.190

Boyce, B. F., & Xing, L. (2007). The RANKL/RANK/OPG pathway. *Current Osteoporosis Reports*, *5*(3), 98–104. doi: 10.1007/s11914-007-0024-y

Boyce, M. K., Trumble, T. N., Carlson, C. S., Groschen, D. M., Merritt, K. A., & Brown, M. P. (2013). Non-terminal animal model of post-traumatic osteoarthritis induced by acute joint injury. *Osteoarthritis and Cartilage*, *21*(5), 746–755. doi: 10.1016/j.joca.2013.02.653

Brama, P. A., Bank, R. A., Tekoppele, J. M., & Van Weeren, P. R. (2001). Training affects the collagen framework of subchondral bone in foals. *Veterinary Journal*, *162*(1), 24–32. doi: 10.1053/tvjl.2001.0570

Brien, S., Prescott, P., Bashir, N., Lewith, H., & Lewith, G. (2008). Systematic review of the nutritional supplements dimethyl sulfoxide (DMSO) and methylsulfonylmethane (MSM) in the treatment of osteoarthritis. *Osteoarthritis and Cartilage*, *16*(11), 1277–1288. doi: 10.1016/j.joca.2008.03.002

Brosseau, L., Rahman, P., Toupin-April, K., Poitras, S., King, J., De Angelis, G., … McEwan, J. (2014). A systematic critical appraisal for non-pharmacological management of osteoarthritis using the appraisal of guidelines research and evaluation II instrument. *Plos One*, *9*(1), e82986. doi: 10.1371/journal.pone.0082986

Buchner, H. H., Savelberg, H. H., Schamhardt, H. C., & Barneveld, A. (1996). Head and trunk movement adaptations in horses with experimentally induced fore- or hindlimb lameness. *Equine Veterinary Journal*, *28*(1), 71–76. doi: 10.1111/j.2042-3306.1996.tb01592.x

Burr, D. B., Martin, R. B., Schaffler, M. B., & Radin, E. L. (1985). Bone remodeling in response to in vivo fatigue microdamage. *Journal of Biomechanics*, *18*(3), 189–200. doi: 10.1016/0021-9290(85)90204-0

Byström, A., Clayton, H. M., Hernlund, E., Roepstorff, L., Rhodin, M., Bragança, F. S., … Egenvall, A. (2021). Asymmetries of horses walking and trotting on treadmill with and without rider. *Equine Veterinary Journal*, *53*(1), 157–166. doi: 10.1111/evj.13252

Cardoso, L., Herman, B. C., Verborgt, O., Laudier, D., Majeska, R. J., & Schaffler, M. B. (2009). Osteocyte apoptosis controls activation of intracortical resorption in response to bone fatigue. *Journal of Bone and Mineral Research*, *24*(4), 597–605. doi: 10.1359/jbmr.081210

Caron, J. P., & Genovese, R. L. (2003). Principles and practices of joint disease treatment. In *Diagnosis and management of lameness in the horse* (pp. 746–764). Elsevier. doi: 10.1016/B978-0-7216-8342-3.50092-9

Chan, M. W. Y., Gomez-Aristizábal, A., Mahomed, N., Gandhi, R., & Viswanathan, S. (2022). A tool for evaluating novel osteoarthritis therapies using multivariate analyses of human cartilage-synovium explant co-culture. *Osteoarthritis and Cartilage*, *30*(1), 147–159. doi: 10.1016/j.joca.2021.09.007

Cheng, D. S., & Visco, C. J. (2012). Pharmaceutical therapy for osteoarthritis. *PM & R: The Journal of Injury, Function, and Rehabilitation*, *4*(5 Suppl), S82-8. doi: 10.1016/j.pmrj.2012.02.009

Chen, X., & Thibeault, S. (2013). Effect of DMSO concentration, cell density and needle gauge on the viability of cryopreserved cells in three dimensional hyaluronan hydrogel. *Annual International Conference of the IEEE Engineering in Medicine and Biology Society. IEEE Engineering in Medicine and Biology Society. Annual International Conference*, *2013*, 6228–6231. doi: 10.1109/EMBC.2013.6610976

Chen, Y.-J., Chang, W.-A., Wu, L.-Y., Huang, C.-F., Chen, C.-H., & Kuo, P.-L. (2019). Identification of Novel Genes in Osteoarthritic Fibroblast-Like Synoviocytes Using Next-Generation Sequencing and Bioinformatics Approaches. *International Journal of Medical Sciences*, *16*(8), 1057–1071. doi: 10.7150/ijms.35611

Chibber, P., Kumar, C., Singh, A., Assim Haq, S., Ahmed, I., Kumar, A., … Singh, G. (2020). Anti-inflammatory and analgesic potential of OA-DHZ; a novel semisynthetic derivative of dehydrozingerone. *International Immunopharmacology*, *83*, 106469. doi: 10.1016/j.intimp.2020.106469

Choi, H. M., Oh, D. H., Bang, J. S., Yang, H.-I., Yoo, M. C., & Kim, K. S. (2010). Differential effect of IL-1β and TNFα on the production of IL-6, IL-8 and PGE2 in fibroblast-like synoviocytes and THP-1 macrophages. *Rheumatology International*, *30*(8), 1025–1033. doi: 10.1007/s00296-009-1089-y

Choi, M.-C., Jo, J., Park, J., Kang, H. K., & Park, Y. (2019). NF-κB Signaling Pathways in Osteoarthritic Cartilage Destruction. *Cells*, *8*(7). doi: 10.3390/cells8070734

Chou, C.-H., Jain, V., Gibson, J., Attarian, D. E., Haraden, C. A., Yohn, C. B., … Kraus, V. B. (2020). Synovial cell cross-talk with cartilage plays a major role in the pathogenesis of osteoarthritis. *Scientific Reports*, *10*(1), 10868. doi: 10.1038/s41598-020-67730-y

Choi, H. M., Oh, D. H., Bang, J. S., Yang, H.-I., Yoo, M. C., & Kim, K. S. (2010). Differential effect of IL-1β and TNFα on the production of IL-6, IL-8 and PGE2 in fibroblast-like synoviocytes and THP-1 macrophages. *Rheumatology International*, *30*(8), 1025–1033. doi: 10.1007/s00296-009-1089-y

Chow, Y. Y., & Chin, K.-Y. (2020). The role of inflammation in the pathogenesis of osteoarthritis. *Mediators of Inflammation*, *2020*, 8293921. doi: 10.1155/2020/8293921

Cohen, J. M., Richardson, D. W., McKnight, A. L., Ross, M. W., & Boston, R. C. (2009). Long-term outcome in 44 horses with stifle lameness after arthroscopic exploration and debridement. *Veterinary Surgery*, *38*(4), 543–551. doi: 10.1111/j.1532-950X.2009.00524.x

Corrigall, V. M., Arastu, M., Khan, S., Shah, C., Fife, M., Smeets, T., … Panayi, G. S. (2001). Functional IL-2 receptor beta (CD122) and gamma (CD132) chains are expressed by fibroblast-like synoviocytes: activation by IL-2 stimulates monocyte chemoattractant protein-1 production. *Journal of Immunology*, *166*(6), 4141–4147. doi: 10.4049/jimmunol.166.6.4141

Cunningham, F., Allen, J. E., Allen, J., Alvarez-Jarreta, J., Amode, M. R., Armean, I. M., … Flicek, P. (2022). Ensembl 2022. *Nucleic Acids Research*, *50*(D1), D988–D995. doi: 10.1093/nar/gkab1049

Davidson, R. K., Jupp, O., de Ferrars, R., Kay, C. D., Culley, K. L., Norton, R., … Clark, I. M. (2014). Sulforaphane represses matrix-degrading proteases and protects cartilage from destruction in vitro and in vivo. *Osteoarthritis and Cartilage*, *22*, S322–S323. doi: 10.1016/j.joca.2014.02.597

de Grauw, J. C., van Loon, J. P. A. M., van de Lest, C. H. A., Brunott, A., & van Weeren, P. R. (2014). In vivo effects of phenylbutazone on inflammation and cartilage-derived biomarkers in equine joints with acute synovitis. *Veterinary Journal*, *201*(1), 51–56. doi: 10.1016/j.tvjl.2014.03.030

De Lasalle, J., Alexander, K., Olive, J., & Laverty, S. (2016). Comparisons among radiography, ultrasonography and computed tomography for ex vivo characterization of stifle osteoarthritis in the horse. *Veterinary Radiology & Ultrasound: The Official Journal of the American College of Veterinary Radiology and the International Veterinary Radiology Association*, *57*(5), 489–501. doi: 10.1111/vru.12370

Diaz-Quinones, A., Figueiredo, M., Sintim, H., & Umbaugh, C. (2011). *Patent No. 11*. U.S. Patent Trademark Office. Retrieved from https://uspto.report/patent/grant/11,022,604#C00002

Dieppe, P. (1999). Subchondral bone should be the main target for the treatment of pain and disease progression in osteoarthritis. *Osteoarthritis and Cartilage*, *7*(3), 325–326. doi: 10.1053/joca.1998.0182

Ding, Y., Wang, L., Zhao, Q., Wu, Z., & Kong, L. (2019). MicroRNA-93 inhibits chondrocyte apoptosis and inflammation in osteoarthritis by targeting the TLR4/NF-κB signaling pathway. *International Journal of Molecular Medicine*, *43*(2), 779–790. doi: 10.3892/ijmm.2018.4033

Dyson, S. J. (2003). Radiography and Radiology. In *Diagnosis and management of lameness in the horse* (pp. 153–166). Elsevier. doi: 10.1016/B978-0-7216-8342-3.50022-X

Elsaid, K. A., Jay, G. D., Warman, M. L., Rhee, D. K., & Chichester, C. O. (2005). Association of articular cartilage degradation and loss of boundary-lubricating ability of synovial fluid following injury and inflammatory arthritis. *Arthritis and Rheumatism*, *52*(6), 1746–1755. doi: 10.1002/art.21038

Elsaid, K. A., Zhang, L., Shaman, Z., Patel, C., Schmidt, T. A., & Jay, G. D. (2015). The impact of early intra-articular administration of interleukin-1 receptor antagonist on lubricin metabolism and cartilage degeneration in an anterior cruciate ligament transection model. *Osteoarthritis and Cartilage*, *23*(1), 114–121. doi: 10.1016/j.joca.2014.09.006

e-Ensembl │ Genonme Browser 106 - Equus_caballus (2022). Retrieved from https://useast.ensembl.org/Equus_caballus/Info/Index

Eskelinen, A. S. A., Tanska, P., Florea, C., Orozco, G. A., Julkunen, P., Grodzinsky, A. J., & Korhonen, R. K. (2020). Mechanobiological model for simulation of injured cartilage degradation via pro-inflammatory cytokines and mechanical stimulus. *PLoS Computational Biology*, *16*(6), e1007998. doi: 10.1371/journal.pcbi.1007998

Estell, E. G., Murphy, L. A., Gangi, L. R., Shah, R. P., Ateshian, G. A., & Hung, C. T. (2021). Attachment of cartilage wear particles to the synovium negatively impacts friction properties. *Journal of Biomechanics*, *127*, 110668. doi: 10.1016/j.jbiomech.2021.110668

Estell, E. G., Murphy, L. A., Silverstein, A. M., Tan, A. R., Shah, R. P., Ateshian, G. A., & Hung, C. T. (2017). Fibroblast-like synoviocyte mechanosensitivity to fluid shear is modulated by interleukin-1α. *Journal of Biomechanics*, *60*, 91–99. doi: 10.1016/j.jbiomech.2017.06.011

Estell, E. G., Silverstein, A. M., Stefani, R. M., Lee, A. J., Murphy, L. A., Shah, R. P., … Hung, C. T. (2019). Cartilage Wear Particles Induce an Inflammatory Response Similar to Cytokines in Human Fibroblast-Like Synoviocytes. *Journal of Orthopaedic Research*, *37*(9), 1979–1987. doi: 10.1002/jor.24340

Evans, C. H., Kraus, V. B., & Setton, L. A. (2014). Progress in intra-articular therapy. *Nature Reviews. Rheumatology*, *10*(1), 11–22. doi: 10.1038/nrrheum.2013.159

Fadok, V. A., & Henson, P. M. (2003). Apoptosis: giving phosphatidylserine recognition an assist--with a twist. *Current Biology*, *13*(16), R655-7. doi: 10.1016/s0960-9822(03)00575-x

Faisal, T. R., Adouni, M., & Dhaher, Y. Y. (2019). The effect of fibrillar degradation on the mechanics of articular cartilage: a computational model. *Biomechanics and Modeling in Mechanobiology, 18*(3), 733–751. doi: 10.1007/s10237-018-01112-2

Fasanello, D. C., Su, J., Deng, S., Yin, R., Colville, M. J., Berenson, J. M., … Reesink, H. L. (2021). Hyaluronic acid synthesis, degradation, and crosslinking in equine osteoarthritis: TNF-α-TSG-6-mediated HC-HA formation. *Arthritis Research & Therapy, 23*(1), 218. doi: 10.1186/s13075-021-02588-7

Fei, J., Liang, B., Jiang, C., Ni, H., & Wang, L. (2019). Luteolin inhibits IL-1β-induced inflammation in rat chondrocytes and attenuates osteoarthritis progression in a rat model. *Biomedicine & Pharmacotherapy (Biomedecine & Pharmacotherapie), 109*, 1586–1592. doi: 10.1016/j.biopha.2018.09.161

Ferris, D. J., Frisbie, D. D., McIlwraith, C. W., & Kawcak, C. E. (2011). Current joint therapy usage in equine practice: a survey of veterinarians 2009. *Equine Veterinary Journal, 43*(5), 530–535. doi: 10.1111/j.2042-3306.2010.00324.x

Fox, A. J. S., Bedi, A., & Rodeo, S. A. (2012). The basic science of human knee menisci: structure, composition, and function. *Sports Health, 4*(4), 340–351. doi: 10.1177/1941738111429419

Frisbie, D. D., Cross, M. W., & McIlwraith, C. W. (2006). A comparative study of articular cartilage thickness in the stifle of animal species used in human pre-clinical studies compared to articular cartilage thickness in the human knee. *Veterinary and Comparative Orthopaedics and Traumatology: V.C.O.T, 19*(3), 142–146. PMID: 16971996.

Frisbie, D. D., McIlwraith, C. W., Kawcak, C. E., & Werpy, N. M. (2013). Evaluation of intra-articular hyaluronan, sodium chondroitin sulfate and N-acetyl-D-glucosamine combination versus saline (0.9% NaCl) for osteoarthritis using an equine model. *Veterinary Journal, 197*(3), 824–829. doi: 10.1016/j.tvjl.2013.05.033

Gabner, S., Ertl, R., Velde, K., Renner, M., Jenner, F., Egerbacher, M., & Hlavaty, J. (2018). Cytokine-induced interleukin-1 receptor antagonist protein expression in genetically engineered equine mesenchymal stem cells for osteoarthritis treatment. *The Journal of Gene Medicine, 20*(5), e3021. doi: 10.1002/jgm.3021

Gaudet, P., Livstone, M. S., Lewis, S. E., & Thomas, P. D. (2011). Phylogenetic-based propagation of functional annotations within the Gene Ontology consortium. *Briefings in Bioinformatics, 12*(5), 449–462. doi: 10.1093/bib/bbr042

Gelse, K., Söder, S., Eger, W., Diemtar, T., & Aigner, T. (2003). Osteophyte development--molecular characterization of differentiation stages. *Osteoarthritis and Cartilage, 11*(2), 141–148. doi: 10.1053/joca.2002.0873

Girden, E. (1992). *ANOVA*. 2455 Teller Road, Thousand Oaks California 91320 United States of America: SAGE Publications, Inc. doi: 10.4135/9781412983419

Goldberg, V. M., & Wera, G. D. (2013). Surgical approaches for treatment of osteoarthritis. In *Addressing unmet needs in osteoarthritis* (pp. 86–97). Unitec House, 2 Albert Place, London N3 1QB, UK: Future Medicine Ltd. doi: 10.2217/ebo.12.200

Gong, Q., Qiu, S., Li, S., Ma, Y., Chen, M., Yao, Y., … Yang, Z. (2014). Proapoptotic PEDF functional peptides inhibit prostate tumor growth--a mechanistic study. *Biochemical Pharmacology*, *92*(3), 425–437. doi: 10.1016/j.bcp.2014.09.012

Goodrich, L. R., & Nixon, A. J. (2006). Medical treatment of osteoarthritis in the horse - a review. *Veterinary Journal*, *171*(1), 51–69. doi: 10.1016/j.tvjl.2004.07.008

Grenier, S., Bhargava, M. M., & Torzilli, P. A. (2014). An in vitro model for the pathological degradation of articular cartilage in osteoarthritis. *Journal of Biomechanics*, *47*(3), 645–652. doi: 10.1016/j.jbiomech.2013.11.050

Guilak, F., Ratcliffe, A., Lane, N., Rosenwasser, M. P., & Mow, V. C. (1994). Mechanical and biochemical changes in the superficial zone of articular cartilage in canine experimental osteoarthritis. *Journal of Orthopaedic Research*, *12*(4), 474–484. doi: 10.1002/jor.1100120404

Guillemin, F., Ricatte, C., Barcenilla-Wong, A., Schoumacker, A., Cross, M., Alleyrat, C., … Hunter, D. J. (2019). Developing a Preliminary Definition and Domains of Flare in Knee and Hip Osteoarthritis (OA): Consensus Building of the Flare-in-OA OMERACT Group. *The Journal of Rheumatology*, *46*(9), 1188–1191. doi: 10.3899/jrheum.181085

Gupta, S. C., Sundaram, C., Reuter, S., & Aggarwal, B. B. (2010). Inhibiting NF-κB activation by small molecules as a therapeutic strategy. *Biochimica et Biophysica Acta*, *1799*(10–12), 775–787. doi: 10.1016/j.bbagrm.2010.05.004

Hada, S., Kaneko, H., Sadatsuki, R., Liu, L., Futami, I., Kinoshita, M., … Ishijima, M. (2014). The degeneration and destruction of femoral articular cartilage shows a greater degree of deterioration than that of the tibial and patellar articular cartilage in early stage knee osteoarthritis: a cross-sectional study. *Osteoarthritis and Cartilage*, *22*(10), 1583–1589. doi: 10.1016/j.joca.2014.07.021

Haffner, A., Figueiredo Neto, M., Umbaugh, C., & Figueiredo, M. (2017). *Investigating novel small compounds and their effects on inflammation and chondrogenesis in joints*. Presented at the Experimental Biology 2017, Chicago, IL.

Haltmayer, E., Ribitsch, I., Gabner, S., Rosser, J., Gueltekin, S., Peham, J., … Jenner, F. (2019). Co-culture of osteochondral explants and synovial membrane as in vitro model for osteoarthritis. *Plos One*, *14*(4), e0214709. doi: 10.1371/journal.pone.0214709

Harrison, S. M., Whitton, R. C., Kawcak, C. E., Stover, S. M., & Pandy, M. G. (2010). Relationship between muscle forces, joint loading and utilization of elastic strain energy in equine locomotion. *Journal of Experimental Biology*, *213*(Pt 23), 3998–4009. doi: 10.1242/jeb.044545

Harrison, S. M., Whitton, R. C., Kawcak, C. E., Stover, S. M., & Pandy, M. G. (2014). Evaluation of a subject-specific finite-element model of the equine metacarpophalangeal joint under physiological load. *Journal of Biomechanics*, *47*(1), 65–73. doi: 10.1016/j.jbiomech.2013.10.001

Harvanova, D., Matejova, J., Slovinska, L., Lacko, M., Gulova, S., Fecskeova, L. K., … Rosocha, J. (2022). The role of synovial membrane in the development of a potential in vitro model of osteoarthritis. *International Journal of Molecular Sciences*, *23*(5). doi: 10.3390/ijms23052475

Haseeb, A., & Haqqi, T. M. (2013). Immunopathogenesis of osteoarthritis. *Clinical Immunology*, *146*(3), 185–196. doi: 10.1016/j.clim.2012.12.011

Hatakeyama, A., Uchida, S., Utsunomiya, H., Tsukamoto, M., Nakashima, H., Nakamura, E., … Sakai, A. (2017). Isolation and Characterization of Synovial Mesenchymal Stem Cell Derived from Hip Joints: A Comparative Analysis with a Matched Control Knee Group. *Stem Cells International*, *2017*, 9312329. doi: 10.1155/2017/9312329

Hawker, G. A., Stewart, L., French, M. R., Cibere, J., Jordan, J. M., March, L., … Gooberman-Hill, R. (2008). Understanding the pain experience in hip and knee osteoarthritis--an OARSI/OMERACT initiative. *Osteoarthritis and Cartilage*, *16*(4), 415–422. doi: 10.1016/j.joca.2007.12.017

Hayami, T., Pickarski, M., Zhuo, Y., Wesolowski, G. A., Rodan, G. A., & Duong, L. T. (2006). Characterization of articular cartilage and subchondral bone changes in the rat anterior cruciate ligament transection and meniscectomized models of osteoarthritis. *Bone*, *38*(2), 234–243. doi: 10.1016/j.bone.2005.08.007

Heinegård, D., & Saxne, T. (2011). The role of the cartilage matrix in osteoarthritis. *Nature Reviews. Rheumatology*, *7*(1), 50–56. doi: 10.1038/nrrheum.2010.198

Hochberg, M. C., Altman, R. D., April, K. T., Benkhalti, M., Guyatt, G., McGowan, J., … American College of Rheumatology. (2012). American College of Rheumatology 2012 recommendations for the use of nonpharmacologic and pharmacologic therapies in osteoarthritis of the hand, hip, and knee. *Arthritis Care & Research*, *64*(4), 465–474. doi: 10.1002/acr.21596

Hsia, A. W., Anderson, M. J., Heffner, M. A., Lagmay, E. P., Zavodovskaya, R., & Christiansen, B. A. (2017). Osteophyte formation after ACL rupture in mice is associated with joint restabilization and loss of range of motion. *Journal of Orthopaedic Research*, *35*(3), 466–473. doi: 10.1002/jor.23252

Huang, H., Zheng, J., Shen, N., Wang, G., Zhou, G., Fang, Y., … Zhao, J. (2018). Identification of pathways and genes associated with synovitis in osteoarthritis using bioinformatics analyses. *Scientific Reports*, *8*(1), 10050. doi: 10.1038/s41598-018-28280-6

Huang, W., Zhang, L., Cheng, C., Shan, W., Ma, R., Yin, Z., & Zhu, C. (2019). Parallel comparison of fibroblast-like synoviocytes from the surgically removed hyperplastic synovial tissues of rheumatoid arthritis and osteoarthritis patients. *BMC Musculoskeletal Disorders*, *20*(1), 591. doi: 10.1186/s12891-019-2977-2

Huh, Y. H., Lee, G., Song, W.-H., Koh, J.-T., & Ryu, J.-H. (2015). Crosstalk between FLS and chondrocytes is regulated by HIF-2α-mediated cytokines in arthritis. *Experimental & Molecular Medicine*, *47*, e197. doi: 10.1038/emm.2015.88

Hunter, D. J., McDougall, J. J., & Keefe, F. J. (2009). The symptoms of osteoarthritis and the genesis of pain. *The Medical Clinics of North America*, *93*(1), 83–100, xi. doi: 10.1016/j.mcna.2008.08.008

Hyttinen, M. M., Holopainen, J., van Weeren, P. R., Firth, E. C., Helminen, H. J., & Brama, P. A. J. (2009). Changes in collagen fibril network organization and proteoglycan distribution in equine articular cartilage during maturation and growth. *Journal of Anatomy*, *215*(5), 584–591. doi: 10.1111/j.1469-7580.2009.01140.x

Ide, Y., Matsui, T., Ishibashi, Y., Takeuchi, M., & Yamagishi, S. (2010). Pigment epithelium-derived factor inhibits advanced glycation end product-elicited mesangial cell damage by blocking NF-kappaB activation. *Microvascular Research*, *80*(2), 227–232. doi: 10.1016/j.mvr.2010.03.015

Ireland, J. L., Wylie, C. E., Collins, S. N., Verheyen, K. L. P., & Newton, J. R. (2013). Preventive health care and owner-reported disease prevalence of horses and ponies in Great Britain. *Research in Veterinary Science*, *95*(2), 418–424. doi: 10.1016/j.rvsc.2013.05.007

Iwanaga, T., Shikichi, M., Kitamura, H., Yanase, H., & Nozawa-Inoue, K. (2000). Morphology and functional roles of synoviocytes in the joint. *Archives of Histology and Cytology*, *63*(1), 17–31. doi: 10.1679/aohc.63.17.

Jiang, A., Xu, P., Sun, S., Zhao, Z., Tan, Q., Li, W., … Leng, H. (2021). Cellular alterations and crosstalk in the osteochondral joint in osteoarthritis and promising therapeutic strategies. *Connective Tissue Research*, *62*(6), 709–719. doi: 10.1080/03008207.2020.1870969

Jin, X.-N., Yan, E.-Z., Wang, H.-M., Sui, H.-J., Liu, Z., Gao, W., & Jin, Y. (2016). Hyperoside exerts anti-inflammatory and anti-arthritic effects in LPS-stimulated human fibroblast-like synoviocytes in vitro and in mice with collagen-induced arthritis. *Acta Pharmacologica Sinica*, *37*(5), 674–686. doi: 10.1038/aps.2016.7

Ji, Q., Xu, X., Zhang, Q., Kang, L., Xu, Y., Zhang, K., … Wang, Y. (2016). The IL-1β/AP-1/miR-30a/ADAMTS-5 axis regulates cartilage matrix degradation in human osteoarthritis. *Journal of Molecular Medicine, 94*(7), 771–785. doi: 10.1007/s00109-016-1418-z

Johnson, K., Zhu, S., Tremblay, M. S., Payette, J. N., Wang, J., Bouchez, L. C., … Schultz, P. G. (2012). A stem cell-based approach to cartilage repair. *Science, 336*(6082), 717–721. doi: 10.1126/science.1215157

Johnson, S., & Symons, J. (2019). Measuring volumetric changes of equine distal limbs: A pilot study examining jumping exercise. *Animals: An Open Access Journal from MDPI, 9*(10). doi: 10.3390/ani9100751

Jones, K., Angelozzi, M., Gangishetti, U., Haseeb, A., de Charleroy, C., Lefebvre, V., & Bhattaram, P. (2021). Human Adult Fibroblast-like Synoviocytes and Articular Chondrocytes Exhibit Prominent Overlap in Their Transcriptomic Signatures. *ACR Open Rheumatology, 3*(6), 359–370. doi: 10.1002/acr2.11255

Joshi, N. S., Bansal, P. N., Stewart, R. C., Snyder, B. D., & Grinstaff, M. W. (2009). Effect of contrast agent charge on visualization of articular cartilage using computed tomography: exploiting electrostatic interactions for improved sensitivity. *Journal of the American Chemical Society, 131*(37), 13234–13235. doi: 10.1021/ja9053306

Kajabi, A. W., Casula, V., Sarin, J. K., Ketola, J. H., Nykänen, O., Te Moller, N. C. R., … Nissi, M. J. (2021). Evaluation of articular cartilage with quantitative MRI in an equine model of post-traumatic osteoarthritis. *Journal of Orthopaedic Research, 39*(1), 63–73. doi: 10.1002/jor.24780

Kamm, J. L., Nixon, A. J., & Witte, T. H. (2010). Cytokine and catabolic enzyme expression in synovium, synovial fluid and articular cartilage of naturally osteoarthritic equine carpi. *Equine Veterinary Journal, 42*(8), 693–699. doi: 10.1111/j.2042-3306.2010.00140.x

Kane, B. A., An, H., Rajasekariah, P., McNeil, H. P., Bryant, K., & Tedla, N. (2019). Differential expression and regulation of the non-integrin 37/67-kDa laminin receptor on peripheral blood leukocytes of healthy individuals and patients with rheumatoid arthritis. *Scientific Reports, 9*(1), 1149. doi: 10.1038/s41598-018-37907-7

Karamanos, N. K. (2019). Extracellular matrix: key structural and functional meshwork in health and disease. *The FEBS Journal, 286*(15), 2826–2829. doi: 10.1111/febs.14992

Karlsson, C., & Lindahl, A. (2009). Articular cartilage stem cell signalling. *Arthritis Research & Therapy, 11*(4), 121. doi: 10.1186/ar2753

Keating, D., Haffner, A., Figueiredo Neto, M., Gimble, J., Lescun, T., & Figueiredo, M. (2019). *The effect of small novel compounds and growth factors on chondrogenic potential of equine mesenchymal stem cells*. Presented at the Van Sickle Research Day.

Kennedy, O. D., Herman, B. C., Laudier, D. M., Majeska, R. J., Sun, H. B., & Schaffler, M. B. (2012). Activation of resorption in fatigue-loaded bone involves both apoptosis and active pro-osteoclastogenic signaling by distinct osteocyte populations. *Bone*, *50*(5), 1115–1122. doi: 10.1016/j.bone.2012.01.025

Kennedy, O. D., Laudier, D. M., Majeska, R. J., Sun, H. B., & Schaffler, M. B. (2014). Osteocyte apoptosis is required for production of osteoclastogenic signals following bone fatigue in vivo. *Bone*, *64*, 132–137. doi: 10.1016/j.bone.2014.03.049

Kiener, H. P., Lee, D. M., Agarwal, S. K., & Brenner, M. B. (2006). Cadherin-11 induces rheumatoid arthritis fibroblast-like synoviocytes to form lining layers in vitro. *The American Journal of Pathology*, *168*(5), 1486–1499. doi: 10.2353/ajpath.2006.050999

Kiener, H. P., Watts, G. F. M., Cui, Y., Wright, J., Thornhill, T. S., Sköld, M., … Lee, D. M. (2010). Synovial fibroblasts self-direct multicellular lining architecture and synthetic function in three-dimensional organ culture. *Arthritis and Rheumatism*, *62*(3), 742–752. doi: 10.1002/art.27285

Kim, H. A., Cho, M.-L., Choi, H. Y., Yoon, C. S., Jhun, J. Y., Oh, H. J., & Kim, H.-Y. (2006). The catabolic pathway mediated by Toll-like receptors in human osteoarthritic chondrocytes. *Arthritis and Rheumatism*, *54*(7), 2152–2163. doi: 10.1002/art.21951

Kim, J. E., Song, D.-H., Kim, S. H., Jung, Y., & Kim, S. J. (2018). Development and characterization of various osteoarthritis models for tissue engineering. *Plos One*, *13*(3), e0194288. doi: 10.1371/journal.pone.0194288

King, M. R., Haussler, K. K., Kawcak, C. E., McIlwraith, C. W., & Reiser, R. F. (2013). Mechanisms of aquatic therapy and its potential use in managing equine osteoarthritis. *Equine Veterinary Education*, *25*(4), 204–209. doi: 10.1111/j.2042-3292.2012.00389.x

Konttinen, Y. T., Li, T. F., Hukkanen, M., Ma, J., Xu, J. W., & Virtanen, I. (2000). Fibroblast biology. Signals targeting the synovial fibroblast in arthritis. *Arthritis Research*, *2*(5), 348–355. doi: 10.1186/ar111

Korhonen, R. K., Laasanen, M. S., Töyräs, J., Lappalainen, R., Helminen, H. J., & Jurvelin, J. S. (2003). Fibril reinforced poroelastic model predicts specifically mechanical behavior of normal, proteoglycan depleted and collagen degraded articular cartilage. *Journal of Biomechanics*, *36*(9), 1373–1379. doi: 10.1016/s0021-9290(03)00069-1

Kramer, J., Keegan, K. G., Kelmer, G., & Wilson, D. A. (2004). Objective determination of pelvic movement during hind limb lameness by use of a signal decomposition method and pelvic height differences. *American Journal of Veterinary Research*, *65*(6), 741–747. doi: 10.2460/ajvr.2004.65.741

Kramer, J., Keegan, K. G., Wilson, D. A., Smith, B. K., & Wilson, D. J. (2000). Kinematics of the hind limb in trotting horses after induced lameness of the distal intertarsal and

tarsometatarsal joints and intra-articular administration of anesthetic. *American Journal of Veterinary Research*, *61*(9), 1031–1036. doi: 10.2460/ajvr.2000.61.1031

Kramer, W. C., Hendricks, K. J., & Wang, J. (2011). Pathogenetic mechanisms of posttraumatic osteoarthritis: opportunities for early intervention. *International Journal of Clinical and Experimental Medicine*, *4*(4), 285–298. PMID: 22140600

Lajeunesse, D. (2004). The role of bone in the treatment of osteoarthritis. *Osteoarthritis and Cartilage*, *12 Suppl A*, S34-8. doi: 10.1016/j.joca.2003.09.013

Lampropoulou-Adamidou, K., Lelovas, P., Karadimas, E. V., Liakou, C., Triantafillopoulos, I. K., Dontas, I., & Papaioannou, N. A. (2014). Useful animal models for the research of osteoarthritis. *European Journal of Orthopaedic Surgery & Traumatology: Orthopedie Traumatologie*, *24*(3), 263–271. doi: 10.1007/s00590-013-1205-2

Lazic, S. E., Clarke-Williams, C. J., & Munafò, M. R. (2018). What exactly is "N" in cell culture and animal experiments? *PLoS Biology*, *16*(4), e2005282. doi: 10.1371/journal.pbio.2005282

Lee, A. K. K., Uhl, E. W., & Osborn, M. L. (2021). Construction of a Realistic, Whole-Body, Three-Dimensional Equine Skeletal Model using Computed Tomography Data. *Journal of Visualized Experiments*, (168). doi: 10.3791/62276

Lee, C. M., Kisiday, J. D., McIlwraith, C. W., Grodzinsky, A. J., & Frisbie, D. D. (2013). Synoviocytes protect cartilage from the effects of injury in vitro. *BMC Musculoskeletal Disorders*, *14*, 54. doi: 10.1186/1471-2474-14-54

Lee, H., & Park, J.-B. (2019). Dimethyl Sulfoxide Leads to Decreased Osteogenic Differentiation of Stem Cells Derived from Gingiva via Runx2 and Collagen I Expression. *European Journal of Dentistry*, *13*(2), 131–136. doi: 10.1055/s-0039-1694904

Leelamankong, P., Estrada, R., Mählmann, K., Rungsri, P., & Lischer, C. (2020). Agreement among equine veterinarians and between equine veterinarians and inertial sensor system during clinical examination of hindlimb lameness in horses. *Equine Veterinary Journal*, *52*(2), 326–331. doi: 10.1111/evj.13144

Lepetsos, P., Papavassiliou, K. A., & Papavassiliou, A. G. (2019). Redox and NF-κB signaling in osteoarthritis. *Free Radical Biology & Medicine*, *132*, 90–100. doi: 10.1016/j.freeradbiomed.2018.09.025

Levick, J. R., & McDonald, J. N. (1995). Fluid movement across synovium in healthy joints: role of synovial fluid macromolecules. *Annals of the Rheumatic Diseases*, *54*(5), 417–423. doi: 10.1136/ard.54.5.417

Ley, C. J., Ekman, S., Hansson, K., Björnsdóttir, S., & Boyde, A. (2014). Osteochondral lesions in distal tarsal joints of Icelandic horses reveal strong associations between hyaline and calcified cartilage abnormalities. *European Cells & Materials*, *27*, 213–236; discussion 234. doi: 10.22203/ecm.v027a16

Liang, S., Wang, Z.-G., Zhang, Z.-Z., Chen, K., Lv, Z.-T., Wang, Y.-T., … Chen, A.-M. (2019). Decreased RIPK1 expression in chondrocytes alleviates osteoarthritis via the TRIF/MyD88-RIPK1-TRAF2 negative feedback loop. *Aging*, *11*(19), 8664–8680. doi: 10.18632/aging.102354

Lim, H., & Kim, H. P. (2011). Matrix metalloproteinase-13 expression in IL-1β-treated chondrocytes by activation of the p38 MAPK/c-Fos/AP-1 and JAK/STAT pathways. *Archives of Pharmacal Research*, *34*(1), 109–117. doi: 10.1007/s12272-011-0113-4

Little, C. B., Barai, A., Burkhardt, D., Smith, S. M., Fosang, A. J., Werb, Z., … Thompson, E. W. (2009). Matrix metalloproteinase 13-deficient mice are resistant to osteoarthritic cartilage erosion but not chondrocyte hypertrophy or osteophyte development. *Arthritis and Rheumatism*, *60*(12), 3723–3733. doi: 10.1002/art.25002

Liu-Bryan, R. (2013). Synovium and the innate inflammatory network in osteoarthritis progression. *Current Rheumatology Reports*, *15*(5), 323. doi: 10.1007/s11926-013-0323-5

Liu, S., Cao, C., Zhang, Y., Liu, G., Ren, W., Ye, Y., & Sun, T. (2019). PI3K/Akt inhibitor partly decreases TNF-α-induced activation of fibroblast-like synoviocytes in osteoarthritis. *Journal of Orthopaedic Surgery and Research*, *14*(1), 425. doi: 10.1186/s13018-019-1394-4

Li, G., Yin, J., Gao, J., Cheng, T. S., Pavlos, N. J., Zhang, C., & Zheng, M. H. (2013). Subchondral bone in osteoarthritis: insight into risk factors and microstructural changes. *Arthritis Research & Therapy*, *15*(6), 223. doi: 10.1186/ar4405

Li, Heng, Li, J., Yu, S., Wu, C., & Zhang, W. (2021). The mechanical properties of tibiofemoral and patellofemoral articular cartilage in compression depend on anatomical regions. *Scientific Reports*, *11*(1), 6128. doi: 10.1038/s41598-021-85716-2

Li, Hongxi, Xie, S., Qi, Y., Li, H., Zhang, R., & Lian, Y. (2018). TNF-α increases the expression of inflammatory factors in synovial fibroblasts by inhibiting the PI3K/AKT pathway in a rat model of monosodium iodoacetate-induced osteoarthritis. *Experimental and Therapeutic Medicine*, *16*(6), 4737–4744. doi: 10.3892/etm.2018.6770

Li, J., Zhang, B., Liu, W.-X., Lu, K., Pan, H., Wang, T., … Chen, D. (2020). Metformin limits osteoarthritis development and progression through activation of AMPK signalling. *Annals of the Rheumatic Diseases*, *79*(5), 635–645. doi: 10.1136/annrheumdis-2019-216713

Li, X., Sun, Y., Zhou, Z., Zhang, D., Jiao, J., Hu, M., … Qin, Y.-X. (2019). Mitigation of Articular Cartilage Degeneration and Subchondral Bone Sclerosis in Osteoarthritis

Progression Using Low-Intensity Ultrasound Stimulation. *Ultrasound in Medicine & Biology*, *45*(1), 148–159. doi: 10.1016/j.ultrasmedbio.2018.08.022

Lopez-Castejon, G., & Brough, D. (2011). Understanding the mechanism of IL-1β secretion. *Cytokine & Growth Factor Reviews*, *22*(4), 189–195. doi: 10.1016/j.cytogfr.2011.10.001

Lord, R. (2019). *The Equine Industry: Competing Beliefs, Changes and Conflicts*. Muma College of Business. Retrieved from http://pubs.mumabusinessreview.org/2019/MBR-2019-03-09-099-120-Lord-EquineIndustry.pdf

Lories, R. J., & Luyten, F. P. (2011). The bone-cartilage unit in osteoarthritis. *Nature Reviews. Rheumatology*, *7*(1), 43–49. doi: 10.1038/nrrheum.2010.197

Lustgarten, M., Redding, W. R., Labens, R., Morgan, M., Davis, W., & Seiler, G. S. (2014). Elastographic characteristics of the metacarpal tendons in horses without clinical evidence of tendon injury. *Veterinary Radiology & Ultrasound: The Official Journal of the American College of Veterinary Radiology and the International Veterinary Radiology Association*, *55*(1), 92–101. doi: 10.1111/vru.12104

Lu, Y., Feng, J., Yang, L., Tang, H., Jin, J., & Xu, X. (2014). Anti-inflammatory effects of a synthetic peptide derived from pigment epithelium-derived factor on H_2O_2-induced corneal injury in vitro. *Chinese Medical Journal*, *127*(8), 1438–1444. PMID: 24762585.

Lyons, T. J., McClure, S. F., Stoddart, R. W., & McClure, J. (2006). The normal human chondro-osseous junctional region: evidence for contact of uncalcified cartilage with subchondral bone and marrow spaces. *BMC Musculoskeletal Disorders*, *7*, 52. doi: 10.1186/1471-2474-7-52

Madry, H., van Dijk, C. N., & Mueller-Gerbl, M. (2010). The basic science of the subchondral bone. *Knee Surgery, Sports Traumatology, Arthroscopy*, *18*(4), 419–433. doi: 10.1007/s00167-010-1054-z

Maeß, M. B., Wittig, B., & Lorkowski, S. (2014). Highly efficient transfection of human THP-1 macrophages by nucleofection. *Journal of Visualized Experiments*, (91), e51960. doi: 10.3791/51960

Mäkelä, J. T. A., Han, S. K., Herzog, W., & Korhonen, R. K. (2015). Very early osteoarthritis changes sensitively fluid flow properties of articular cartilage. *Journal of Biomechanics*, *48*(12), 3369–3376. doi: 10.1016/j.jbiomech.2015.06.010

Maliye, S., Voute, L. C., & Marshall, J. F. (2015). Naturally-occurring forelimb lameness in the horse results in significant compensatory load redistribution during trotting. *Veterinary Journal*, *204*(2), 208–213. doi: 10.1016/j.tvjl.2015.03.005

Manzano, S., Manzano, R., Doblaré, M., & Doweidar, M. H. (2015). Altered swelling and ion fluxes in articular cartilage as a biomarker in osteoarthritis and joint immobilization: a computational analysis. *Journal of the Royal Society, Interface*, *12*(102), 20141090. doi: 10.1098/rsif.2014.1090

Marcu, K. B., Otero, M., Olivotto, E., Borzi, R. M., & Goldring, M. B. (2010). NF-kappaB signaling: multiple angles to target OA. *Current Drug Targets*, *11*(5), 599–613. doi: 10.2174/138945010791011938

Martel-Pelletier, J., Boileau, C., Pelletier, J.-P., & Roughley, P. J. (2008). Cartilage in normal and osteoarthritis conditions. *Best Practice & Research. Clinical Rheumatology*, *22*(2), 351–384. doi: 10.1016/j.berh.2008.02.001

Martig, S., Hitchens, P. L., Lee, P. V. S., & Whitton, R. C. (2020). The relationship between microstructure, stiffness and compressive fatigue life of equine subchondral bone. *Journal of the Mechanical Behavior of Biomedical Materials*, *101*, 103439. doi: 10.1016/j.jmbbm.2019.103439

Martin, J. A., Anderson, D. D., Goetz, J. E., Fredericks, D., Pedersen, D. R., Ayati, B. P., … Buckwalter, J. A. (2017). Complementary models reveal cellular responses to contact stresses that contribute to post-traumatic osteoarthritis. *Journal of Orthopaedic Research*, *35*(3), 515–523. doi: 10.1002/jor.23389

Mathiessen, A., & Conaghan, P. G. (2017). Synovitis in osteoarthritis: current understanding with therapeutic implications. *Arthritis Research & Therapy*, *19*(1), 18. doi: 10.1186/s13075-017-1229-9

Matsui, T., Higashimoto, Y., Taira, J., & Yamagishi, S. (2013). Pigment epithelium-derived factor (PEDF) binds to caveolin-1 and inhibits the pro-inflammatory effects of caveolin-1 in endothelial cells. *Biochemical and Biophysical Research Communications*, *441*(2), 405–410. doi: 10.1016/j.bbrc.2013.10.074

Matsui, T., Higashimoto, Y., & Yamagishi, S. (2014). Laminin receptor mediates anti-inflammatory and anti-thrombogenic effects of pigment epithelium-derived factor in myeloma cells. *Biochemical and Biophysical Research Communications*, *443*(3), 847–851. doi: 10.1016/j.bbrc.2013.12.060

Ma, B., Zhou, Y., Liu, R., Zhang, K., Yang, T., Hu, C., … Qi, H. (2021). Pigment epithelium-derived factor (PEDF) plays anti-inflammatory roles in the pathogenesis of dry eye disease. *The Ocular Surface*, *20*, 70–85. doi: 10.1016/j.jtos.2020.12.007

McCoy, A. M., Kemper, A. M., Boyce, M. K., Brown, M. P., & Trumble, T. N. (2020). Differential gene expression analysis reveals pathways important in early post-traumatic osteoarthritis in an equine model. *BMC Genomics*, *21*(1), 843. doi: 10.1186/s12864-020-07228-z

McIlwraith, C. Wayne. (2013). Oral joint supplements in the management of osteoarthritis. In *Equine applied and clinical nutrition* (pp. 549–557). Elsevier. doi: 10.1016/B978-0-7020-3422-0.00033-X

McIlwraith, C W, Frisbie, D. D., Kawcak, C. E., Fuller, C. J., Hurtig, M., & Cruz, A. (2010). The OARSI histopathology initiative - recommendations for histological assessments of osteoarthritis in the horse. *Osteoarthritis and Cartilage, 18 Suppl 3*, S93-105. doi: 10.1016/j.joca.2010.05.031

McIlwraith, C W, Frisbie, D. D., & Kawcak, C. E. (2012). The horse as a model of naturally occurring osteoarthritis. *Bone & Joint Research*, *1*(11), 297–309. doi: 10.1302/2046-3758.111.2000132

McIlwraith, C Wayne, & Lattermann, C. (2019). Intra-articular Corticosteroids for Knee Pain-What Have We Learned from the Equine Athlete and Current Best Practice. *The Journal of Knee Surgery*, *32*(1), 9–25. doi: 10.1055/s-0038-1676449

McNary, S. M., Athanasiou, K. A., & Reddi, A. H. (2012). Engineering lubrication in articular cartilage. *Tissue Engineering. Part B, Reviews*, *18*(2), 88–100. doi: 10.1089/ten.TEB.2011.0394

Millerand, M., Sudre, L., Nefla, M., Pène, F., Rousseau, C., Pons, A., … Jacques, C. (2020). Activation of innate immunity by 14-3-3 ε, a new potential alarmin in osteoarthritis. *Osteoarthritis and Cartilage*, *28*(5), 646–657. doi: 10.1016/j.joca.2020.03.002

Moradi, B., Rosshirt, N., Tripel, E., Kirsch, J., Barié, A., Zeifang, F., … Hagmann, S. (2015). Unicompartmental and bicompartmental knee osteoarthritis show different patterns of mononuclear cell infiltration and cytokine release in the affected joints. *Clinical and Experimental Immunology*, *180*(1), 143–154. doi: 10.1111/cei.12486

Musumeci, G. (2016). The effect of mechanical loading on articular cartilage. *Journal of Functional Morphology and Kinesiology*, *1*(2), 154–161. doi: 10.3390/jfmk1020154

Myller, K. A. H., Korhonen, R. K., Töyräs, J., Salo, J., Jurvelin, J. S., & Venäläinen, M. S. (2019). Computational evaluation of altered biomechanics related to articular cartilage lesions observed in vivo. *Journal of Orthopaedic Research*, *37*(5), 1042–1051. doi: 10.1002/jor.24273

Nair, A., Kanda, V., Bush-Joseph, C., Verma, N., Chubinskaya, S., Mikecz, K., … Scanzello, C. R. (2012). Synovial fluid from patients with early osteoarthritis modulates fibroblast-like synoviocyte responses to toll-like receptor 4 and toll-like receptor 2 ligands via soluble CD14. *Arthritis and Rheumatism*, *64*(7), 2268–2277. doi: 10.1002/art.34495

Nakamura, D. S., Hollander, J. M., Uchimura, T., Nielsen, H. C., & Zeng, L. (2017). Pigment Epithelium-Derived Factor (PEDF) mediates cartilage matrix loss in an age-dependent manner under inflammatory conditions. *BMC Musculoskeletal Disorders*, *18*(1), 39. doi: 10.1186/s12891-017-1410-y

Nelson, B. B., Stewart, R. C., Kawcak, C. E., Freedman, J. D., Patwa, A. N., Snyder, B. D., … Grinstaff, M. W. (2021). Quantitative Evaluation of Equine Articular Cartilage Using Cationic Contrast-Enhanced Computed Tomography. *Cartilage*, *12*(2), 211–221. doi: 10.1177/1947603518812562

Neundorf, R. H., Lowerison, M. B., Cruz, A. M., Thomason, J. J., McEwen, B. J., & Hurtig, M. B. (2010). Determination of the prevalence and severity of metacarpophalangeal joint osteoarthritis in Thoroughbred racehorses via quantitative macroscopic evaluation. *American Journal of Veterinary Research*, *71*(11), 1284–1293. doi: 10.2460/ajvr.71.11.1284

Ni, Z., Kuang, L., Chen, H., Xie, Y., Zhang, B., Ouyang, J., … Chen, L. (2019). The exosome-like vesicles from osteoarthritic chondrocyte enhanced mature IL-1β production of macrophages and aggravated synovitis in osteoarthritis. *Cell Death & Disease*, *10*(7), 522. doi: 10.1038/s41419-019-1739-2

Nissinen, M. T., Hänninen, N., Prakash, M., Mäkelä, J. T. A., Nissi, M. J., Töyräs, J., … Tanska, P. (2021). Functional and structural properties of human patellar articular cartilage in osteoarthritis. *Journal of Biomechanics*, *126*, 110634. doi: 10.1016/j.jbiomech.2021.110634

Nixon, A. J., Grol, M. W., Lang, H. M., Ruan, M. Z. C., Stone, A., Begum, L., … Guse, K. (2018). Disease-Modifying Osteoarthritis Treatment With Interleukin-1 Receptor Antagonist Gene Therapy in Small and Large Animal Models. *Arthritis & Rheumatology (Hoboken, N.J.)*, *70*(11), 1757–1768. doi: 10.1002/art.40668

Noble, P., Collin, B., Lecomte-Beckers, J., Magnée, A., Denoix, J. M., & Serteyn, D. (2010). An equine joint friction test model using a cartilage-on-cartilage arrangement. *Veterinary Journal*, *183*(2), 148–152. doi: 10.1016/j.tvjl.2008.12.003

Novakofski, K. D., Williams, R. M., Fortier, L. A., Mohammed, H. O., Zipfel, W. R., & Bonassar, L. J. (2014). Identification of cartilage injury using quantitative multiphoton microscopy. *Osteoarthritis and Cartilage*, *22*(2), 355–362. doi: 10.1016/j.joca.2013.10.008

Núñez Miguel, R., Wong, J., Westoll, J. F., Brooks, H. J., O'Neill, L. A. J., Gay, N. J., … Monie, T. P. (2007). A dimer of the Toll-like receptor 4 cytoplasmic domain provides a specific scaffold for the recruitment of signalling adaptor proteins. *Plos One*, *2*(8), e788. doi: 10.1371/journal.pone.0000788

O'Connell, J. X. (2000). Pathology of the synovium. *American Journal of Clinical Pathology*, *114*(5), 773–784. doi: 10.1309/LWW3-5XK0-FKG9-HDRK

Ohata, J., Zvaifler, N. J., Nishio, M., Boyle, D. L., Kalled, S. L., Carson, D. A., & Kipps, T. J. (2005). Fibroblast-like synoviocytes of mesenchymal origin express functional B cell-activating factor of the TNF family in response to proinflammatory cytokines. *Journal of Immunology*, *174*(2), 864–870. doi: 10.4049/jimmunol.174.2.864

Oke, S., McIlwraith, C., & Moyer, W. (2010). Review of the economic impact of osteoarthritis and oral joint-health supplements in horses. Retrieved from https://aaep.org/sites/default/files/issues/proceedings-10proceedings-z9100110000012.pdf.

Olive, J., Lambert, N., Bubeck, K. A., Beauchamp, G., & Laverty, S. (2014). Comparison between palpation and ultrasonography for evaluation of experimentally induced effusion in the distal interphalangeal joint of horses. *American Journal of Veterinary Research*, *75*(1), 34–40. doi: 10.2460/ajvr.75.1.34

Pan, J., Zhou, X., Li, W., Novotny, J. E., Doty, S. B., & Wang, L. (2009). In situ measurement of transport between subchondral bone and articular cartilage. *Journal of Orthopaedic Research*, *27*(10), 1347–1352. doi: 10.1002/jor.20883

Pap, T., Dankbar, B., Wehmeyer, C., Korb-Pap, A., & Sherwood, J. (2020). Synovial fibroblasts and articular tissue remodelling: Role and mechanisms. *Seminars in Cell & Developmental Biology*, *101*, 140–145. doi: 10.1016/j.semcdb.2019.12.006

Park, H., Hong, J., Yin, Y., Joo, Y., Kim, Y., Shin, J., … Kim, J. (2020). TAP2, a peptide antagonist of Toll-like receptor 4, attenuates pain and cartilage degradation in a monoiodoacetate-induced arthritis rat model. *Scientific Reports*, *10*(1), 17451. doi: 10.1038/s41598-020-74544-5

Parsons, K. J., Spence, A. J., Morgan, R., Thompson, J. A., & Wilson, A. M. (2011). High speed field kinematics of foot contact in elite galloping horses in training. *Equine Veterinary Journal*, *43*(2), 216–222. doi: 10.1111/j.2042-3306.2010.00149.x

Petersen, W., & Tillmann, B. (1998). Collagenous fibril texture of the human knee joint menisci. *Anatomy and Embryology*, *197*(4), 317–324. doi: 10.1007/s004290050141

Prado, A. A. F., Favaron, P. O., da Silva, L. C. L. C., Baccarin, R. Y. A., Miglino, M. A., & Maria, D. A. (2015). Characterization of mesenchymal stem cells derived from the equine synovial fluid and membrane. *BMC Veterinary Research*, *11*, 281. doi: 10.1186/s12917-015-0531-5

Pretzel, D., Pohlers, D., Weinert, S., & Kinne, R. W. (2009). In vitro model for the analysis of synovial fibroblast-mediated degradation of intact cartilage. *Arthritis Research & Therapy*, *11*(1), R25. doi: 10.1186/ar2618

Pulai, J. I., Chen, H., Im, H.-J., Kumar, S., Hanning, C., Hegde, P. S., & Loeser, R. F. (2005). NF-kappa B mediates the stimulation of cytokine and chemokine expression by human articular chondrocytes in response to fibronectin fragments. *Journal of Immunology*, *174*(9), 5781–5788. doi: 10.4049/jimmunol.174.9.5781

Qiao, L., Li, Y., & Sun, S. (2020). Insulin Exacerbates Inflammation in Fibroblast-Like Synoviocytes. *Inflammation*, *43*(3), 916–936. doi: 10.1007/s10753-020-01178-0

Qiao, Z., Tang, J., Wu, W., Tang, J., & Liu, M. (2019). Acteoside inhibits inflammatory response via JAK/STAT signaling pathway in osteoarthritic rats. *BMC Complementary and Alternative Medicine*, *19*(1), 264. doi: 10.1186/s12906-019-2673-7

Rao, X., Huang, X., Zhou, Z., & Lin, X. (2013). An improvement of the 2ˆ(-delta CT) method for quantitative real-time polymerase chain reaction data analysis. *Biostatistics, Bioinformatics and Biomathematics*, *3*(3), 71–85. PMID: 25558171

Rattner, J. B., Sciore, P., Ou, Y., van der Hoorn, F. A., & Lo, I. K. Y. (2010). Primary cilia in fibroblast-like type B synoviocytes lie within a cilium pit: a site of endocytosis. *Histology and Histopathology*, *25*(7), 865–875. doi: 10.14670/HH-25.865

Reesink, Heidi L, Sutton, R. M., Shurer, C. R., Peterson, R. P., Tan, J. S., Su, J., … Nixon, A. J. (2017). Galectin-1 and galectin-3 expression in equine mesenchymal stromal cells (MSCs), synovial fibroblasts and chondrocytes, and the effect of inflammation on MSC motility. *Stem Cell Research & Therapy*, *8*(1), 243. doi: 10.1186/s13287-017-0691-2

Reesink, H L, Watts, A. E., Mohammed, H. O., Jay, G. D., & Nixon, A. J. (2017). Lubricin/proteoglycan 4 increases in both experimental and naturally occurring equine osteoarthritis. *Osteoarthritis and Cartilage*, *25*(1), 128–137. doi: 10.1016/j.joca.2016.07.021

Rhee, D. K., Marcelino, J., Baker, M., Gong, Y., Smits, P., Lefebvre, V., … Carpten, J. D. (2005). The secreted glycoprotein lubricin protects cartilage surfaces and inhibits synovial cell overgrowth. *The Journal of Clinical Investigation*, *115*(3), 622–631. doi: 10.1172/JCI22263

Ribitsch, I., Peham, C., Ade, N., Dürr, J., Handschuh, S., Schramel, J. P., … Jenner, F. (2018). Structure-Function relationships of equine menisci. *Plos One*, *13*(3), e0194052. doi: 10.1371/journal.pone.0194052

Richardson, D. W. (2008). Complications of orthopaedic surgery in horses. *The Veterinary Clinics of North America. Equine Practice*, *24*(3), 591–610, viii. doi: 10.1016/j.cveq.2008.11.001

Riemenschneider, P. E., Rose, M. D., Giordani, M., & McNary, S. M. (2019). Compressive fatigue and endurance of juvenile bovine articular cartilage explants. *Journal of Biomechanics*, *95*, 109304. doi: 10.1016/j.jbiomech.2019.07.048

Roemer, F. W., Collins, J., Kwoh, C. K., Hannon, M. J., Neogi, T., Felson, D. T., … Guermazi, A. (2020). MRI-based screening for structural definition of eligibility in clinical DMOAD trials: Rapid OsteoArthritis MRI Eligibility Score (ROAMES). *Osteoarthritis and Cartilage*, *28*(1), 71–81. doi: 10.1016/j.joca.2019.08.005

Rosenberg, J. H., Rai, V., Dilisio, M. F., & Agrawal, D. K. (2017). Damage-associated molecular patterns in the pathogenesis of osteoarthritis: potentially novel therapeutic targets. *Molecular and Cellular Biochemistry, 434*(1–2), 171–179. doi: 10.1007/s11010-017-3047-4

Rosenberg, J. H., Rai, V., Dilisio, M. F., Sekundiak, T. D., & Agrawal, D. K. (2017). Increased expression of damage-associated molecular patterns (DAMPs) in osteoarthritis of human knee joint compared to hip joint. *Molecular and Cellular Biochemistry*, *436*(1–2), 59–69. doi: 10.1007/s11010-017-3078-x

Ross, M. W. (2003a). Arthroscopic Examination. In *Diagnosis and management of lameness in the horse* (pp. 226–230). Elsevier. doi: 10.1016/B978-0-7216-8342-3.50030-9

Ross, M. W. (2003b). Conformation and Lameness. In *Diagnosis and management of lameness in the horse* (pp. 15–31). Elsevier. doi: 10.1016/B978-0-7216-8342-3.50011-5

Ross, M. W. (2003c). Lameness in Horses: Basic Facts before Starting. In *Diagnosis and management of lameness in the horse* (pp. 3–8). Elsevier. doi: 10.1016/B978-0-7216-8342-3.50009-7

Sadeghi, H., Shepherd, D. E. T., & Espino, D. M. (2015). Effect of the variation of loading frequency on surface failure of bovine articular cartilage. *Osteoarthritis and Cartilage*, *23*(12), 2252–2258. doi: 10.1016/j.joca.2015.06.002

Sato, T., Konomi, K., Yamasaki, S., Aratani, S., Tsuchimochi, K., Yokouchi, M., … Nakajima, T. (2006). Comparative analysis of gene expression profiles in intact and damaged regions of human osteoarthritic cartilage. *Arthritis and Rheumatism*, *54*(3), 808–817. doi: 10.1002/art.21638

Scanzello, C. R., & Goldring, S. R. (2012). The role of synovitis in osteoarthritis pathogenesis. *Bone*, *51*(2), 249–257. doi: 10.1016/j.bone.2012.02.012

Schröder, A., Nazet, U., Muschter, D., Grässel, S., Proff, P., & Kirschneck, C. (2019). Impact of Mechanical Load on the Expression Profile of Synovial Fibroblasts from Patients with and without Osteoarthritis. *International Journal of Molecular Sciences*, *20*(3). doi: 10.3390/ijms20030585

Schwarzbach, S. V., Melo, C. F., Xavier, P. L. P., Roballo, K. C., Cordeiro, Y. G., Ambrósio, C. E., … Carregaro, A. B. (2019). Morphine, but not methadone, inhibits microsomal prostaglandin E synthase-1 and prostaglandin-endoperoxide synthase 2 in lipopolysaccharide-stimulated horse synoviocytes. *Biochimie*, *160*, 28–33. doi: 10.1016/j.biochi.2019.02.004

Setton, L. A., Elliott, D. M., & Mow, V. C. (1999). Altered mechanics of cartilage with osteoarthritis: human osteoarthritis and an experimental model of joint degeneration. *Osteoarthritis and Cartilage*, *7*(1), 2–14. doi: 10.1053/joca.1998.0170

Shaktivesh, S., Malekipour, F., Whitton, R. C., Hitchens, P. L., & Lee, P. V. (2020). Fatigue behavior of subchondral bone under simulated physiological loads of equine athletic training. *Journal of the Mechanical Behavior of Biomedical Materials*, *110*, 103920. doi: 10.1016/j.jmbbm.2020.103920

Sharma, A. R., Jagga, S., Chakraborty, C., & Lee, S.-S. (2020). Fibroblast-Like-Synoviocytes Mediate Secretion of Pro-Inflammatory Cytokines via ERK and JNK MAPKs in Ti-Particle-Induced Osteolysis. *Materials*, *13*(16). doi: 10.3390/ma13163628

Shen, S., Guo, J., Luo, Y., Zhang, W., Cui, Y., Wang, Q., … Wang, T. (2014). Functional proteomics revealed IL-1β amplifies TNF downstream protein signals in human synoviocytes in a TNF-independent manner. *Biochemical and Biophysical Research Communications*, *450*(1), 538–544. doi: 10.1016/j.bbrc.2014.06.008

Shikichi, M., Kitamura, H. P., Yanase, H., Konno, A., Takahashi-Iwanaga, H., & Iwanaga, T. (1999). Three-dimensional ultrastructure of synoviocytes in the horse joint as revealed by the scanning electron microscope. *Archives of Histology and Cytology*, *62*(3), 219–229. doi: 10.1679/aohc.62.219

Shi, J.-H., & Sun, S.-C. (2018). Tumor Necrosis Factor Receptor-Associated Factor Regulation of Nuclear Factor κB and Mitogen-Activated Protein Kinase Pathways. *Frontiers in Immunology*, *9*, 1849. doi: 10.3389/fimmu.2018.01849

Silber, M., Miller, I., Bar-Joseph, H., Ben-Ami, I., & Shalgi, R. (2020). Elucidating the role of pigment epithelium-derived factor (PEDF) in metabolic PCOS models. *The Journal of Endocrinology*, *244*(2), 297–308. doi: 10.1530/JOE-19-0297

Silverstein, A. M., Stefani, R. M., Sobczak, E., Tong, E. L., Attur, M. G., Shah, R. P., … Hung, C. T. (2017). Toward understanding the role of cartilage particulates in synovial inflammation. *Osteoarthritis and Cartilage*, *25*(8), 1353–1361. doi: 10.1016/j.joca.2017.03.015

Simmons, E. J., Bertone, A. L., & Weisbrode, S. E. (1999). Instability-induced osteoarthritis in the metacarpophalangeal joint of horses. *American Journal of Veterinary Research*, *60*(1), 7–13. PMID: 9918142

Singh, Y. P., Moses, J. C., Bhardwaj, N., & Mandal, B. B. (2021). Overcoming the Dependence on Animal Models for Osteoarthritis Therapeutics - The Promises and Prospects of In Vitro Models. *Advanced Healthcare Materials*, *10*(20), e2100961. doi: 10.1002/adhm.202100961

Smith, Malcolm D. (2011). The normal synovium. *The Open Rheumatology Journal*, *5*, 100–106. doi: 10.2174/1874312901105010100

Smith, M D, Barg, E., Weedon, H., Papengelis, V., Smeets, T., Tak, P. P., … Ahern, M. J. (2003). Microarchitecture and protective mechanisms in synovial tissue from clinically and arthroscopically normal knee joints. *Annals of the Rheumatic Diseases*, *62*(4), 303–307. doi: 10.1136/ard.62.4.303

Sokolove, J., & Lepus, C. M. (2013). Role of inflammation in the pathogenesis of osteoarthritis: latest findings and interpretations. *Therapeutic Advances in Musculoskeletal Disease*, *5*(2), 77–94. doi: 10.1177/1759720X12467868

Sotelo, E. D. P., Vendruscolo, C. P., Fülber, J., Seidel, S. R. T., Jaramillo, F. M., Agreste, F. R., … Baccarin, R. Y. A. (2020). Effects of Joint Lavage with Dimethylsulfoxide on LPS-Induced Synovitis in Horses-Clinical and Laboratorial Aspects. *Veterinary Sciences*, *7*(2). doi: 10.3390/vetsci7020057

Stefani, R. M., Halder, S. S., Estell, E. G., Lee, A. J., Silverstein, A. M., Sobczak, E., … Hung, C. T. (2019). A Functional Tissue-Engineered Synovium Model to Study Osteoarthritis Progression and Treatment. *Tissue Engineering. Part A*, *25*(7–8), 538–553. doi: 10.1089/ten.TEA.2018.0142

Steinmeyer, J., Bock, F., Stöve, J., Jerosch, J., & Flechtenmacher, J. (2018). Pharmacological treatment of knee osteoarthritis: Special considerations of the new German guideline. *Orthopedic Reviews*, *10*(4), 7782. doi: 10.4081/or.2018.7782

Straticò, P., Guerri, G., Palozzo, A., Di Francesco, P., Vignoli, M., Varasano, V., & Petrizzi, L. (2021). Elastosonographic features of the metacarpophalangeal joint capsule in horses. *BMC Veterinary Research*, *17*(1), 202. doi: 10.1186/s12917-021-02897-8

Ströbel, S., Loparic, M., Wendt, D., Schenk, A. D., Candrian, C., Lindberg, R. L. P., … Martin, I. (2010). Anabolic and catabolic responses of human articular chondrocytes to varying oxygen percentages. *Arthritis Research & Therapy*, *12*(2), R34. doi: 10.1186/ar2942

Sun, H.-Y., Hu, K.-Z., & Yin, Z.-S. (2017). Inhibition of the p38-MAPK signaling pathway suppresses the apoptosis and expression of proinflammatory cytokines in human osteoarthritis chondrocytes. *Cytokine*, *90*, 135–143. doi: 10.1016/j.cyto.2016.11.002

Sun, K., Luo, J., Jing, X., Xiang, W., Guo, J., Yao, X., … Xu, T. (2021). Hyperoside ameliorates the progression of osteoarthritis: An in vitro and in vivo study. *Phytomedicine: International Journal of Phytotherapy and Phytopharmacology*, *80*, 153387. doi: 10.1016/j.phymed.2020.153387

Suri, S., & Walsh, D. A. (2012). Osteochondral alterations in osteoarthritis. *Bone*, *51*(2), 204–211. doi: 10.1016/j.bone.2011.10.010

Tang, Q., Hao, L., Peng, Y., Zheng, Y., Sun, K., Cai, F., … Liao, Q. (2015). RNAi Silencing of IL-1β and TNF-α in the Treatment of Post-traumatic Arthritis in Rabbits. *Chemical Biology & Drug Design*, *86*(6), 1466–1470. doi: 10.1111/cbdd.12611

Tetsunaga, T., Nishida, K., Furumatsu, T., Naruse, K., Hirohata, S., Yoshida, A., … Ozaki, T. (2011). Regulation of mechanical stress-induced MMP-13 and ADAMTS-5 expression by RUNX-2 transcriptional factor in SW1353 chondrocyte-like cells. *Osteoarthritis and Cartilage*, *19*(2), 222–232. doi: 10.1016/j.joca.2010.11.004

Thomsen, L. N., Thomsen, P. D., Downing, A., Talbot, R., & Berg, L. C. (2017). FOXO1, PXK, PYCARD and SAMD9L are differentially expressed by fibroblast-like cells in equine synovial membrane compared to joint capsule. *BMC Veterinary Research*, *13*(1), 106. doi: 10.1186/s12917-017-1003-x

Thermo Fisher Scientific │Trypan Blue Exclusion - US. (2022). Retrieved from https://www.thermofisher.com/us/en/home/references/gibco-cell-culture-basics/cell-culture-protocols/trypan-blue-exclusion.html

Tsunoda, T., & Takagi, T. (1999). Estimating transcription factor bindability on DNA. *Bioinformatics*, *15*(7–8), 622–630. doi: 10.1093/bioinformatics/15.7.622

Tu, J., Huang, W., Zhang, W., Mei, J., Yu, Z., & Zhu, C. (2020). TWIST1-MicroRNA-10a-MAP3K7 Axis Ameliorates Synovitis of Osteoarthritis in Fibroblast-like Synoviocytes. *Molecular Therapy. Nucleic Acids*, *22*, 1107–1120. doi: 10.1016/j.omtn.2020.10.020

Uhlir, C., Licka, T., Kübber, P., Peham, C., Scheidl, M., & Girtler, D. (1997). Compensatory movements of horses with a stance phase lameness. *Equine Veterinary Journal. Supplement*, (23), 102–105. doi: 10.1111/j.2042-3306.1997.tb05065.x

Umbaugh, C. S., Diaz-Quiñones, A., Neto, M. F., Shearer, J. J., & Figueiredo, M. L. (2018). A dock derived compound against laminin receptor (37 LR) exhibits anti-cancer properties in a prostate cancer cell line model. *Oncotarget*, *9*(5), 5958–5978. doi: 10.18632/oncotarget.23236

United States Department of Agriculture. (2000). Lameness and laminitis in U.S. Horses. *National Animal Health Monitoring System.* Retrieved from https://www.aphis.usda.gov/animal_health/nahms/equine/downloads/equine98/Equine98_dr_Lameness.pdf

Valencia, X., Higgins, J. M. G., Kiener, H. P., Lee, D. M., Podrebarac, T. A., Dascher, C. C., … Brenner, M. B. (2004). Cadherin-11 provides specific cellular adhesion between fibroblast-like synoviocytes. *The Journal of Experimental Medicine*, *200*(12), 1673–1679. doi: 10.1084/jem.20041545

van Lent, P. L. E. M., Blom, A. B., Schelbergen, R. F. P., Slöetjes, A., Lafeber, F. P. J. G., Lems, W. F., … van den Berg, W. B. (2012). Active involvement of alarmins S100A8 and S100A9 in the regulation of synovial activation and joint destruction during mouse and human osteoarthritis. *Arthritis and Rheumatism*, *64*(5), 1466–1476. doi: 10.1002/art.34315

van Weeren, P. R. (2016). General anatomy and physiology of joints. In *Joint disease in the horse* (pp. 1–24). Elsevier. doi: 10.1016/B978-1-4557-5969-9.00001-2

Verborgt, O., Gibson, G. J., & Schaffler, M. B. (2000). Loss of osteocyte integrity in association with microdamage and bone remodeling after fatigue in vivo. *Journal of Bone and Mineral Research*, *15*(1), 60–67. doi: 10.1359/jbmr.2000.15.1.60

Verbruggen, G., Wittoek, R., Vander Cruyssen, B., & Elewaut, D. (2012). Tumour necrosis factor blockade for the treatment of erosive osteoarthritis of the interphalangeal finger joints: a double blind, randomised trial on structure modification. *Annals of the Rheumatic Diseases*, *71*(6), 891–898. doi: 10.1136/ard.2011.149849

Viana, M. N., Leiguez, E., Gutiérrez, J. M., Rucavado, A., Markus, R. P., Marçola, M., … Fernandes, C. M. (2020). A representative metalloprotease induces PGE2 synthesis in fibroblast-like synoviocytes via the NF-κB/COX-2 pathway with amplification by IL-1β and the EP4 receptor. *Scientific Reports*, *10*(1), 3269. doi: 10.1038/s41598-020-59095-z

Wang, C., Zeng, L., Zhang, T., Liu, J., & Wang, W. (2016). Tenuigenin Prevents IL-1β-induced Inflammation in Human Osteoarthritis Chondrocytes by Suppressing PI3K/AKT/NF-κB Signaling Pathway. *Inflammation*, *39*(2), 807–812. doi: 10.1007/s10753-016-0309-3

Wang, G.-D., Zhao, X.-W., Zhang, Y.-G., Kong, Y., Niu, S.-S., Ma, L.-F., & Zhang, Y.-M. (2017). Effects of miR-145 on the inhibition of chondrocyte proliferation and fibrosis by targeting TNFRSF11B in human osteoarthritis. *Molecular Medicine Reports*, *15*(1), 75–80. doi: 10.3892/mmr.2016.5981

Wang, T., & He, C. (2018). Pro-inflammatory cytokines: The link between obesity and osteoarthritis. *Cytokine & Growth Factor Reviews*, *44*, 38–50. doi: 10.1016/j.cytogfr.2018.10.002

Watkins, A. R., & Reesink, H. L. (2020). Lubricin in experimental and naturally occurring osteoarthritis: a systematic review. *Osteoarthritis and Cartilage*, *28*(10), 1303–1315. doi: 10.1016/j.joca.2020.05.009

Weishaupt, M. A., Wiestner, T., Hogg, H. P., Jordan, P., & Auer, J. A. (2006). Compensatory load redistribution of horses with induced weight-bearing forelimb lameness trotting on a treadmill. *Veterinary Journal*, *171*(1), 135–146. doi: 10.1016/j.tvjl.2004.09.004

Wei, Y., & Bai, L. (2016). Recent advances in the understanding of molecular mechanisms of cartilage degeneration, synovitis and subchondral bone changes in osteoarthritis. *Connective Tissue Research*, *57*(4), 245–261. doi: 10.1080/03008207.2016.1177036

Wen, H., Liu, M., Liu, Z., Yang, X., Liu, X., Ni, M., … Lu, H. (2017). PEDF improves atherosclerotic plaque stability by inhibiting macrophage inflammation response. *International Journal of Cardiology*, *235*, 37–41. doi: 10.1016/j.ijcard.2017.02.102

Wen, Y., Qin, J., Deng, Y., Wang, H., Magdalou, J., & Chen, L. (2014). The critical role of UDP-galactose-4-epimerase in osteoarthritis: modulating proteoglycans synthesis of the articular chondrocytes. *Biochemical and Biophysical Research Communications*, *452*(4), 906–911. doi: 10.1016/j.bbrc.2014.08.148

Whitton, C., Murray, R. C., & Dyson, S. J. (2003). Magnetic Resonance Imaging. In *Diagnosis and management of lameness in the horse* (pp. 216–222). Elsevier. doi: 10.1016/B978-0-7216-8342-3.50028-0

Woods, B., Manca, A., Weatherly, H., Saramago, P., Sideris, E., Giannopoulou, C., … Sculpher, M. (2017). Cost-effectiveness of adjunct non-pharmacological interventions for osteoarthritis of the knee. *Plos One*, *12*(3), e0172749. doi: 10.1371/journal.pone.0172749

Wu, J., Liu, W., Bemis, A., Wang, E., Qiu, Y., Morris, E. A., … Yang, Z. (2007). Comparative proteomic characterization of articular cartilage tissue from normal donors and patients with osteoarthritis. *Arthritis and Rheumatism*, *56*(11), 3675–3684. doi: 10.1002/art.22876

Wu, X., Song, W., Zheng, C., Zhou, S., & Bai, S. (2015). Morphological study of mechanoreceptors in collateral ligaments of the ankle joint. *Journal of Orthopaedic Surgery and Research*, *10*, 92. doi: 10.1186/s13018-015-0215-7

Yang, S.-L., Chen, S.-L., Wu, J.-Y., Ho, T.-C., & Tsao, Y.-P. (2010). Pigment epithelium-derived factor induces interleukin-10 expression in human macrophages by induction of PPAR gamma. *Life Sciences*, *87*(1–2), 26–35. doi: 10.1016/j.lfs.2010.05.007

Yang, W., Bai, X., Luan, X., Min, J., Tian, X., Li, H., … Sun, L. (2022). Delicate regulation of IL-1β-mediated inflammation by cyclophilin A. *Cell Reports*, *38*(11), 110513. doi: 10.1016/j.celrep.2022.110513

Yatim, N., Jusforgues-Saklani, H., Orozco, S., Schulz, O., Barreira da Silva, R., Reis e Sousa, C., … Albert, M. L. (2015). RIPK1 and NF-κB signaling in dying cells determines cross-priming of $CD8^+$ T cells. *Science*, *350*(6258), 328–334. doi: 10.1126/science.aad0395

Yoshitomi, H. (2019). Regulation of Immune Responses and Chronic Inflammation by Fibroblast-Like Synoviocytes. *Frontiers in Immunology*, *10*, 1395. doi: 10.3389/fimmu.2019.01395

Yusuf, E. (2016). Pharmacologic and Non-Pharmacologic Treatment of Osteoarthritis. *Current Treatment Options in Rheumatology*, *2*(2), 111–125. doi: 10.1007/s40674-016-0042-y

Zahir, H., Dehghani, B., Yuan, X., Chinenov, Y., Kim, C., Burge, A., … Otero, M. (2021). In vitro responses to platelet-rich-plasma are associated with variable clinical outcomes in patients with knee osteoarthritis. *Scientific Reports*, *11*(1), 11493. doi: 10.1038/s41598-021-90174-x

Zamiri, P., Masli, S., Streilein, J. W., & Taylor, A. W. (2006). Pigment epithelial growth factor suppresses inflammation by modulating macrophage activation. *Investigative Ophthalmology & Visual Science*, *47*(9), 3912–3918. doi: 10.1167/iovs.05-1267

Zarka, M., Hay, E., Ostertag, A., Marty, C., Chappard, C., Oudet, F., … Cohen-Solal, M. (2019). Microcracks in subchondral bone plate is linked to less cartilage damage. *Bone*, *123*, 1–7. doi: 10.1016/j.bone.2019.03.011

Zhang, W., Nuki, G., Moskowitz, R. W., Abramson, S., Altman, R. D., Arden, N. K., … Tugwell, P. (2010). OARSI recommendations for the management of hip and knee osteoarthritis: part III: Changes in evidence following systematic cumulative update of research published through January 2009. *Osteoarthritis and Cartilage*, *18*(4), 476–499. doi: 10.1016/j.joca.2010.01.013

Zhang, X., Egan, B., & Wang, J. (2015). Structural and Functional features of Major Synovial Joints and Their Relevance to Osteoarthritis. In Q. Chen (Ed.), *Osteoarthritis - Progress in Basic Research and Treatment*. InTech. doi: 10.5772/59978

Zhao, C. (2021). Identifying the hub gene and immune infiltration of osteoarthritis by bioinformatical methods. *Clinical Rheumatology*, *40*(3), 1027–1037. doi: 10.1007/s10067-020-05311-0

Zhao, W., Zhang, C., Shi, M., Zhang, J., Li, M., Xue, X., … Zhang, Y. (2014). The discoidin domain receptor 2/annexin A2/matrix metalloproteinase 13 loop promotes joint destruction in arthritis through promoting migration and invasion of fibroblast-like synoviocytes. *Arthritis & Rheumatology (Hoboken, N.J.)*, *66*(9), 2355–2367. doi: 10.1002/art.38696

Zhen, G., Wen, C., Jia, X., Li, Y., Crane, J. L., Mears, S. C., … Cao, X. (2013). Inhibition of TGF-β signaling in mesenchymal stem cells of subchondral bone attenuates osteoarthritis. *Nature Medicine*, *19*(6), 704–712. doi: 10.1038/nm.3143

Zhou, X., Li, F., Kong, L., Chodosh, J., & Cao, W. (2009). Anti-inflammatory effect of pigment epithelium-derived factor in DBA/2J mice. *Molecular Vision*, *15*, 438–450. PMID: 19247457

Zhou, Yachuan, Shu, B., Xie, R., Huang, J., Zheng, L., Zhou, X., … Chen, D. (2019). Deletion of Axin1 in condylar chondrocytes leads to osteoarthritis-like phenotype in temporomandibular joint via activation of β-catenin and FGF signaling. *Journal of Cellular Physiology*, *234*(2), 1720–1729. doi: 10.1002/jcp.27043

Zhou, Yingyao, Zhou, B., Pache, L., Chang, M., Khodabakhshi, A. H., Tanaseichuk, O., … Chanda, S. K. (2019). Metascape provides a biologist-oriented resource for the analysis of systems-level datasets. *Nature Communications*, *10*(1), 1523. doi: 10.1038/s41467-019-09234-6

Zhu, W., Wang, D., Lu, W., Han, Y., Ou, Y., Zhou, K., … Zhang, X. (2012). Gene expression profile of the synovium and cartilage in a chronic arthritis rat model. *Artificial Cells, Blood Substitutes, and Immobilization Biotechnology*, *40*(1–2), 70–74. doi: 10.3109/10731199.2011.592493

Ziemian, S. N., Witkowski, A. M., Wright, T. M., Otero, M., & van der Meulen, M. C. H. (2021). Early inhibition of subchondral bone remodeling slows load-induced posttraumatic osteoarthritis development in mice. *Journal of Bone and Mineral Research*, *36*(10), 2027–2038. doi: 10.1002/jbmr.4397